The role of the miR-17-92 cluster in macrophage driven innate immunity

Vorgelegt von

H. James Stunden

aus
Melbourne (Australia)

Bonn, Februar, 2018

Angefertigt mit Genehmigung der Mathematisch-

Naturwissenschaftlichen Fakultät der Rheinischen Friedrich-

Wilhelms-Universität Bonn

Gutachter: Prof. Dr. med. Eicke Latz

Gutachter: Prof. Dr. med. Joachim L. Schultze

Supervised by

Prof. Dr. med. Eicke Latz

Dr Michael P. Gantier

Tag der Promotion: 12.11.2018

Erscheinungsjahr: 2018

Summary

Research into miRNA, discovered in 1993, has exploded and revolutionized our understanding of molecular regulation in biological systems. MicroRNAs are now a well established as a regulatory mechanism of many pathways and functions within cells of eukaryotic organisms, though much needs to be learnt about the intricacies of such regulation. In recent years, targeting this system of post-translational regulation has been a goal of many therapeutics, but requires much greater insight into how miRNA work, and the broadness of their activity.

The innate immune system is critical for mounting an effective response against invading pathogens and protecting the host from damage. But being such a powerful system, unchecked it can wreak havoc on the host itself. While the innate immune system is tightly regulated by many mechanisms, further understanding could lead to major advances in therapeutics of autoimmune diseases. As the miR-17-92 cluster has already been identified as a regulator of innate immune functions, and continued research in animal models is necessary for therapeutics to become a reality.

This thesis focuses on the role and function of the miR-17-92 cluster within macrophages, which are a major component of the innate immune system. It highlights the complexity and often subtle nature of microRNA regulation in biological systems. It describes the generation of a mouse line with a myeloid-specific deletion of the miR-17-92 cluster is described, and shown that despite this deletion, there is no change both to the innate immune response of these mice, or to the TLR signalling cascade. It is postulated that while the miR-17-92 cluster affects innate immune signaling in some other cell types, it is unlikely to have a similar role in macrophages.

Contents

1 Introduction

1.1 miRNA

MicroRNAs (miRNAs) are small ~22 nucleotide RNA molecules that regulate the expression of genes in a sequence-dependent manner. They bind to complementary sequences, often within the 3' UTR of messenger RNA (mRNA) and sequester, deadenylate, inhibit ribosomal translation, or in cases of exact complementarity, enzymatically cleave a target mRNA [1]. Such mechanisms destabilise the mRNA molecule, and thus prevent protein translation. Initially discovered as critical regulators of worm growth [2], miRNA quickly become understood as a key mechanism of gene regulation in cells [3].

miRNAs, like genes, are differentially expressed in tissues and can be further influenced by stimulation, activation and environmental factors. Their regulatory effect is recognised as a integral component for the survival of organisms and cells, tuning critical processes including apoptosis, inflammation, and metabolism [4]. miRNA use a "seed sequence" of 6 nucleotides, between positions 2-8 of its 5' terminal end to bind target mRNA, at a site known as the miRNA Response Element (MRE). As the complementary sequences to these seed sequences are repeated both perfectly and imperfectly many thousands of times in the genome, the number of genes a single mature miRNA binds to quickly multiplies to several hundred [5, 6, 7, 8]. Furthermore, imperfect sequence complementarity, as well as different numbers of MREs found on a single mRNA allows for a variety of strength in interactions between mature miRNA and different target sequences. This observation of has led groups to develop software and algorithms to predict miRNA interactions with target mRNA 3'UTRs [9, 10].

As some miRNA share seed sequences with other miRNA, they are likely to target the same genes, and are therefore considered part of the same miRNA family. As such, the dysregulation of a single miRNA can either have widespread consequences for aberrant epigenetic regulation, not least considering other transcription factors that are downstream of such modulation, or redundancy by expression of other miRNA family members can mediate the effects [6]. However, because of the potential breadth of these effects, the dysregulation of a single, or groups of miRNA are often associated with diseases, including arthritis [11, 12, 13], cholesterol metabolism and atherosclerosis [14, 15], and colitis [16] to name a few.

1.2 Biogenesis and processing of miRNA

The pathway to a mature miRNA begins in the nucleus as a primary transcript (pri-miRNA) is generated by RNA polymerase II, which folds on itself to form a large hairpin structure. pri-miRNA can be a part of other genes, found within introns, or expressed independently with their own genomic regulatory elements and promoters [17]. Stem-loop structures found in the pri-miRNA, after folding in on itself, are recognised by DGCR8, binding to the junction between the single-stranded RNA and double-stranded RNA of the pri-miRNA. DGCR8 then recruits Drosha, which in turn cleaves the molecule ~11bp from this junction [18]. The resulting stem-loops are called precursor-miRNA (pre-miRNA), and contain mature miRNA sequences in the stem section. These pre-miRNA are exported to the cytoplasm by Exportin 5 [19] (Fig. 1), where once in the cytoplasm, another RNAse enzyme, Dicer, cleaves the loop off the pre-miRNA to form a miRNA duplex with a 3' overhang. Either strand of the duplex miRNA is now loaded in the RNA-Induced Silencing Complex (RISC), a structure comprising of an Argonaute protein, TRBP and Dicer, to form the mature miRNA [20, 21]. miRNA can regulate target mRNA by either repressing ribosomal activity, cleaving the target, or deadenylation [22, 23]. As mature miRNA can arise from either complementary strand of pre-miRNA, modern nomenclature states that the mature miRNA loaded RISC with the 5'end of the stem-loop are termed -5p (ie. mmu-miR-19b-5p), while those from the 3'end are called -3p (ie. mmu-miR-19b-3p).

The miRNA gene silencing pathway has been found to be useful in biological research, as hijacking the biogenesis pathway results in targeted silencing of genes, commonly known today as Short Hairpin RNA (shRNA) gene silencing [24]. However, the use of RNA silencing technologies for therapeutics has been slow to develop, mostly due to difficulties and complications with the delivery and efficacy of such drugs to target cells without undesirable side-effects [25]. Others have had more success, using polymer nanoparticle based delivery systems to inhibit miR-155 *in vivo* [26], while others have used SELEX-based approaches to develop cell-specific aptamers [27]. More recently, new methods of "zipping" miRNA together have been developed, however questions still remain regarding *in vivo* evidence, off-target effects, and nucleic acid acid-sensing PRR activation [28].
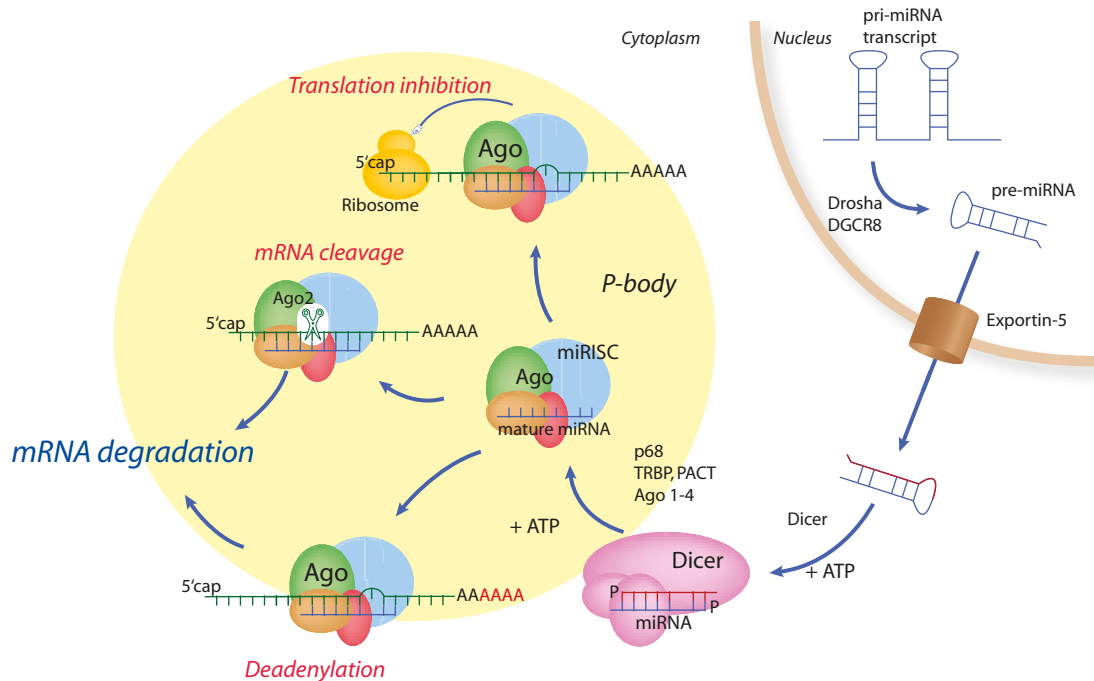
Figure 1:

Biogenesis and effector mechanisms of miRNA. Pri-miRNA are generated in the nucleus, where they are cleaved by Drosha and DGCR8 into hairpin structures, that are exported to the cytoplasm by Exportin-5. Once in the cytoplasm, the loop is trimmed by Dicer, and one of the strands of the miRNA will become a core component of the RISC. Now, the mature miRNA will guide the RISC to inhibit, and often destabilise messenger RNA, resulting in its degradation. Image adapted with permission from M.P. Gantier.

1.3 miR-17-92

The miR-17-92 cluster (Fig. 2), also known as oncomiR-1, is a major focus of cancer research [29, 30]. Initially it was discovered as a novel gene, chromosome 13 open reading from 25 (c13orf25) in human B-cell lymphoma, where the region was significantly upregulated [31]. Currently identified as Mir17HG, it encodes 6 separate miRNAs from 4 different families, miR-17, miR-18a, miR-19a, miR-20a, miR-19b-1, and miR-92a. There are also two identified paralogues of the miR-17-92 cluster, called the miR-106a-363 and miR-106b-25 clusters, expressed on chromosomes X and 7 respectively [32].

Even though there are 6 mature miRNAs from a single transcript, each individual mature miRNA is expressed at different levels. In a recent study, the complex secondary and tertiary structure of the miR-17-92 cluster was published, and indicated that the Drosha cleavage sites were inac-

cessible for pri-miR-18a, -19a and -20a due to its folding [33]. Furthermore, another part of the pre-miR-17-92 sequence (termed NPSL2) even binds and sequesters a component required to form the basal helix structure for pri-miR-92a, preventing Drosha processing at all. This led the authors to believe that the tertiary structure provides a first layer of regulation for the expression of each individual pri-miRNA. Furthermore, this indicates that other factors must act to expose these cleavage sites and allow processing, possibly providing a secondary layer of miRNA expression control. One potential candidate is KHSRP, previously published to enhance miR-20 expression, however the precise mechanism is unknown [34]. Previously, hnRNP A1 was shown to bind pri-miR-18a before Drosha processing, indicating another potential candidate for multilayer regulation of miR-17-92 mature miRNA expression [35].

The mir-17-92 cluster was found to be upregulated by the transcription factor c-myc, and could facilitate the inhibition apoptosis, resulting in accelerated tumour growth [36]. Deleting the cluster in mice resulted in the death of animals shortly after birth with developmental defects of the heart, lungs and skeletal structure, a reduced body mass, and a near complete ablation of pre-B cells [37]. Later work established that the lung hypoplasia is due to the combined contribution of miR-17, miR-18 and miR-92 deletion, while miR-17 and miR-18 deletion was responsible for the ablation of mature B-cells [38]. A role of the miR-17-92 cluster was then established in adaptive immunity, especially in B-cell survival, B-cell related cancers, including lymphomas [39].

Further studies have published that miR-19 modulates the stability of several negative regulators of NF-κB, thus enhancing pro-inflammatory cytokine production [40], while other groups have confirmed these discoveries in T cells [41], and have further identified miR-19 as an indicator in T_H2 driven asthma by the targeting the same genes [42]. However, miR-19 is not solely responsible for all immune-related diseases are caused by dysregulation of the cluster, as miR-92a has also been discovered to have a role in Type I diabetes in T cells [43], and miR-18a was also described to target PIAS3; the regulator of STAT3 signalling in hepatocytes [44], and miR-20a targets ASK1, decreasing LPS induced cytokine release in arthritis models [12]. It is also indicated that miR-18 expression is induced via TNFa, which could play a role in other cells. To this end, it has also been found that miR-18a is induced by NF-κB in Rheumatoid arthritis Synovial Fibroblasts, and by increasing the expression of miR-18a, there was also an increase in Il-8, RANTES and other pro-inflammatory markers [45]. More recently, ILC2s were also found to harbor important roles for the miR-17-92 cluster, where dampened expression of the cluster resulted in reduced counts of ILC2 cells in the lungs of mice, defective IL-33 driven

proliferation and inhibited the IL-13 and IL-5 response to the allergen papain [46]. Overexpressing the cluster had the opposite effect, and most of the effects were attributed to miR-19, which when expression was recapitulated *in vivo* reversed much of the miR-17-92 deficient observations. A critical challenge for researchers trying to study the miR-17-92 cluster is that it affects such a wide variety of pathways in the cell. Making a complete KO cell is made difficult when the cluster is critical for cell survival [32], which explains why other studies have had trouble using and making miR-17-92 KO cells lines [42].

1.4 Innate immune system and inflammation

The innate immune system is the first line of defense against invading pathogens in complex multicellular organisms. It consists of physical barriers including the skin and secreted fluids, like saliva and mucus, that non-specifically limit the invasion by pathogens into the body, and then effector cells and mechanisms, including (but not limited to), macrophages, dendritic cells, and mast cells. Indeed, most cells in the body, such as fibroblasts, possess some function for innate immunity, sensing microbial pathogens and activating transcription factors that activate chemokine release, encouraging the mobilisation of other effector cells to the site of infection.

Pathogen Associated Molecular Patterns (PAMPs) are conserved structures and components of pathogens, and Danger Associated Molecular patterns (DAMPs) are molecules from the host organisms, that would not normally be found in the extracellular space, but their presence may indicate an infection or damage to the host. Both PAMPs and DAMPs can be specifically recognised by conserved receptors, called Pattern Recognition Receptors (PRRs), which are found in and on different innate immune cells. Included in this family of receptors are the Toll-like receptors (TLRs), the NOD-like receptors, RIG-I like receptors and C-type lectin receptors, all of which are evolutionarily conserved to recognise particular motifs from bacteria, viruses, parasites and fungi [48, 49].

Inflammation is one of the major responses to invading pathogens, typified by a reddening and swelling of the affected tissue, often accompanied with tenderness or pain. PRRs from either local epithelial cells, tissue resident macrophages or dendritic cells identify foreign material from bacteria, viruses, and other invading pathogens, and release pro-inflammatory signals such as cytokines. This signal results in a rush of blood and fluids to the affected area, bringing with it recruited activated effector cells such as neutrophils and monocyte-derived macrophages. This rush in blood and fluid reddens the area, and increases the swelling of the tissue.
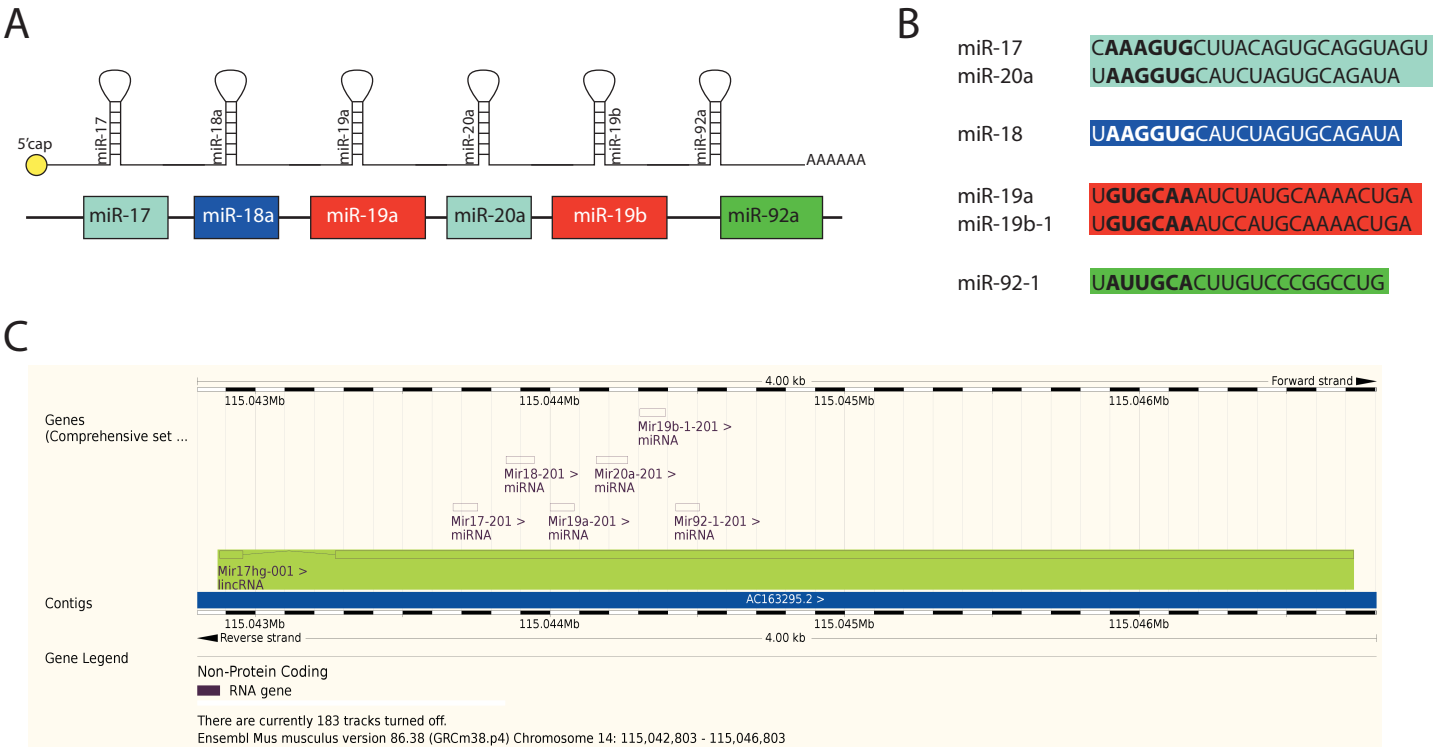
Figure 2:

The miR-17-92 cluster. A. Stylized schematic indicating the relative positions of the miRNA inside the cluster. The colour coding indicates the family into which each miRNA belongs. **B.** The arrangement according the family members of each miRNA with the seed sequence highlighted. **C.** Genomic mapping of the Mir17HG, accessed from Ensembl, Release 91 [47].

16

The detection of PAMPS triggers a signalling cascade from the recruitment of the adaptor molecules MyD88, with or without TRIF, and switches on signalling networks that induce the production and secretion of pro-inflammatory cytokines, chemokines, interferons (IFNs) and other anti-microbial agents, which mount responses to fight infection by pathogens. Typically, when tissue resident macrophages encounter an invading pathogen, their PRRs are activated, and they begin to phagocytose, followed by the release of the cytokines TNFα, IL-6, and IL-1β, and sometimes more, depending on the PRR activated [50].

Macrophages typically clear dead cells, pathogens and debris, while dendritic cells remove antigens, and migrate to the local lymph nodes to activate and mature T and B cells.

1.5 Macrophages

First described as "Big Eaters" by their discoverer, Elie Metchnikoff, macrophages have become recognized as critical cells of the innate immune system [51, 52]. There are many subpopulations of macrophages identified, typically distinguished by their location in the body, and are derived from embryonic precursor cells [53, 54]. Tissue resident macrophages include peritoneal macrophages, microglia in the brain, and kupfer cells in the liver to name a few. Macrophages have diverse and important functions in the body, patrolling for invading pathogens, initiating innate immune responses, remodelling and repairing of tissues following an infection or inflammation, and resolving the inflammatory response. In the event of inflammation or other stimuli, monocytes that are recruited to the site of infection may also differentiate into macrophages, given the right conditions and presence of macrophage colony stimulating factor (M-CSF). Their major function is the phagocytosis of invading pathogens and antigens, which can be degraded by the macrophage itself using lysosomal compartments filled with degradative enzymes. If a macrophage is activated by the detection of a PAMP or DAMP, a rapid change in metabolism and gene expression is observed, and the cell may release pro-inflammatory cytokines IL-1, IL-6 and TNFa. Other release cytokines include IL-8 to recruit and attract neutrophils, and IL-12 to activate NK cells, and initiate the differentiation of TH1 cells. Other macrophages will also try and resolve the response by secreting IL-10, returning the conditions back to normal [55].

Critical functions of macrophages are known to be regulated by many miRNA. For example, miR-146a and -146b are both upregulated following stimulation of cell surface receptors [56, 14]. More recently, expression of miR-146a was found to be controlled by PU.1 and ApoE in mouse macrophages [15]. These miRNA target TRAF6, IRAK1, IRAK2, all components of the

myddosome, a protein scaffold required for many TLR and TNFR signalling cascades [57]. As a consequence of miR-146a/b targeting of these regulatory components, expression and release of many inflammatory cytokines such as IL-8 and RANTES following stimulation are reduced [57, 58]. Because of these mechanisms, miR-146 has also been associated with diseases and disease processes such as atherosclerosis, cholesterol efflux and metabolism to name a few [15, 14].

Other effects are not as direct, such as miR-132, which was found to target acetylcholinesterase (AChE) in murine macrophages [59]. AChE breaks down acetylcholine, which is released by the vagus nerve to dampen peripheral inflammatory responses [60, 61]. In macrophages, miR-132 was reduced upon LPS stimulation allowing for miR-132 regulation to permit acetylcholine driven inflammatory regulation. By mutating the miR-132 target site in AChE in a mouse model, the mice exhibited enhanced pro-inflammatory cytokine release when challenged with LPS [59].

miRNA expression may also be regulated by environmental stresses or stimuli. IL-10, a critical anti-inflammatory cytokine released by macrophages also inhibits the induction of miR-155 by TLR signalling in macrophages [62]. This is a critical step to reduce and control inflammation in macrophages [63]. miRNA also have very complicated roles in macrophages and may also have delicate interplay may be important for context dependent responses. As both miR-146 and miR-155 are induced by NF-κB mechanisms, and where miR-146 is more anti-inflammatory [64], miR-155 has a wide range of effects on NF-κB, but is not limited to just pro-inflammatory roles [62, 63, 65]. While miR-146$^{-/-}$ macrophages were found to be pro-inflammatory, the effect was entirely dependent on the expression of miR-155 [66].

1.6 Regulation of NF-kB and Inflammation

The NF-κB family of transcription factors (consisting of p50, p52, RelA, RelB, and c-Rel) is one of the major drivers of inflammation, and were initially found in B-cells in 1986 [67]. NF-κB members are found in the cytoplasm of most cells pre-formed in homo- or heterodimers of 13 different forms, but are sequestered by bound proteins; Inhibitors of κB (IκBα, IκBβ, IκBε, and more) [49, 68, 69, 70, 71]. The N-terminal subdomain is responsible for DNA recognition and binding, while the C-terminal domain of these family members is responsible or dimer formation and inhibition. Furthermore, with such a wide variety of NF-κB dimers possible, it is easy to see that these subtle differences may allow for different affinities to unique sequences of DNA. There are two methods of activating NF-κB to translocate to the nucleus, the Classical pathway

and the Alternative pathway. It is largely accepted that the Classical pathway is associated with response to infectious agents and inflammatory insults, while the alternative pathway is for developmental signals [71].

For the Classical pathway, a surface receptor such as a PRR or TNFR undergoes a conformational change allowing for interaction with downstream molecules including MyD88, IRAK-1, IRAK-4, RIPK1, TRADD, TAK1 and TRAF6, depending on the specific receptor activated. This activation is often concurrent with the addition of a K63 ubiquitin chain to these adaptor proteins [72, 73, 74]. These adaptor proteins will trigger a signalling cascade that results in the activation of Inhibitor of kB Kinases (IKKα, IKKβ and IKKγ), whose function is to phosphorylate the IkBs, triggering their ubiquitination and degradation, and thus releasing NF-κB dimers to migrate to the nucleus [75, 76, 49, 77, 71, 78]. Once there, NF-κB binds in a sequence dependent manner to the DNA sequence 5'-GGGRNWYYCC-3' (N, any base; R, purine; W, adenine or thymine; Y, pyrimidine), called kB, which modulates expression of specific genes [71]. Genes associated with cytokine expression are often upregulated, and the cells shift towards a glycolytic metabolic setting, as the cell begins to produce lots of cytokines and other proteins associated with combating the invading pathogen [79, 80]. It is quite clear that with several NF-κB family members and multiple possible dimers, the potential for differential DNA binding and recognition can result in many transactivation mechanisms [70].

Continual low-grade inflammation can, in time, result in an imbalance of the immune homeostasis, leading to tissue damage, autoimmune and inflammatory diseases such as arthritis, and cancers [81, 50]. The control of inflammatory signals is also critical for normal development, as NF-κB has been found important in the development of many tissues [82]. To prevent dysregulation of inflammation, there are many negative regulators that are induced following an inflammatory signal that try to shut down NF-κB and the inflammatory response. These built-in negative feedback loops allow for a pulsatile response, continually keeping the system under self-check [83, 84, 85]. *Tnfaip3* (A20) is among these genes, which edits the ubiquitination of TRAF6 and RIPK1. Upon activation and translocation of NF-κB to the nucleus, genes including *Tnfaip3* are induced [86, 87, 88]that then remove the K63 polyubiquitin from TRAF6 and RIPK1, and replace them with K48-linked polyubiquitin [72]. Importantly, the biogenesis of miRNA is also modified by activation of inflammatory cascades and transcription factors [89, 84, 90], thus bringing a new dimension to miRNA regulation of gene expression.

As inflammation is such an important pathway that must be tightly regulated, it makes sense

that miRNA can modulate such cellular responses. Indeed, miR-146a, miR-155 and miR-132 were found to be induced following LPS stimulation. Furthermore, miR-146a could regulate *IRAK1* and *TRAF6*, hence providing a negative feedback loop to curb the inflammatory signalling cascade [56, 91, 92]. Independent analysis shows that miR-155 was indeed induced by LPS and TNFa, further highlighting their roles as regulators of inflammation and endotoxic shock [93, 94]. Even more importantly, miRNA are also under the control of negative regulators of NF-κB and inflammation, as was discovered when IL-10, an anti-inflammatory cytokine could inhibit the induction of miR-155 following TLR activation [62]. Furthermore, miR-125a and -125b have been previously shown to regulate A20 expression in primary bronchial epithelial cells which results in an impaired regulation of inflammatory cytokines. Interestingly, COPD patients had increased miR-125 levels, resulting in an impairment of not only A20 regulation of inflammatory signalling, but also MAVS, thus reducing the patients antiviral response and further worsening the condition of the patients [95]. However, when inhibiting the miRNA, there was a more marked reduction in viral replication than of inflammatory markers, indicating that miR-125a and b target MAVS preferentially to A20.

Critically, miR-19 has been identified to regulate several controllers of NF-κB, including SOCS3 [96], A20 and Rnf11 [40, 97], and CYLD [98]. Given the knowledge that miR-19 is a potent regulator of inflammation *in vitro,* experiments must be done to assess its effect *in vivo.*

1.7 Cre recombinase

Cre recombinase technology is based on the use of the Cre recombinase enzyme, which recognizes and recombines sequences of genomic DNA, called lox sites [99]. The LysMCre animal was produced in 1999 to allow for myeloid specific deletion of genes [100]. Cre recombinase is expressed upon activation of the Lyz2 promoter, activated specifically in macrophages and monocytes. When bred with an animal with a gene flanked by specific lox sites, this allows for cell specific gene deletion. When combined with the miR-17-92fl/fl, this should theoretically provide a myeloid specific deletion of this miRNA cluster. This will hopefully mitigate the issue of a full miR-17-92 cluster being fatal.

2 Aims

As the miR-17-92 cluster has been shown to regulate NF-κB driven innate immune signalling, it would be interesting to investigate wether this cluster has an effect in macrophages, a major component of the innate immune response, and a critical determinable factor in disease. As little investigative work has been done to elucidate this topic, this project intends to examine the effect of the miR-17-92 on cytokine production and NF-κB signalling in macrophages. The aims of this study are as follows:

- Generate a miR-17-92 mø specific transgenic animal.

- Investigate if the miR-17-92 cluster regulates cytokine production in Macrophages.

- Investigate if modulation of the miR-17-92 cluster affects the innate immune response *in vivo*.

- Develop a Modular Nanostring Panel that can be used by multiple projects to assess macrophage response by transcription.

3 Materials and Methods

3.1 Software

Software	Company
Adobe Illustrator CS6	Adobe
FloJo 10.3	FlowJo LLC
Geneious 8.1.5	Biomatters
ImageStudio 3.1.4	LI-COR
Microsoft Office for Mac 2016	Microsoft
nSolver 4.0	Nanostring Technologies, Inc.
Oligo7	Molecular Biology Insights, Inc.
Papers3	Digital Science and Research Solutions Inc.
Partek Genomics Suite 6.6	Partek, Inc.
Partek Flow	Partek, Inc.
Prism6	GraphPad Software
LyX- LaTeX document writer	Free Software Foundation, Inc.

3.2 Media and buffers

LB medium

20g LB media Powder (Roth) in 1L water. Autoclaved and Ampicillin or Kanamycin added fresh.

LB agar

32g LB agar powder (Roth) in 1L water. Autoclaved and Ampicillin or Kanamycin added before poured into clean petri dishes.

Complete DMEM

Gibco DMEM, High glucose, L-Glutamine (Thermo Fisher) with 10% (v/v) Heat-inactivated sterile filtered FBS and 1% (v/v) penicillin and streptomycin.

ELISA washing buffer

0.01% (v/v) Tween20 (Roth) in 1x PBS.

ELISA blocking buffer

0.01% (w/v) BSA in 1x PBS

MACS buffer

1% (w/v) BSA, 2mM EDTA in 1xPBS

Duplex buffer

Ingredient	
Potassium Acetate	100mM
HEPES	30mM

Adjust pH to 7.5.

6x Laemllie lysis buffer

Ingredient	
SDS	1.2g
Bromophenol Blue	6mg
Glycerol	4.7ml
1M TRIS pH6.8	1.2ml
Water	2.1ml

Dilute to 1x before use and add 50mM DTT and 1/1000 dilution of benzonase (Thermo Fisher).

MOPS buffer

NuPAGE 20x MOPS SDS running buffer (Thermo Fisher) diluted in water.

Transfer buffer

100ml 10x Tris-Glycine Buffer (Thermo Fisher), 150ml Methanol, 750ml water.

TBS-T

100ml 10x TBS (Thermo Fisher), 0.1% Tween20 (Roth) and 900ml water.

iCLIP buffers

iCLIP cell lysis buffer	
1M TRIS pH7	2.5ml
1M TRIS pH8	2.5ml
5M NaCl	2ml
10% Igepal	10ml
10% SDS	1ml
5% Sodium deoxycholate	10ml
Water	71ml
Add Protease inhibitors	

iCLIP High Salt Wash	
1M TRIS pH7	2.5ml
1M TRIS pH8	2.5ml
5M NaCl	20ml
10% Igepal	10ml
10% SDS	1ml
5% Sodium deoxycholate	10ml
Water	53ml
Add Protease inhibitors	

PNK wash buffer	
1M TRIS pH7	1ml
1M TRIS pH8	1ml
1M MgCl	1ml
10% Tween20	2ml
Water	95ml

5xPNK pH6.5 buffer	
1M TRIS pH6.5	350µl
1M MgCl	50µl
1M DTT	5µl
Water	555µl

2xPK Buffer	
1M TRIS pH7	10ml
1M TRIS pH8	10ml
5M NaCl	2ml
0.5M EDTA	4ml
Water	74ml

3.3   Mice

3.3.1   Breeding miR-17-92fl/fl - CD11b-Cre

CD11b-Cre mice were a kind gift from Prof. Andreas Zimmer. They were bred with a miR-17-92fl/fl animal, purchased from Jax Laboratories (JAX stock #008458) [37]. An animal of the progeny, miR-17-92fl/- Cd11b+/- were then bred with mir-17-9fl/fl mice, and then the progeny

Primer name	Sequence
miR-17-92^{fl} fwd	TCGAGTATCTGACAATGTGG
miR-17-92^{fl} rev	TAGCCAGAAGTTCCAAATTGG
CD11b-Cre fwd	CATTTGGGCCAGCTAAACAT
CD11b-Cre rev	CCCGGCAAAACAGGTAGTTA
LysMCre fwd	CATTTGGGCCAGCTAAAC
LysMCre rev	CCCGGCAAAACAGGTAGT

Table 1: Genotyping Primers

that are miR-17-92fl/fl - CD11b-Cre+/- are then kept by breeding with miR-17-92fl/fl. The progeny of these are then used for experiments and maintaining the line. All breeding and housing was performed at the Haus für Experimentelle Therapie (HET) at the Universität Klinikum Bonn.

3.3.2 Breeding miR-17-92fl/fl - LysMCre

LysM-Cre mice were a kind gift from Imgard Förster [100]. They were bred with a miR-17-92fl/fl animal, purchased from Jax Laboratories (JAX stock #008458) [37]. An animal of the progeny, miR-17-92fl/- LysM-Cre+/- were then bred with mir-17-9fl/fl mice, and then the progeny that are miR-17-92fl/fl - LysM-Cre+/- are then kept by breeding with miR-17-92fl/fl. The progeny of these are then used for experiments and maintaining the line. Genotyping was performed using the primers in table 1, a WT animal for miR-17-92fl/fl was expected to have a band of 255bp, while a homozygous miR-17-92fl/fl animal has a band of 289bp. Genotyping for LysMCre was performed with a simple positive or negative PCR, using the priers outlined in table 1.All breeding and housing was performed at the Haus für Experimentelle Therapie (HET) at the University Klinikum Bonn.

3.3.3 Animal sacrifice

Animals were handled as little as possible, and euthanased by cervical dislocation.

3.3.4 Peritoneal Cavity

Immediately following euthanasia, the fur was pulled away from the abdomen. To collect cytokines from the cavity, 2ml of PBS+2mM EDTA was injected through the abdominal fat pad, with care to avoid internal organs, the belly was shaken thoroughly, and then 1ml of fluid was collected, spun down at 300g, and then transferred to a new 1.5ml Eppendorf tube and frozen. Another 8ml of PBS+2mM EDTA was injected into the peritoneal cavity, shaken again and collected, before the cell pellet from the previous collection is added. This suspension is spun and then resuspended in DMEM +10%FCS +P/S, before counting and plating for adherent cells.

If collection is only for peritoneal lavage cells, 10ml of PBS +2mM EDTA injected through the abdominal fat pad, the belly is shaken, and then as much fluid is collected as possible. This is spun down at 300g, and then resuspended in DMEM +10%FCS +P/S, before gross counting and plating for adherent cells.

Alternatively, cells may be pelleted and subjected to MACS magnetic selection (3.3.8).

3.3.5   Spleen preparation

The spleen was removed from the mouse and then trimmed of as much fat as possible, and placed in RPMI +0.1% FCS on ice until use. It is then crushed using a syringe plunger through a 70μm cell strainer, and washed with 5-10ml RPMI+0.1% FCS. The suspension is spun at 300g for 8 minutes at 4˚C, then a red blood cell lysis is performed for 2 minutes following the manufacturers instructions, before being stopped with PBS. The suspension is then spun at 300g again for 5 minutes at 4˚C, the supernatant is discarded, and the pellet is resuspended in 1ml MACS buffer. The suspension is then passed through a 40μm cell strainer, washed with MACS buffer, and then spun again at 300g for 5 minutes. The cell pellet is then resuspended with 200μl of MACS buffer per spleen, before proceeding to magnetic bead binding (3.3.8).

3.3.6   BMDM preparation

Femurs and tibias from 6 - 10 week old mice were isolated, the muscle and tissue was removed and then briefly soaked in 70% ethanol. An end of the bone was cut and bone marrow was flushed using a fine-gauge needle and DMEM supplemented with 10% FCS and pen/strep. Bone marrow was collected, filtered through a 70 μm Nylon cell strainer, and pelleted (5 min at 340 x g), resuspended in 40 ml of DMEM supplemented with either 20% L929 supernatant or 40 ng/ml M-CSF (R&D Systems). BMDMs were differentiated over 7 days in 20 ml of media in T175 flasks. Adherent BMDMs were harvested by removing media, washing cells in PBS and then incubating cells at 4°C for 10 min in cold PBS supplemented with 2 % FCS and 2 mM EDTA. Gentle tapping dislodged cells and scraping dislodged any remaining adherent cells. Cells were collected, pelleted (5 min at 340 x g) and resuspended in DMEM with 10% FCS and pen/strep and plated for experiments.

3.3.7   *In vivo* LPS injection

In accordance with ethics form 84-02.04.2014.A151, mice were injected with low dose LPS (0.5μg per gram animal weight in 100μl of sterile PBS) or sterile PBS intraperitoneally. Ani-

mals were monitored for temperature fluctuations and behavioral changes every 30 minutes until 6 hours post-injection. Animals were then sacrificed by cervical dislocation, then spleen, peritoneal lavage and leg bones were removed. The spleen was processed as per 3.3.5, peritoneal lavage as per 3.3.4, and leg bone as per 3.3.6 before being frozen at -80°C. All *in vivo* experiments were performed with the supervision of a certified animal handler.

3.3.8 MACS Cd11b and F4/80 cell magnetic selection

Cells from the peritoneum, spleen or blood were washed with MACS buffer, and incubated with FC blocker (Miltenyi Biotec) for 10 minutes before incubation with CD11b microbeads (Miltenyi Biotec) for a further 15 minutes. The cells are washed once with MACS buffer, before passing through an MS column (peritoneum and blood) or LS column (spleen)(Miltenyi Biotec). The column was washed twice with MACS buffer, before a plunger was used to extract the selected cells, for downstream applications.

3.4 Cell Culture

3.4.1 Immortalised BMDMs

Immortalised BMDMs were generated as previously described[101]. Cells were grown in DMEM with 10% FCS and antibiotics in flasks. Cells were passaged by removing media from adherent cells, washing cells with PBS, then incubating adherent cells with Trypsin-EDTA (Invitrogen/Gibco) for 5 min at 37°C. Cells were then collected with addition of DMEM with 10% FCS and antibiotics, spun in a centrifuge at 300g for 5 minutes, and diluted with fresh DMEM with 10% FCS and antibiotics in new flasks.

3.4.2 Immortalised MEFs

A pregnant mouse with embryos between 13.5 and 14.5 days was euthanized with CO_2 asphyxiation, and the uterus was removed in a sterile hood to a dish with sterile BBS on ice. The embryos were removed from the uterus and washed thoroughly with PBS, then the heads and all red matter were removed. The remainder was finely minced with sterile scalpels and incubated with Trypsin-EDTA for 5 minutes. DMEM with 10% FCS and antibiotics was added to stop Trypsin reaction, the mixture was spun at 300g for 5 minutes, and then the cells were resuspended in fresh DMEM with 10% FCS and antibiotics, then incubated in a flask overnight. The following day, adherent cells were washed with PBS, and then collected with Trypsin-EDTA, before being plated into 2 wells of a 6 well plate, one diluted at 1/4 and the other well at 1/6

dilution. 1µl GeneJuice transfection reagent was mixed with 2µg of SV40-T antigen expressing plasmid (donated by Michael Gantier) in 100µl of Optimem for 20 minutes, before being added to the MEF cells and incubated overnight. The next day, cells were washed with PBS and fresh DMEM with 10% FCS and antibiotics was added. Cells were allowed to grow until confluent and then split into flasks. After growth of cells in flasks is to confluency again, the cells are immortalised and can be frozen and used for experiments.

3.4.3 MEF cells

MEF cells were grown in DMEM with 10% FCS and antibiotics in flasks. Cells were passaged by removing media from adherent cells, washing cells with PBS, then incubating adherent cells with Trypsin-EDTA (Invitrogen/Gibco) for 5 min at 37°C. Cells were then collected with addition of DMEM with 10% FCS and antibiotics, spun in a centrifuge at 300g for 5 minutes, and diluted with fresh DMEM with 10% FCS and antibiotics in new flasks.

3.4.4 Virus generation

$4x10^5$ HEK 293T cells were plated into a well of a 6 well plate, and left to rest overnight at 37°C in an incubator. The next day, cells were transfected with 100ng VSV-G plasmid, 1µg of gag-pol plasmid, and 2µg of vector plasmid, using 8µl of GeneJuice transfection reagent and 110µl of optimem. The following day, cells were observed for colour tag production (if any) to confirm transfection, and media was removed and replaced with DMEM 30% FCS and antibiotics, then left overnight at 37°C in an incubator. The following day, the viral supernatant was collected with a blunt needle and syringe, and filtered through a 0.45µm filter. This filtered supernatant can now be used to infect a target cell. Plasmids maps are in Fig 3.

3.4.5 BMDM virus infection

BM of an animal is prepared as previously described in 3.3.6 and is plated into 3 T75 flasks. 2 days later, 10ml of viral supernatant from 3.4.4 is given to each flask, supplemented with 10ng/ml M-CSF or 20% volume L929 conditioned media, as desired. The following day, the media is removed, and the cells are washed with PBS before replacing the media with normal DMEM with 10% FCS, antibiotics, and M-CSF or L929 supplements. The BMDMS are allowed to differentiate until day 7 after initial plating, collected as described in 3.3.6 and experiments are performed.
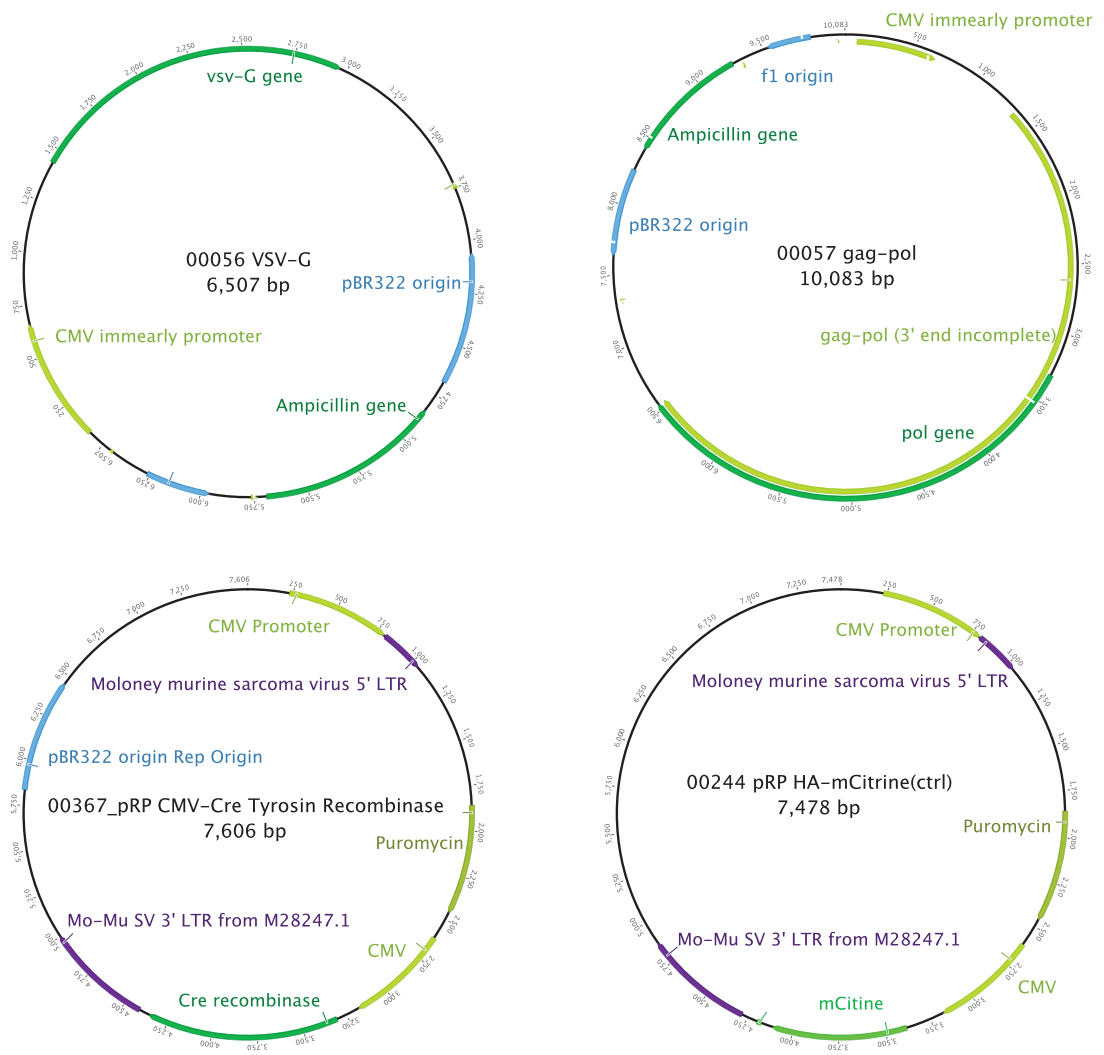
Figure 3:
Plasmid maps. Plasmids used to generate virus. See 3.4.4 for protocol used.

Name	Sequence
NC1 ZEN AMO	5'-GCGUAUUAUAGCCGAUUAACG-3'
miR-17-5p ZEN AMO	5'-CUACCUGCACUGUAAGCACUUU-3'
miR-18-5p ZEN AMO	5'-CUAUCUGCACUAGAUGCACCUU-3'
miR-19a-3p ZEN AMO	5'-UCAGUUUUGCAUAGAUUUGCAC-3'
miR-19b–1-3p ZEN AMO	5'-UCAGUUUUGCAUGGAUUUGCAC-3'
miR-92a-3p ZEN AMO	5'-ACAGGCCGGGACAAGUGCAAU-3'
RD	5'-UAACACGCGACAGGCCAACUU-3'
B-406AS-1	5'-UAAUUGGCGUCUGGCCUUCUU-3'

Table 2: *AMO and immunostimulatory sequences.*

3.4.6 AMOs and transfection

AMOs were purchased from Integrated DNA Technologies (IDT) with ZEN modifications to pre-vent exonuclease digestion and 2'OMe modifications to each base. Stocks were stored at 50µM in Duplex buffer, and diluted to 4µM before use. RD control ssRNA and B-406AS-1 are not made with ZEN or 2'OMe modifications. RD and B-406AS-1 stocks are at 80µM.

AMOs were transfected into cells with DOTAP (Roche). AMO was first diluted in 32µl DMEM, and 1.05µl DOTAP was mixed and incubated in 37µl DMEM in parallel, and incubated both separately for 5 min. Mix both solutions and incubate for a further 10 minutes, before adding 25µl of this to a well of a 96 well plate, with 80×10^3 BMDMs in 150µl of DMEM.

To stimulate TLR7, mix 1.35µl of 80µM B-406AS-1 in 37µl DMEM, and 4.75µl DOTAP in 33µl DMEM in parallel, and incubate both separately for 5 minutes. Mix both together, incubate for a further 10 minutes, before adding 25µl to a well of a 96 well plate with BMDMs and AMOs.

MEF cells were transfected using a reverse transfection method. 1.35µl Lipofectamine 2000 (Invitrogen) was diluted in 150µl Optimem and 1.5µl of 4µM AMO was added. This mixture is incubated for 20 minutes, before 50µl was pipetted per well of a 96 well plate. Then 150µl of DMEM with 8×10^3 MEF cells were pipetted on top, and incubated overnight in an incubator.

3.4.7 Actinomycin D

Cells were cultured as previously described (3.3.6) and stimulated with LPS for indicated times. Actinomycin D (Sigma) was diluted for a final concentration of 5µg/ml in media and LPS was incubated with the cells for the indicated times.

3.5 Biochemistry

3.5.1 ELISAs

Mouse IL-6 and TNFa ELISAs were purchased from BD Biosciences. NUNC Maxisorp plates were coated with 50 µl Capture antibody diluted in PBS overnight at room temperature. Plates were blocked with 1% BSA in PBS for 1 hour, then supernatants and standard dilutions were added for 2 hours at room temperature. 50µl of detection antibody in 1% BSA PBS were then incubated for a further 2 hours, before a working dilution of 50µl Streptavidin-HRP in 1% BSA PBS was added for 20 minutes. Between each step, plates were washed with 0.05% TWEEN-20 PBS using an automated washer. 50µl of TMB substrate was used to develop the ELISA, and the reaction was stopped with 1M Sulfuric Acid and absorbances at 450nm and 570nm were read using a Spectramax i3.

3.5.2 Western blots

Protein lysates were prepared from cells using RIPA or laemmli buffer, supplemented with phosstop and proteinase inhibitors (Sigma-Aldrich). Lysates were frozen at -20°C for storage, and were then thawed on ice for use. Supernatants were spun at maximum speed, 4°C in a centrifuge to pellet nucleic acid material. If lysed with RIPA, the protein diluents were added to appropriate dilutions of NuPAGE LDS buffer (4x) and Reducing agent (10x). The lysates of either laemmli or RIPA are then heated at 90°C for 10 minutes. Heated protein lysates were then loaded into well of a NuPAGE™ 4-12% BIS-TRIS gels (Invitrogen), and run using MOPS running buffer, at 100v for ~1.5-2 hours, or until the protein front reached the bottom of the gel in a XCell SureLock™ Mini-Cell Electrophoresis System (Invitrogen). Ladder used was a PageRuler™ Plus Pre-statined Protein (ThermoFisher). The separeted proteins were then transferred to a PVDF membrane using a wet TRIS-Glycine transfer system in an XCell II™blot module (Invitrogen), at 32V for 1.5 hours. Membranes were then blocked with 3% BSA TBS for 1 hour at room temperature, before incubation with primary antibodies overnight at 4°C. Membranes were washed with 0.1% TWEEN-20 TBS before incubation with a fluorescent secondary antibody for 2 hours. Membranes were washed again and then imaged using a LI-COR Odyssey device. Quantification was performed using the ImageStudioLite software from LI-COR. For antibodies

Antibody name	Company	Product no.	Use
A20/TNFAIP3 (D13H3) Rabbit mAb	Cell Signaling	5630S	Western Primary
β-Actin Mouse Monoclonal Antibody	Li-Cor	926-42212	Western Primary
Phospho-NF-κB p65 (Ser536) (93H1) Rabbit mAb	Cell Signaling	3033S	Western Primary
IRDye 800CW Donkey Anti-Rabbit IgG (H+L)	Li-Cor	926-32213	Western Secondary
IRDye 680LT Goat anti-Mouse IgM (mu chain specific), 0.1 mg	Li-Cor	925-68080	Western Secondary
Anti-NK1.1-APC, mouse	Miltenyi Biotec	130-095-869	FACS
BV510 Rat Anti-Mouse B220/CD45R Clone RA3-6B2	BD	563103	FACS
CD8a-FITC, mouse (CD8)	Miltenyi	130-091-605	FACS
Anti-Mouse CD3e PE-Cyanine7	eBioscience	25-0031-81	FACS
CD4 Monoclonal Antibody (OKT4 (OKT-4)), PerCP-Cyanine5.5	eBioscience	45-0048-42	FACS
BV421 Rat Anti-Mouse CD62L Clone MEL-14	BD	562910	FACS
APC-Cy7 Rat Anti-Mouse CD16/CD32 Clone 2.4G2	BD	560541	FACS
PerCP-Cy™5.5 Rat Anti-Mouse Ly-6C Clone AL-21	BD	560525	FACS
Pe/Cy7 anti-mouse Ly6G (1A8)	Biolegend	127618	FACS
Anti-Mouse CD11b PE	eBioscience	12-0112-81	FACS
BV421 Armenian Hamster Anti-Mouse CD11c Clone N418	BD	565451	FACS
Anti-mouse I-A/I-E (MHCII) (clone M5/114.15.2)	Biolegend	107627	FACS

Table 3: *FACS and Western Blot Antibodies*

used, refer to table 3.

3.5.3 CTB assay

CellTiter-Blue® Cell Viability Assay (Promega) was aliquoted and stored at -20˚C. 10μl of CTB reagent was diluted in 50μl of Complete DMEM per well of a 96 well plate. To perform the assay, media was removed from the cells in culture, and 50μl of diluted CTB reagent/Complete DMEM was put onto the cells. Cells were incubated for a further 1 hour at 37˚C before measuring the fluorescence with excitation of 560nm and emission of 590nm.

3.5.4 Seahorse cellular metabolism assay

Cells were plated into a special Agilent Seahorse XF 96-well plate, and treated according to the experiment. The cells are then washed thoroughly three times with assay medium, before resting for 1 hour in a non-carbonated incubator. The 4-port injector plate is prepared with 20μl 100mM Glucose, 22μl oligomycin, 25μl FCCP and 27μl Antimycin A / Rotenone. Assay was performed on a Agilent Seahorse XFe96. Thanks to Mario Lauterbach for operating the device.

For the analysis, the average of the three readings between treatments was used. For Basal Glycolysis: ECAR(Glucose-null), glycolytic capacity: ECAR(Glucose-null), Spare glycolytic reserve: ECAR(oligo-glucose), ATP production: OCR(null-oligo), Maximum respiration: OCR(FCCP-AA/ROT), Basal Respiration: OCR(null-AA/ROT).

3.5.5 Magpix multiplex cytokine assay

Samples were diluted 1:1 with with universal assay buffer, with guidance from Christian Kolbe and Mario Lauterbach. Beads coated in antibodies were washed twice before incubating with either the standard or with diluted samples. After a 2 hour incubation, 100µl of detection antibody mix was added to each well, and incubated for a half an hour. Streptavidin-PE was then added to the beads, and incubated for half an hour again, before being washed, resuspended and then detected on a Luminex MAGPIX®

3.6 RNA, cDNA and qRT-PCR

3.6.1 RNA preparation

Samples are lysed using 350µl of Qiazol, and homogenised, before freezing at -80°C. Frozen samples are thawed and then RNA is isolated using the miRNeasy kit (Qiagen) following the manufacturers instructions, and gDNA is digested using the on column DNAse protocol of Qiagen.

3.6.2 mRNA cDNA preparation

500ng of RNA per sample, or a pool of all samples is mixed in a volume of 12.9µl with 1µl of Oligo dT, and put on a thermocycler for 5 minutes at 65°C, before being moved back to ice for 2 minutes. Then, 4µl of 5x First strand buffer, 1µl 10mM dNTPs, 1µl 0.1M DTT, and 0.2µl SuperScript III are mixed in. The sample is put back onto the thermocycler at 50°C for 50 minutes, 85°C for 5 minutes and then put back on ice. cDNA is then diluted 1:10 with nuclease free water. qRT-PCR was performed using 5µl Maxima SYBR Green/ROX qPCR Master Mix, 2µl of mixed 2µM forward and reverse gene-specific primers, 1µl of nuclease free water, and 2µl of diluted cDNA. qPCR was performed in 10µl reactions, following the manufacturers instructions using a QuantStudio 6 Flex Real-Time PCR System from Applied Biosystems.

3.6.3 miRNA cDNA and RT-qPCR

miRNA cDNA was generated using a modified protocol of the Taqman® small RNA Assays protocol from Applied Biosystems. 1µl of up to 3 stem-loop miRNA RT primers were mixed together with Multiscribe Reverse Transcriptase (Applied Biosystems), 1.5µl of 10x buffer and 10ng of total RNA.

qPCR was performed in 10µl reactions, following the manufacturers instructions using a QuantStu-

Primer Name	Sequence	Primer Name	Sequence
mTnfaip3_RT_For	TGCCCACAGTTCCGAGAGAT	mll-6_RT_For	CAAAGCCAGAGTCCTTCAGAG
mTnfaip3_RT_Rev	TGAGGCAGTTTCCATCACCA	mll-6_RT_Rev	GTCCTTAGCCACTCCTTCTG
mFbxl11_RT_For	TTGCTGACTCCACCCACAGA	mCxcl1_RT_For	ATGGCTGGGATTCACCTCAA
mRbxl11_RT_Rev	GAGACAAAAGGGGCATGTGG	mCxcl1_RT_Rev	AGGGAGCTTCAGGGTCAAGG
mRnf11_RT_For	GCTTTCTTCCTCCCGCAGAT	pri-miR-155-RT_For	AAACCAGGAAGGGGAAGTGT
mRnf11_RT_Rev	GACTCGTGAAGCAGGGAGATG	pri-miR-155-RT_Rev	ATCCAGCAGGGTGACTCTTG
mAtg16l1-RT-Fwd	CTGGATTCAAATGCGGCTCT	pri-miR-146a-RT_For	GTGTGTATCCCCAGCTCTGA
mAtg16l1-RT-Rev	TTCCCTGTCAGCACACTCCA	pri-miR-146a-RT_Rev	CTTCACCCCACTCTCTCCAC
mll-10_RT_For	AAGCATGGCCCAGAAATCAA	mHprt_RT_For	TGAAGTACTCATTATAGTCAAGGGCA
mll-10_RT_Rev	TCACAGGGGAGAAATCGATGA	mHprt_RT_Rev	CTGGTGAAAAGGACCTCTCG
mll-1b_RT_For	TTGACGGACCCCAAAAGATG	Cre_RT_For	GTTCACTCATGGAAAATAGC
mll-1b_RT_Rev	CAGCTTCTCCACAGCCACAA	Cre_RT_Rev	TATCTTTAACCCTGATCCTG
mTnfa_RT_For	CCAAATGGCCTCCCTCTCAT	mMir17hg_RT_For	ACAGAGCTAAAGTTTTCCAT
mTnfa_RT_Rev	TGGTGGTTTGCTACGACGTG	mMir17hg_RT_Rev	AATTCTGGTCACTCACAATC

Table 4: *qRT-PCR Primers*

dio 6 Flex Real-Time PCR System from Applied Biosystems. A list of qRT-PCR primers is found in Table 4.

3.6.4   Lexogen 3' sequencing.

Samples were prepared using the QuantSeq 3' mRNA-Seq Library Prep Kit FWD for Illumina (Lexogen) by the NGS Core Facility, Institute of Human Genetics, Division of Genomics at the university of Bonn. Sequencing was performed to 20 million reads per sample, and data was analysed using Partek Flow. The pipeline for the analysis was provided by Dr Simit Patel, Partek. Briefly, the reads provided with the adapters trimmed from the NGS Core Facility, then were aligned using STAR 2.5.3a, the genes and transcripts were quantified to Ensemble mm10 whole genome, and the normalisation and analysis was performed using DESeq2[102]. Genes with ≤1 read count were excluded from further analysis. Volcano plots were created using FDR-stepup corrected p-values.

3.7   Nanostring

3.7.1   Nanostring Elements

Master stocks of Probes A and B were prepared according to the Manufacturer's guidelines. 5µl of each Probe A stock (1µM) or Probe B (5µM) were pipetted, and TE buffer was added to make a final volume of 1ml. 2µl of this was aliquoted into microfuge tubes and frozen at -80°C as single use tubes, yielding a final concentration in the Master Probe A stock of 5nM each, and 25nM in

the Master Probe B stock. For each set of 12 samples, 14.5µl of 0.1% TE-TWEEN was added to the aliquoted Master Probe A and B stocks, which are now at 30x Working concentrations of 20pM and 3nM respectively.

3µl of total cell lysate (10,000 mouse BMDMs, or 20,000 human PBMCs per µl) in RLT buffer with βME, or 100ng of total RNA extracted using the miRNeasy kit (Qiagen) was incubated with 13µl of 30x Working Probe A and 13µl of 30x Working Probe B, with hybridisation buffer, following the manufacturer's instructions for 24 hours at 67˚C, and a lid temperature of 72˚C. 24 hours was chosen because the manufacturer's Package Insert claims and increase of 5% in target counts per hour up to 24 hours without increase in background signal[1]. Following hybridisation the samples were moved to the Nanostring Prep Station immediately for processing.

3.7.2   Nanostring miRNA

100ng of total RNA was prepared as outlined in 3.6.1 and then diluted to 33ng/µl using nuclease free water. miRNAs were then hybridized and ligated to nCounter miRNA Tag Reagents as per the manufacturer's instructions. Following ligation, the samples are then hybridized with the Reporter CodeSet and Capture ProbeSet for a minimum of 16 hours, before immediately proceeding to use the Nanostring Prep Station.

3.8   Nanostring Normalisation and Data processing

3.8.1   Nanostring Elements

Analysis was done using the nSolver 4.0 (alpha build) software, a gift from Dr Maik Pruess of Nanostring. Raw data was imported as .RCC files, and data was manually inspected for quality control flags, binding density and technical performance before proceeding. Background subtraction was performed using the geometric mean of included negative controls. Then positive Control Normalisation was done using the geometric mean of the positive controls (for technical normalisation of the samples for assay performance), and then finally Content normalisation was done using Rpl19, Hprt, Actb, Gapdh, and Eef1g.

---

[1]nCounter Elements General Purpose Reagents Package Insert, Version 03, created 2013-12, Ref LBL-C0266-03.

Data was then exported from nSolver 4.0 (alpha build) software as log2 counts, and then opened in Microsoft Excel. Removal of low counts before analysis was done previously by other groups[103]. For the purposes of our own analysis, a mean of the values for a gene across all samples was identified, and all genes with an average detection below the highest negative control were excluded from subsequent analysis. Furthermore, all ratio-metric comparisons of unstimulated to stimulated conditions must take into account if the gene was not detected in unstimulated conditions (such as Il-6 and Il-1b).

3.8.2   Nanostring miRNA

Analysis was done using the nSolver 4.0 (alpha build) software, a gift from Dr Maik Pruess of Nanostring. Raw data was imported as .RCC files, and data was manually inspected for quality control flags, binding density and technical performance before proceeding. Background subtraction was performed using the geometric mean of included negative controls. Then positive Control Normalisation was done using the geometric mean of the positive controls (for technical normalisation of the samples for assay performance), and then finally Content normalisation was done using the geometric means of the included Reference genes; *Actb, B2m, Gapdh* and *Rpl19*.

Data was then exported from nSolver 4.0 (alpha build) as log2 counts and ranked according to expression in the WT samples. Batch correction was performed in Partek for date of processing.

3.8.3   Partek Analysis

Log2 counts of data is imported to Partek, PCA analysis is performed for uniformity of data, and batch corrections made if necessary. Two-way ANOVA was performed, and multiple test corrected using FDR step-up. Volcano plots were then created with these p-values.

3.8.4   Partek miRNA analysis

Log2 counts of data is imported to Partek, PCA analysis is performed for uniformity of data, and batch corrections made if necessary. Batch corrected data was exported to Prism for graphing

of individual miRNA, and analysis using Tukey's multiple correction test. In Partek, two-way ANOVA was performed, and multiple test corrected using FDR step-up, for all conditions. Volcano plots were then created with these p-values. miRNA lists were created from analysis of interest, and a gene list is created using Partek's in-built feature to search Targetscan.org for predicted targets of miRNA identified in the list. This gene list is then used in Partek to search for pathway enrichment.

3.9   iCLIP

The original protocol is from Huppertz et al[104], and adapted by Tim Sadlon. Minor alterations were made with guidance by Dr Kate Jeffrey.

In brief, $3x10^7$ cells were cross-linked with UV irradiation (Biol-link 254, Vilber), collected, and the cell pellet was frozen. The pellet was lysed and treated with RNAse I briefly to shorten RNA molecules, before immediately stopping. Samples were then immunoprecipatated with Dynabeads™ Protein A (ThermoFisher, 10001D) with Pan-AGO antibody (Diagenode, Clone 2A8, C15200167) or IgG control (Jackson Immunoresearch, 315-005-008). Cross-linked immunoprecipitated RNA was then 3' de-phosphorylated and an L3 adaptor ligated. The 5' end was labelled with ^{32}p-γATP, and a western blot was performed using a 4-12% BIS-TRIS gel. The protein as cross-linked RNA were transferred to a nitrocellulose membrane before phosphorimaging to ensure transfer. Using the image as a guide, small sections of each sample were cut out of the membrane corresponding to the weight of AGO, and treated with proteinase K to digest the protein and release the RNA from the membrane. The RNA is then isolated and cDNA is made using RT primers containing Illumina sequencing barcodes. The cDNA is then purified using a urea gel, before circularising the cDNA, and then incubated with Cut_oligo to form a double-stranded molecule over an inserted BamHI site. This BamHI site is then cleaved, and the newly linearized cDNA libraries can then amplified and sent for sequencing.

Sequence Name	Sequence
RT -2	5'Phos/NNACAANNNAGATCGGAAGAGCGTCGTGgatcCTGAACCGC
RT -6	5'Phos/NNCCGGNNNAGATCGGAAGAGCGTCGTGgatcCTGAACCGC
RT -10	5'Phos/NNGACCNNNAGATCGGAAGAGCGTCGTGgatcCTGAACCGC
RT -15	5'Phos/NNTATTNNNAGATCGGAAGAGCGTCGTGgatcCTGAACCGC
Cut_oligo	GTTCAGGATCCACGACGCTCTTCaaaa
P5	5'-AATGATACGGCGACCACCGAGATCTACACTCTTTCCCTACACGACGCTCTTCCGATCT-3'
P3	5'-CAAGCAGAAGACGGCATACGAGATCGGTCTCGGCATTCCTGCTGAACCGCTCTTCCGATCT-3'
L3 adaptor	5rApp/AGATCGGAAGAGCGGTTCAG/3ddC/

Table 5: *Sequences used for iCLIP.*

4 Results

4.1 Decrease of Cytokines following miR-17-92 modulation

miR-19 of the miR-17-92 cluster has been previously shown to inhibit many regulators of NF-κB and inflammation [40, 96, 42]. *In silico* analysis of miRNA interaction between members of the miR-17-92 cluster and other known regulators of inflammation indicate that the majority of regulation is likely due to miR-19. To get an idea of the scale of potential regulation by the miR-17-92 cluster of genes involved in inflammation in mouse, the predicted targets of each family of the cluster was collected from TargetscanMouse and compiled in the table 6. By filtering for genes with known regulatory effects of inflammation, it becomes clear that any effect will be mostly driven by miR-19 and miR-17 families of miRNA. While it is important to note that these are *in silico* predictions, many interactions have already been published (indicated by the *, further references in Supplementary Table 9). Of important note, most of these publications featured regulating these miRNA families in B cells, T cells and epithelial cells mostly, or showed data that was cell-agnostic by using artificial means such as luciferase assays to indicate gene regulation by miRNA.This has led to a shift in focus from expecting the physiological effect of a miRNA being related to modulation of a single gene to understanding that it is likely the augmentative effect of a miRNA regulating many genes within a pathway [40].

To confirm that decreasing the levels of miR-17 and miR-19 could also decrease the release of cytokines, MEF cells were transfected with AMOs against miR-17, miR-19a and -19b, or non-targeting control, and then stimulated with low doses of either LPS or PAM3csk4, previously found to be the EC_{50} dose for these cells. Figure 4 shows that IL6 release was reduced, and the cell viability was not affected by transfection of AMOs. Importantly, this is the first indication that the response to TLR4 is also reduced, indicating that, with previous results from TNF stimulation, the modulation of response by miRNA is not receptor specific, but rather affecting multiple mechanisms of NF-κB activation. There is also no significant modulation of cell viability, if ever the cells are more viable when the miRNA are inhibited.

To further investigate this, differentiating miR-17-92fl/fl BMDMs were infected with virus expressing Cre recombinase to induce recombination of the miR-17-92 cluster, and were grown for a further 4 days to allow for reduction of mature miRNA, as it has been shown that mature miRNA are very stable and require several days to be reduced significantly [106]. Stimulation with several TLR ligands resulted in reduced release of Tnfα, compared to control virus infected

	miR-17/20a	miR-18a	miR-19a/b	miR-92a
Tnfaip3*		7mer(1)	8mer(1) 7mer(1)	
Rnf11*			8mer(2)	
Fbxl11*	8mer(1) 6mer(1)	8mer(1) 6mer(1)	7mer(2)	
Cyld*			7mer(2) 6mer(1)	
Atg16l1*	8mer(1) 6mer(1)		7mer(2)	
Otud7b			8mer(1)	
Tnip1			8mer(1)	
Itch*	7mer(1)		7mer(1)	
Zfand4	8mer(1) 6mer(4)			
Zfand5			7mer(1)	
Zfand6			7mer(1)	
Ikzf1*			8mer(1)	
Ikzf4*	8mer(1) 7mer(1) 6mer(3)			8mer(1) 6mer(1)
Socs1*			8mer(1)	
Socs3*			8mer(1) 6mer(1)	
Socs5		7mer(1)	7mer(1)	7mer(1)
Socs6*	7mer(2)		7mer(1) 6mer(1)	8mer(1)
Tax1bp1		8mer(1) 6mer(3)	8mer(1) 7mer(2) 6mer(1)	
Hif1a*	7mer(2) 6mer(1)	7mer(1) 6mer(1)	7mer(1)	7mer(1) 6mer(1)
Pten*	8mer(1) 7mer(2) 6mer(2)	7mer(2) 6mer(1)	8mer(1) 7mer(1) 6mer(1)	
Fxr1	7mer(1) 6mer(2)		7mer(1) 6mer(1)	8mer(1)
S1pr1*	8mer(1) 7mer(2)		8mer(1) 7mer(2)	7mer(1) 6mer(1)
Bcl2l11*	8mer(1) 7mer(1) 6mer(3)		7mer(2)	8mer(1) 7mer(1)
Klhl20	7mer(2) 6mer(3)	7mer(2)	8mer(1) 7mer(2) 6mer(1)	

Legend: 8mer · 7mer · 6mer

Table 6:

Targetscan predicted targeting by the miR-17-92 cluster. A representation of regulators of NF-κB and inflammation are targeted by various members of the miR-17-92 cluster. The number and strength of the MRE is represented from Targetscan data [105], including both conserved and non-conserved sites within the mouse transcriptome used only. Validated targets of one or more members of the miR-17-92 cluster are marked with an *. See Table 9 for references.

Figure 4:

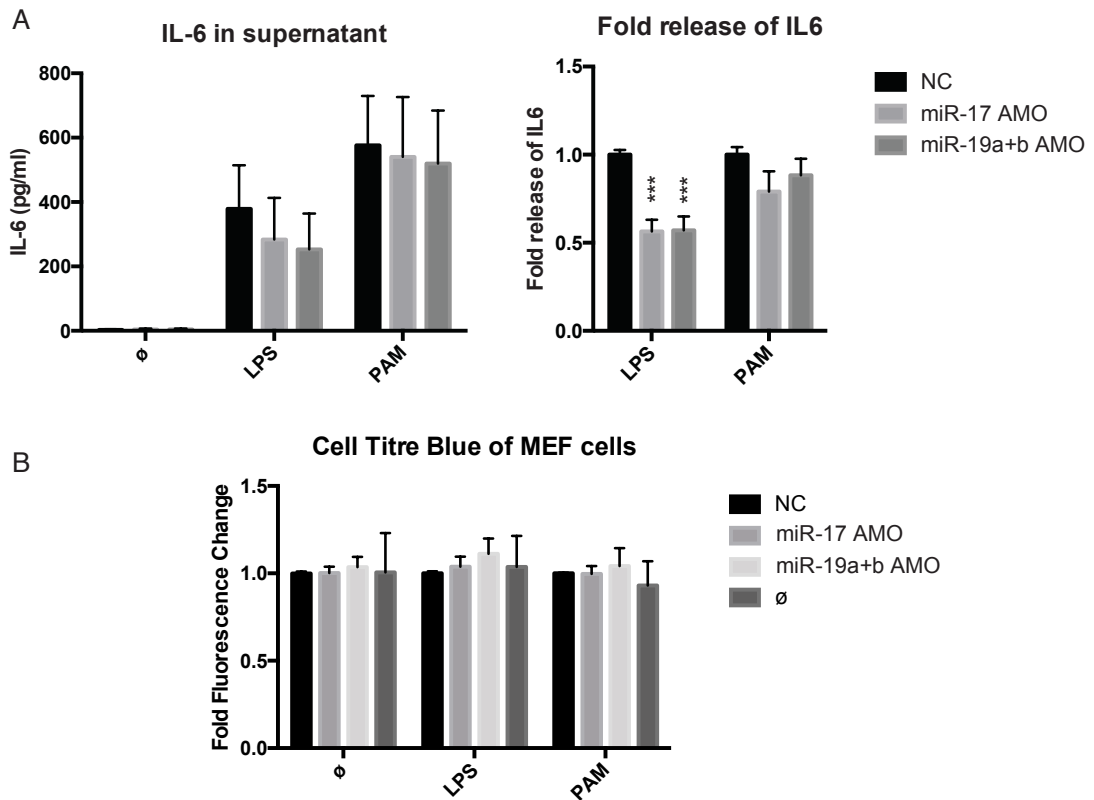***Modulation of IL6 from MEF cells with reduced miRNA.*** **A.** IL-6 measured from supernatants following stimulation with LPS or PAM3csk4. Both raw and fold change are depicted here. **B.** CTB assay was performed to measure cell viability. Values are means with SEM of three independent experiments. Two-way ANOVA was performed comparing the RD control, with Dunnett's multiple comparisons test, and an alpha set to 0.05.
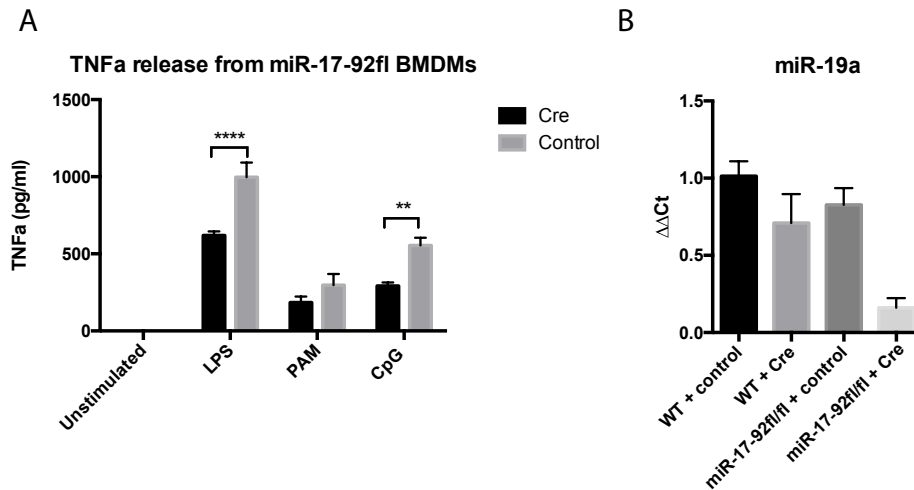
A

TNFa release from miR-17-92fl BMDMs

B

miR-19a

Figure 5:

Reduced mTnfα release from miR-17-92fl/fl-Cre BMDMs. **A.** Tnfα release from BMDMs following miR-17-92fl recombination. BM was differentiated in M-CSF media after infection with either Cre-recombinase virus or mCitrine control virus with and stimulated for 8 hours. **B.** miR-19a expression from samples in A. Mean and SEM of 3 independent experiments. Two-way ANOVA was performed, with Dunnett's multiple comparisons test, and an alpha set to 0.05.

miR-17-92fl cells (Figure 5).

4.2 Generation of miR-17-92 mø-specific transgenic mice.

4.2.1 CD11b-Cre

The miR-17-92 cluster is a critical cluster for growth and development of an organism. This was demonstrated by the initial attempt to make a KO mouse, where mice born as miR-17-92$^{-/-}$ died within minutes of birth, with hypoplasia of the heart and lungs [37]. This raises several points about the critical role that this miRNA cluster plays in the development of an organism, and not just its role in cancer or immunity. In order to modify the expression of these miRNA after birth of the animal, a Cre-recombinase approach was employed. The most obvious, allowing for any cell in the body would be an inducible-cre model, such as the Esr1^{Cre}. Unfortunately, tamoxifen has known interactions with the immune system, and so the Esr1^{Cre} animal would likely have non-specific effects when generating a model for immune specific model [107, 108]. It was therefore decided to use the CD11b-Cre model, which would allow for the observation of miRNA modulation in macrophages and microglial cells [109].

To breed these animals, miR-17-92fl/fl mice was paired with a Cd11b-Cre mouse, both of the BL/6 backgrounds. Then, using the miR-17-92$^{+/fl}$- Cd11b-Cre$^{+/-}$ of the F1 generation to then breed back with the miR-17-92$^{fl/fl}$resulted in 50% of the F2 generation with a homozygous expression for miR-17-92$^{fl/fl}$, and of those, half were CD11b-Cre$^{+/-}$. These mice were use for further breeding with mice of the miR-17-92$^{fl/fl}$background, and Cd11b-Cre was kept to heterozygous expression in only 50% of the offspring. This would allow for the generation of mice that could be littermate controls to miR-17-92$^{fl/fl}$- Cd11b-Cre$^{+/-}$mice. Furthermore, by design, the level of Cre recombinase is kept to a minimum to avoid known Cre toxicity effects [110, 111].

However, initial testing of the mice BMDMs indicated that there was no deletion of the miR-17-92 cluster, as there were equivalent mature miRNA amounts between either CD11b-Cre+ mice, and their CD11b-Cre- littermates. The cells were then tested for the expression of Cre recombinase and there is no discernible difference between the two mice, indicating that the lack of Cre expression is the cause of the fault. Figure 6 show that the levels of miRNA were the same when tested by qPCR, and that there is a lack of Cre expression, especially compared to the later generated miR-17-92$^{fl/fl}$ - LysMCre mice. These results were echoed by a study published subsequently from another group attempting to measure Cre recombinase genetic manipulation using the CD11b-Cre transgenic mice, indicating that it is a unreliable model for myeloid specific deletion of target genes [112]. In conclusion, the CD11b-Cre model was unable to delete the miR-17-92 cluster in BMDMs, and so what not used further.

4.2.2   miR-17-92fl/fl - LysMCre

After failing to successfully produce macrophages with a reduced miR-17-92 expression using the CD11b-Cre mice, a new breeding program was set up using the well established LysM-Cre mouse. While this model will not allow for myeloid deletion of the miR-17-92 cluster, it has been used successfully in several other miRNA studies [66]. Breeding followed the same pattern and reasoning as the miR-17-92$^{fl/fl}$ - CD11b-Cre$^{+/-}$ animals, (hereafter referred to as miR-17-92$^{\Delta}$, and littermate controls as WT, unless otherwise stated) with the F2 generation being used to maintain the line for experiments. This new animal genotype was much more successful at deleting the miR-17-92 cluster in BMDMs and in peritoneal cells, as shown in figure 7. Interestingly, the effectiveness of Cre-driven miRNA deletion appeared to be more
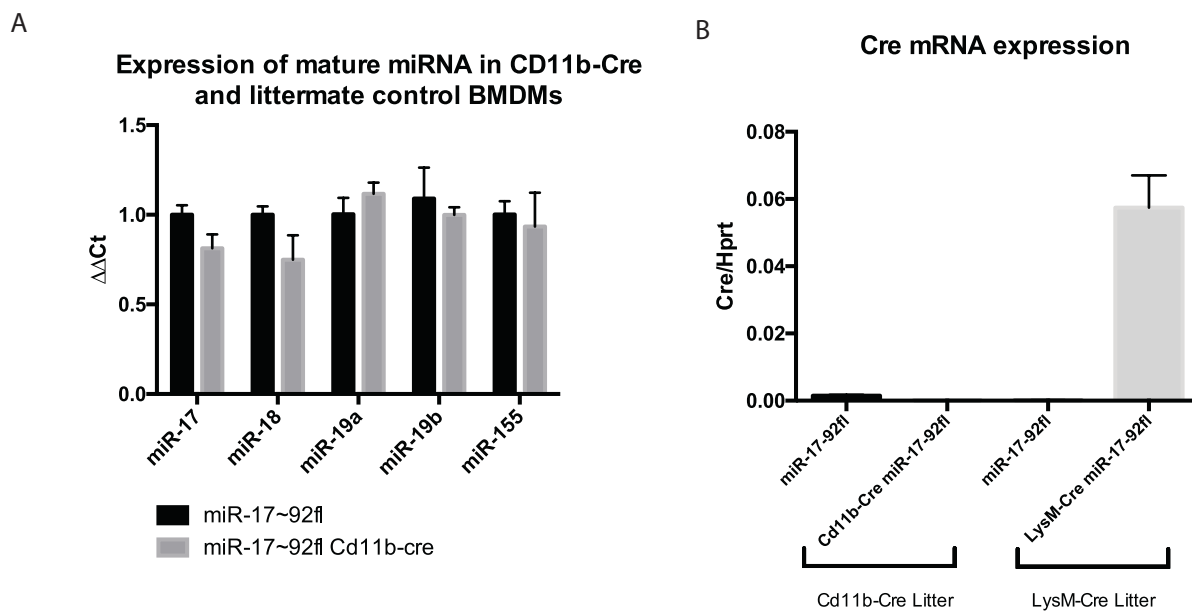
A

Expression of mature miRNA in CD11b-Cre and littermate control BMDMs

B

Cre mRNA expression

Figure 6:

Expression of miRNA and Cre recombinase in CD11b-Cre expressing BMDMs. **A.** The expression of mature miRNA from BMDMs from miR-17-92fl/Cd11b-Cre and littermate control mice was determined with qPCR. The expression of miRNA was not significantly different between the two genotypes, indicating that the miRNA expression was unchanged in the CD11b-Cre mice. **B.** The expression of Cre recombinase mRNA was determined using qPCR, and using LysM-Cre expressing mice as positive controls, it is evident that the CD11b-Cre BMDMs did not express Cre recombinase, hence had not recombined the miR-17-92fl locus.
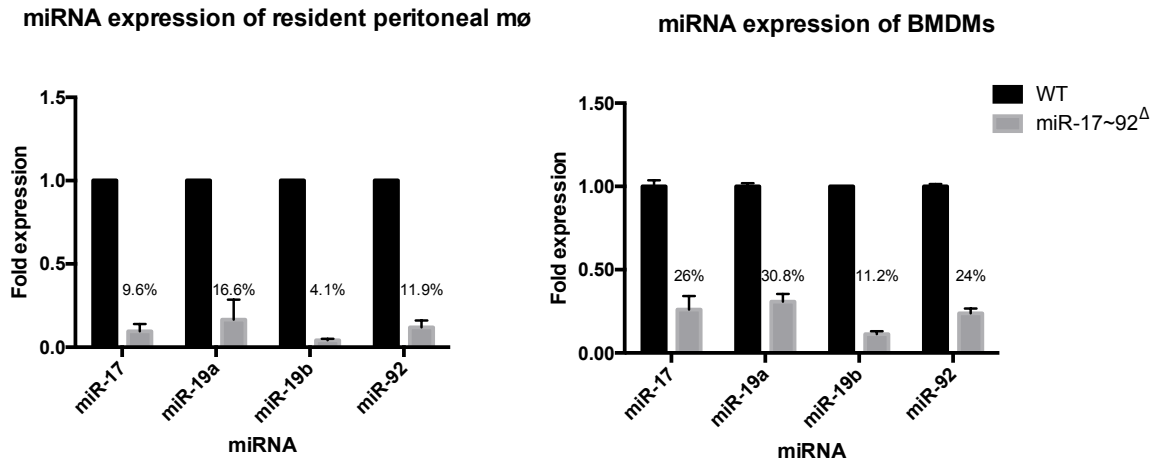
miRNA expression of resident peritoneal mø

miRNA expression of BMDMs

Figure 7:

miRNA expression in miR-17-92fl/fl$^\Delta$ Macrophages. Expression of miRNA determined by qPCR of BMDMs and Peritoneal cells and bone marrow, showing steady deletion of the miRNA cluster. Data is of 3 independent experiments, with data normalised to the WT.

complete in the peritoneal cells than in the BMDMs. This may be in part due to how old the cells are. As previously noted, mature miRNA are often long-lived molecules, and so when deleted, may take several days to be reduced further, not to mention that Cre-recombination in an incomplete activity [113, 106, 114].

When investigating the kinetics of miRNA deletion using LysM-Cre, it was noted that the expression of several miRNA from the miR-17-92 cluster were not changed in the bone marrow of mice, but rather only after differentiation into BMDMs using L929 conditioned media. Figure 8 outlines this transition, and also shows that the expression of miR-19b and miR-92 are decreased slightly in the WT BMDMs compared to their progenitor bone marrow. This is expected, as is has been previously published that the expression of the miR-17-92 cluster must be down-regulated in a PU.1-dependant manner for proper macrophage maturation [115].

Mice were also born with normal ratio of genders and with normal ratio of LysM-Cre$^{+/-}$ to $^{-/-}$ mice, with a slight tendency towards LsyM-Cre$^{-/-}$. No developmental abnormalities were observed, mice behaved the same, and no visual differences could be detected between mice.

Next, to investigate the specificity of deletion in tissues, the blood, spleen and peritoneal lavage were harvested from mice and digested to single cells suspensions if necessary, before magnetically enriching CD11b+ cells. miR-17 was used as a measure of miRNA deletion from the cluster, and it was noted that there was no observable difference between the mice in the blood
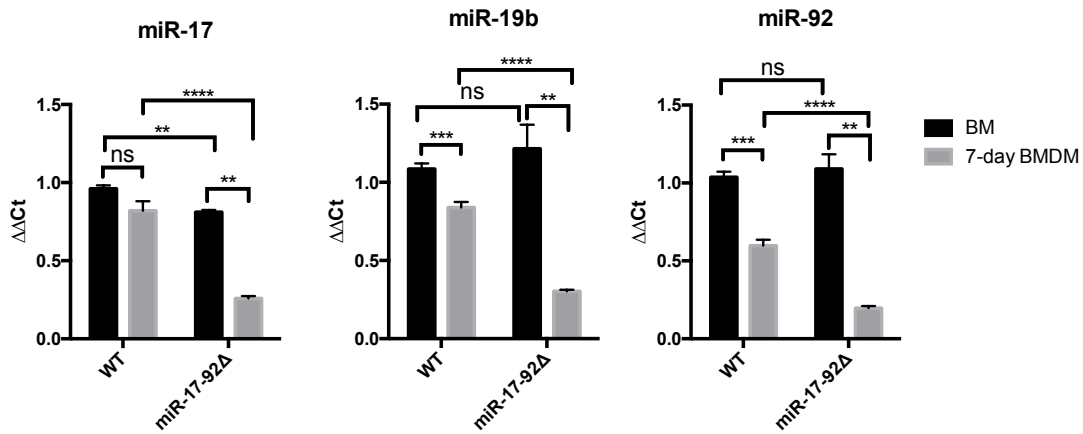
Figure 8:

Expression of miRNA decreased following differentiation of BM to BMDMs. Using L929 conditioned media to induce BM HSC to BMDM differentiation reduced the expression of miRNA of the miR-17-92 cluster, whereas M-CSF does not change them, other than miR-92. LysM-Cre however does not delete the miRNA in BM, and is only activated upon differentiation of cells to BMDMs. Mann-Whitney U test between BM and BMDMs of each genotype are performed, *P<0.05, **P<0.01, ***P<0.001 ****P< 0.0001

A

	WT	LysMCre	Total
Female	23.47%	22.07%	45.54%
Male	30.99%	23.47%	54.46%
Total	54.46%	45.54%	

B
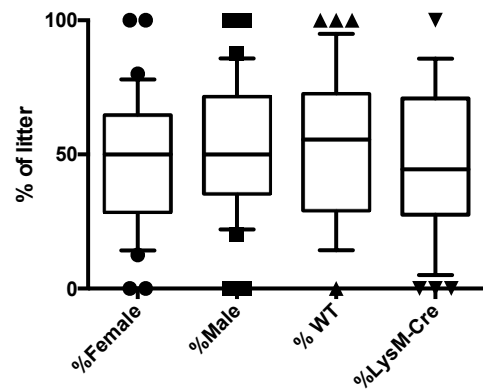
Figure 9:

Distribution of mice in litters. Data from 33 litters. **A**. Distribution of animals in the whole population, with a nearly 50% distribution of animals between both gender and genotypes, indicating that the mi-17-92fl/fl-LysM-Cre genotype does not confer a advantage to survival. **B.** Distribution of mice within litters, represented as a percentage. There is no significant difference between the distribution of female and male mice inside litters, however, more litters had a total of wt mice within them.

Ratio expression of miR-17 from mice

Figure 10:

LysM-Cre driven miRNA deletion is specific to peritoneal cells in vivo. Whole blood, spleen or peritoneal lavage cells were selected with CD11b magnetic beads, and lysed for miRNA. qPCR for mature miR-17 was perf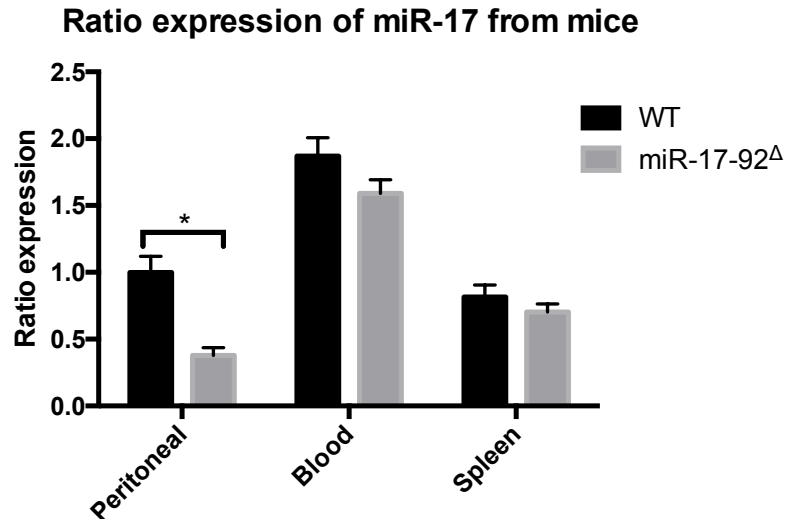ormed, and ratio expression is represented here to WT peritoneal samples. Unpaired T-tests were performed, with correction for multiple comparisons using the Holm-Sidak method.

or spleen compartments. It is entirely possible that given the mice are housed in a clean facility, mø of the spleen and circulating in the blood have not had a significant enough NF-κB activation to induce LysM expression, and by extent, LysM-Cre [116].

Investigating the cell composition of the spleen did not produce any significant differences, with perhaps slightly lower, yet insignificant amounts of T-cells and macrophages.

4.3   Response of miR-17-92$^\Delta$ BMDMs

4.3.1   Immortalisation of miR-17-92KO cell lines.

To investigate the role of the miR-17-92 cluster in macrophages, some BMDMs were harvested from two sibling mice, one miR-17-92fl/fl (WT) and the other miR-17-92fl/fl - LysM-Cre -/+ (KO). The cells are then grown in DMEM with 40ng/ml M-CSF initially, and infected with the J2Cre virus [117], to immortalise them. In Figure 12, at the beginning of the immortalisation process while the cells were still dependent on growth factors, the cells displayed a ~50% reduction in mature miRNA of the floxed cluster. However, after weening the cells off extra growth factors, the miRNA levels had equalised between the two cell populations. Genotyping of both cell types indicated that they were still the correct genotype, and the cells had not been cross-
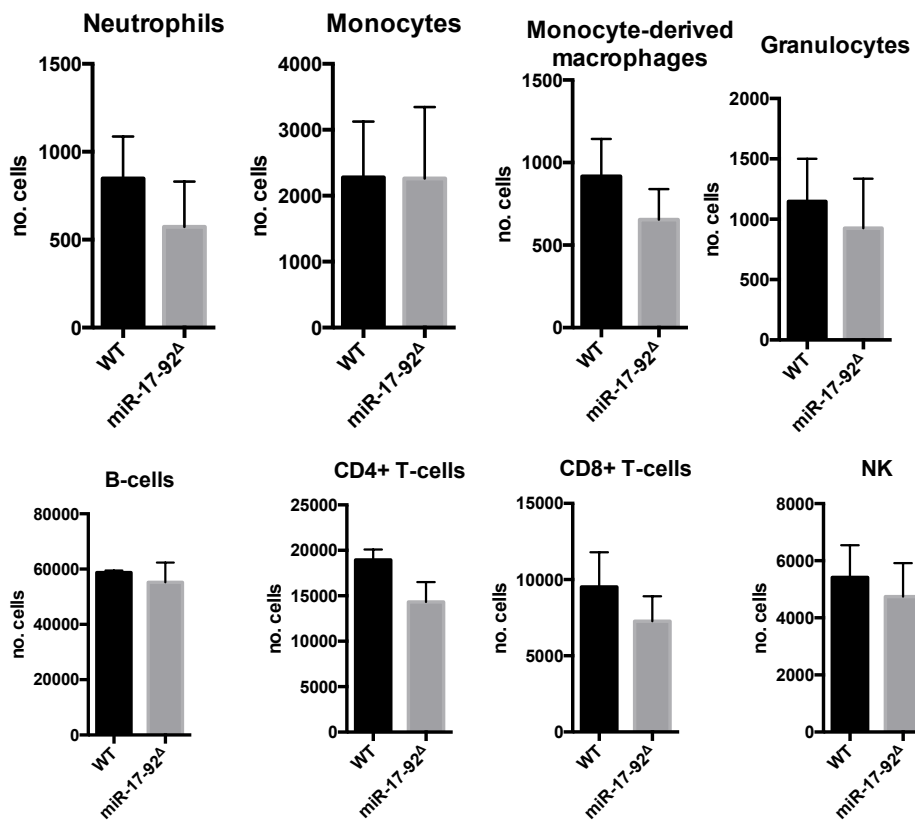
Figure 11:

FACS analysis of spleen from WT and miR-17-92$^\Delta$ mice. Spleens were taken of WT and miR-17-92$^\Delta$ mice, and were analysed for cellular composition. No distinct differences are seen. FACS experiment performed by Dr Bianca Martin, analysis by H. James Stunden.

contaminated (Figure 12C). Furthermore, the expression of Cre recombinase was reduced in the immortalised cells when compared to freshly prepared BMDMs (7 days, M-CSF)(Figure 12D). This is likely connected to either the fact that cre-recombinase is toxic to cells in high concentration, and that prolonged expression has caused some genetic damage [110, 111], or that deletion of the miR-17-92 cluster is incompatible with life, even at the cellular level. This has also been previously observed, where cre-driven deletion of the miR-17-92 cluster resulted in proliferation defects [42]. As these cells were not viable, further experiments were performed using primary cells only.

To investigate the release of cytokines, BMDMs were differentiated with M-CSF, as this gave the greatest difference between genotypes (Figure8), and cells were stimulated with EC_{50} doses of LPS, R848, PAM3csk4 or CpG to stimulate TLR4, TLR7/8, TLR2 or TLR9 respectively. Surprisingly, there was very little difference between the two genotypes, with mildly enhanced Tnfα production, but no difference in the release of either IL-6 nor IL-12 (Figure 13). It has been shown that Tnfα is a target of miR-19 [118, 42], and this would explain that Tnfα is higher, it was not fully clear why there was no difference in IL-6 or IL-12 release. To confirm that there isn't a kinetics difference that cause these results, BMDMs were stimulated over the course of 24 hours and gene expression was measured by qPCR. By measuring both early and late stage NF-κB induced genes, there was no discernible difference observed between the WT and miR-17-92$^\Delta$ BMDMs (Figure 14). One interesting observation is that the expression of the *Mir17HG* is enhanced in the miR-17-92$^\Delta$ BMDMs. It is possible that the cells are responding to a reduced expression of the mature miRNA, and are attempting to express more. Furthermore, while observed in the miR-17-92$^\Delta$ cells, the expression pattern is decreased, potentially indicating that the expression is to be reduced following stimulation anyway, in order to not regulate expression of NF-κB regulating genes, including *Tnfaip3*. Furthermore, known targets of the miR-19 do not show enhanced stability once translation is inhibited by actinomycin D. This implies that miR-19 does not significantly regulate *Tnfaip3*, *Rnf11* or Fbxl11 in macrophages.

Data shown in Figure 19 and table 7 indicates that only the miRNA of the miR-17-92 cluster are largely adjusted following cre recombinase deletion of the cluster in BMDMs. This potentially means that the current model is useful to determine the effects of this miRNA cluster alone. However, there is still a large amount of mature miRNA of the miR-17-92 cluster present, even after LysM-Cre deletion. Given that LysM-Cre is only activated during differentiation of bone marrow with growth factors into macrophages, and these miRNA are present at equal levels in

miRNA levels of miR-17-92 cluster and Cre recombinase in immortalised macrophages.

A.

C.
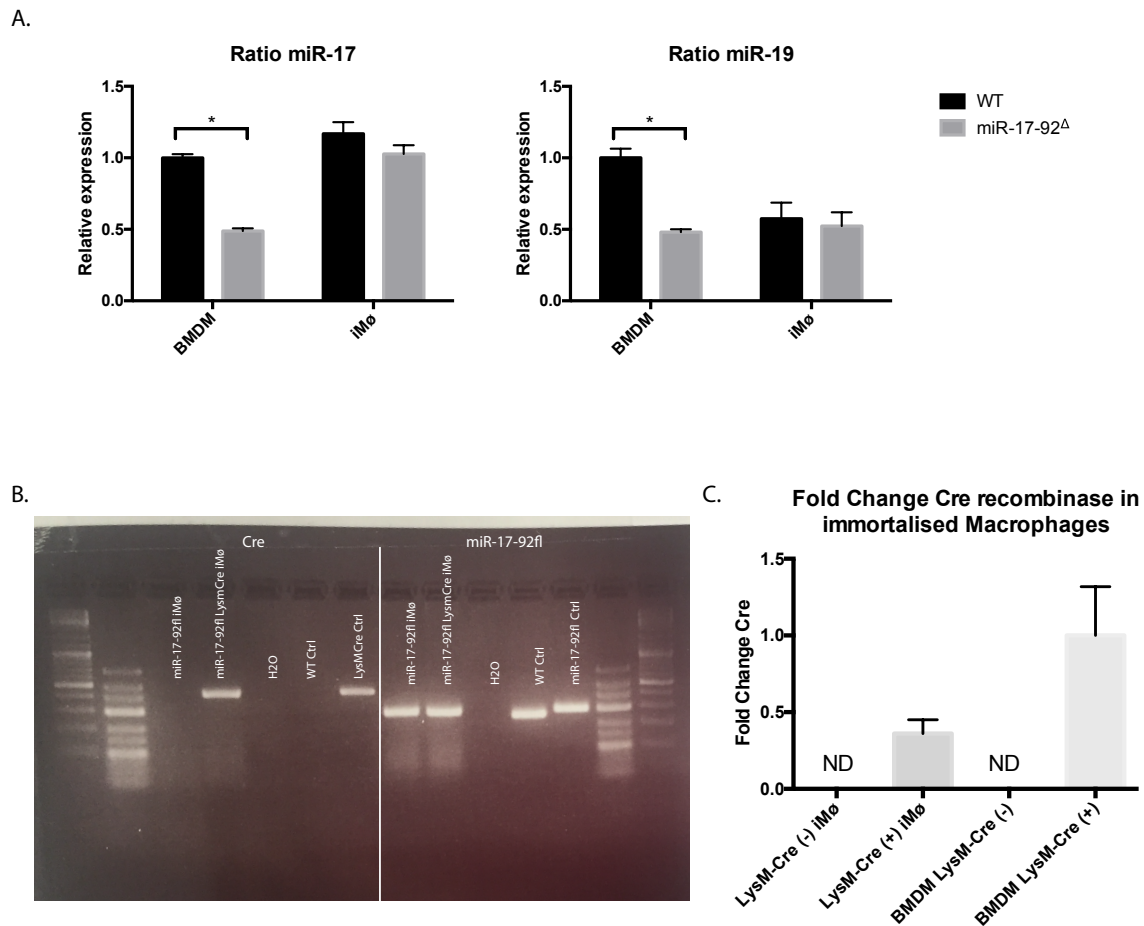
Figure 12:

Immortalisation of miR-17-92$^\Delta$ BMDMs. miRNA and Cre recombinase RNA levels in immortalised BMDMs of the miR-17-92$^\Delta$ mice changed during the immortalisation process. **A.** Levels of mature miR-17 and miR-19a determined by qPCR in the early stages of BMDM immortalisation and after the cells were immortalised. Unpaired T-tests were performed, with correction for multiple comparisons using the Holm-Sidak method. **B.** Genotyping of immortalised BMDMs showed that the cells were of the correct genotype, and were not incorrectly prepared. **C.** A fold change of Cre recombinase mRNA determined by qPCR, comparing the immortalised BMDMs to freshly prepared BMDMS. ND=Not detected.
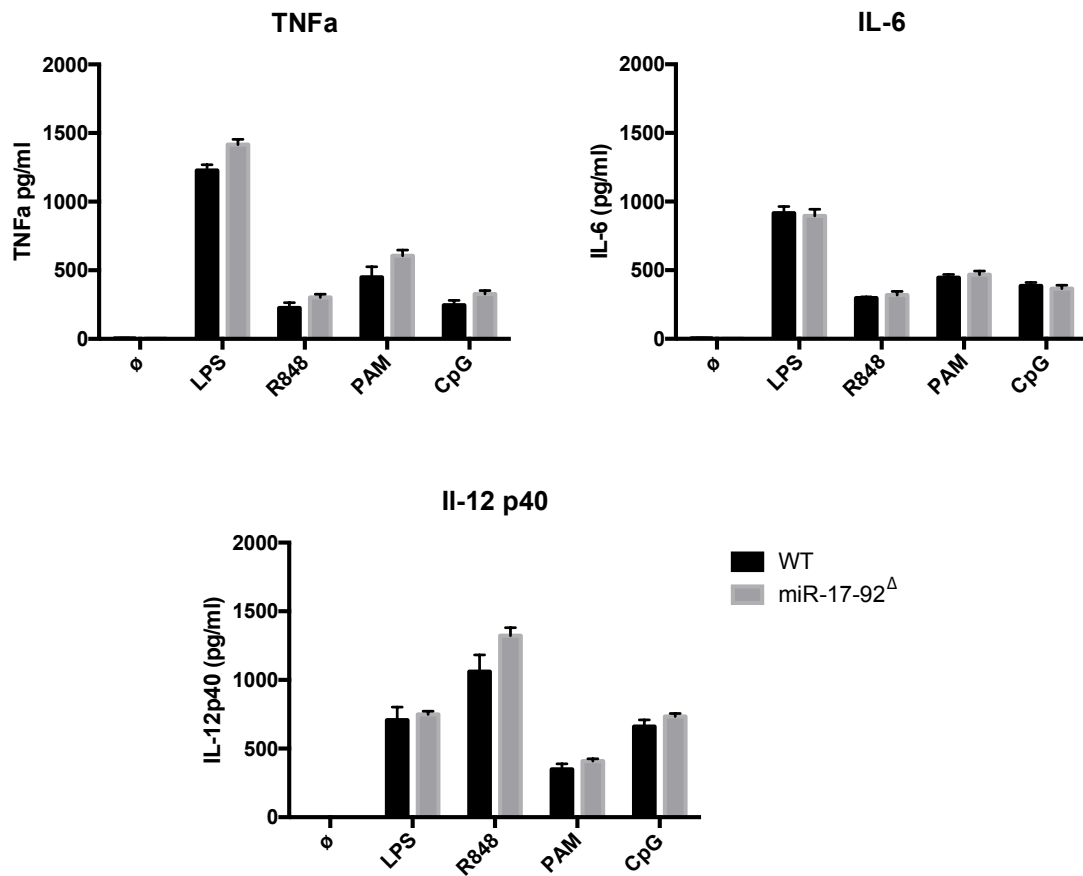
Figure 13:

Release of Cytokines from BMDMs. BMDMS were stimulated for 6 hours with different TLR ligands and supernatants were collected for cytokine analysis with ELISA. No statistically significant differences were found between WT and miR-17-92$^{\Delta}$ stimulated BMDMs. Mean ± SEM of 3 independent experiments (each performed in pairs).
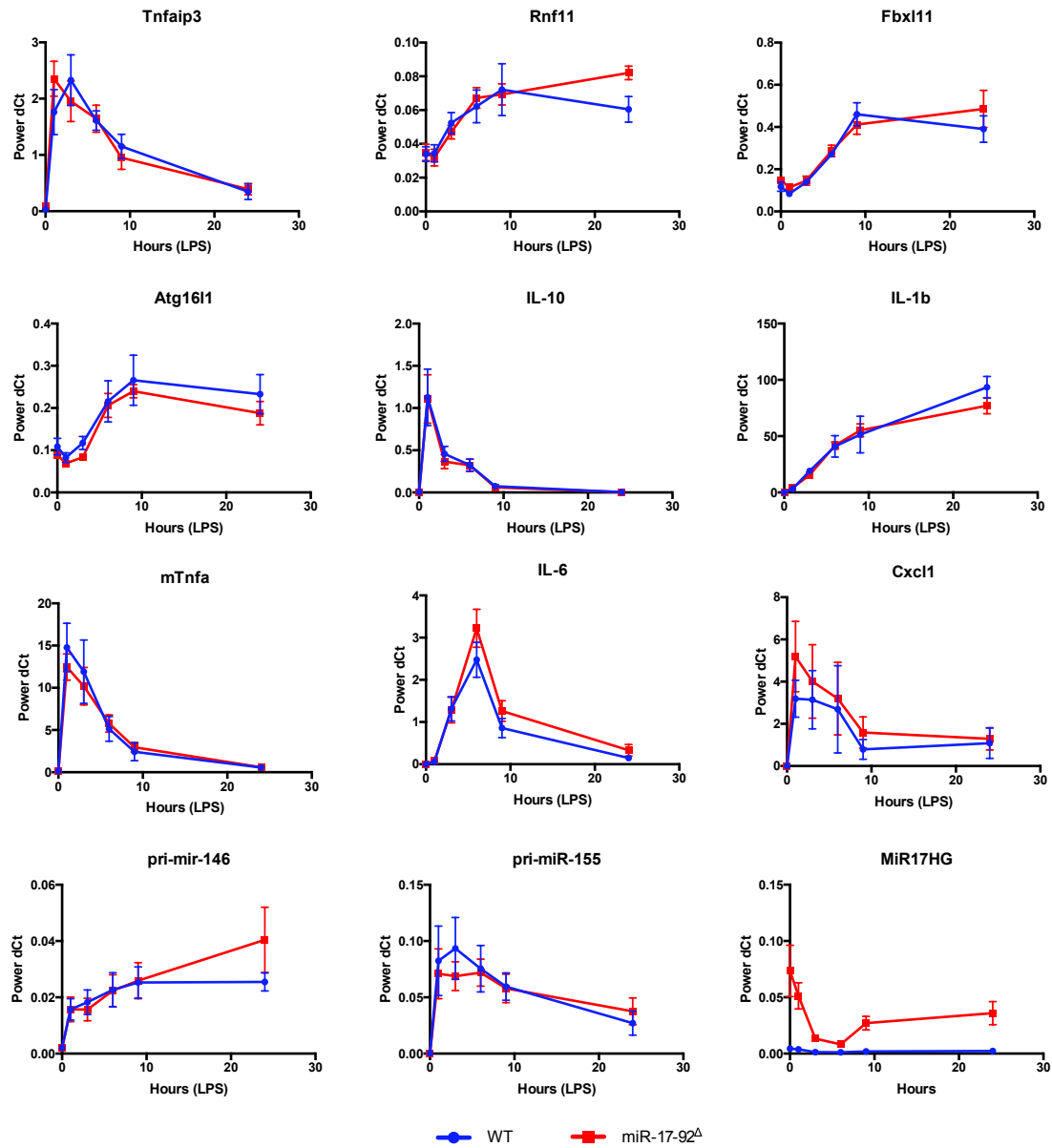
Figure 14:

mRNA kinetics following stimulation. Stimulation of primary BMDMs with LPS showed no difference in the kinetics of gene expression between miR-17-92$^\Delta$ and littermate controls. Values graphed are expression normalised with Hprt.
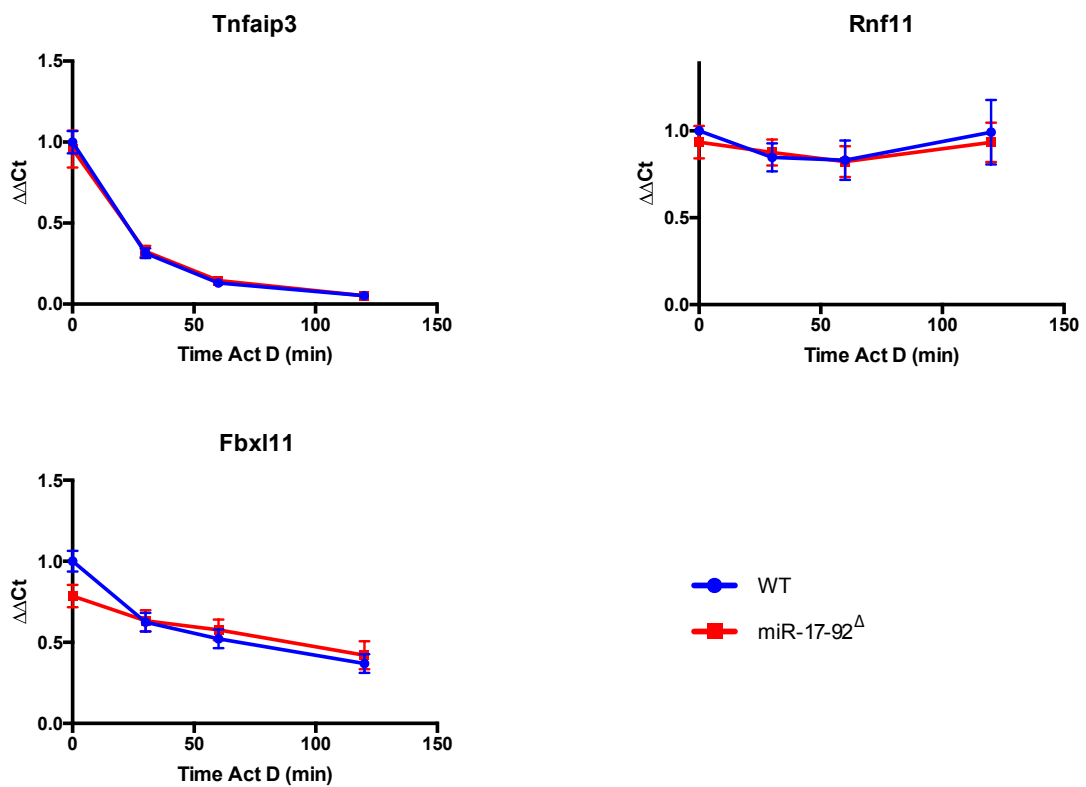
Figure 15:

Actinomycin D RNA stability. BMDMs were stimulated for 3 hours with LPS and then treated with Actinomycin D to inhibit mRNA production for the indicated times. RNA was collected and qPCR was performed to determine the stability of mRNA. Data is of 3 experiments, mean± SEM.

the Bone Marrow between the two genotypes (Fig. 8), this difference is because of both the degradation of the mature miRNA and the lack of biogenesis of new miRNA [106].

4.3.2 p-p65 and A20 response in miR-17-92$^\Delta$ BMDMs

By looking at phosphorylated p-65, a measure of NF-κB activation, in the immediate duration after LPS challenge, there is a slight trend that the miR-17-92$^\Delta$ BMDMs have a little less activation than the miR-17-92fl littermate controls. This difference is however insignificant, and furthermore there is no change in the protein levels of A20 following stimulation either. This indicates that despite having lower miR-17-92 expression, any modulation of the immune system is mild at best, and is not necessarily regulated by A20 in this model, but perhaps by something else. To investigate this further, the scope of analysis must be widened.

4.3.3 Metabolic changes to stimuli of miR-17-92$^\Delta$ BMDMs

In response to external stimuli, cells change their metabolic profile in order to better adapt to the changing requirements of the situation. Immune cells, such as macrophages, are known to adopt a more glycolytic setting upon activating of TLRs in order to quickly produce the energy required for cellular proliferation and cytokine production [119]. To measure these changes, BMDMs of miR-17-92$^\Delta$and littermate controls were incubated with or without a low dose of LPS for 8 hours and the metabolic reprogramming of the cells were measured using a Seahorse assay. Interestingly, in basal conditions, the miR-17-92$^\Delta$ BMDMs displayed slightly enhanced, albeit insignificant ATP production, and non-mitochondrial respiration. There is however a significant difference in the maximal respiration of the cells at basal conditions, however this difference is not as significant following LPS stimulation. This indicates that the miR-17-92$^\Delta$ BMDMs have a more oxidative phenotype, while interestingly also maintaining a greater glycolytic capacity to respond to stimuli. Furthermore, the presence of the miR-17-92 cluster may promote Warburg metabolism, and its loss may inhibit it. While it is known that miR-17, 18a and 20a/b target Hif-1α [120, 121, 122], and that miR-19 is upregulated in endothelial cells by Hif-1α activation [123], it makes sense that the reduction of these miRNA would results in a more oxidative phosphorylation phenotype, given they also have roles in promoting cancer, which often has Warburg metabolism. Furthermore, relieving miR-19 targeting of PTEN would also inhibit AKT-mTOR signalling, reducing glycolysis within the cell [39].
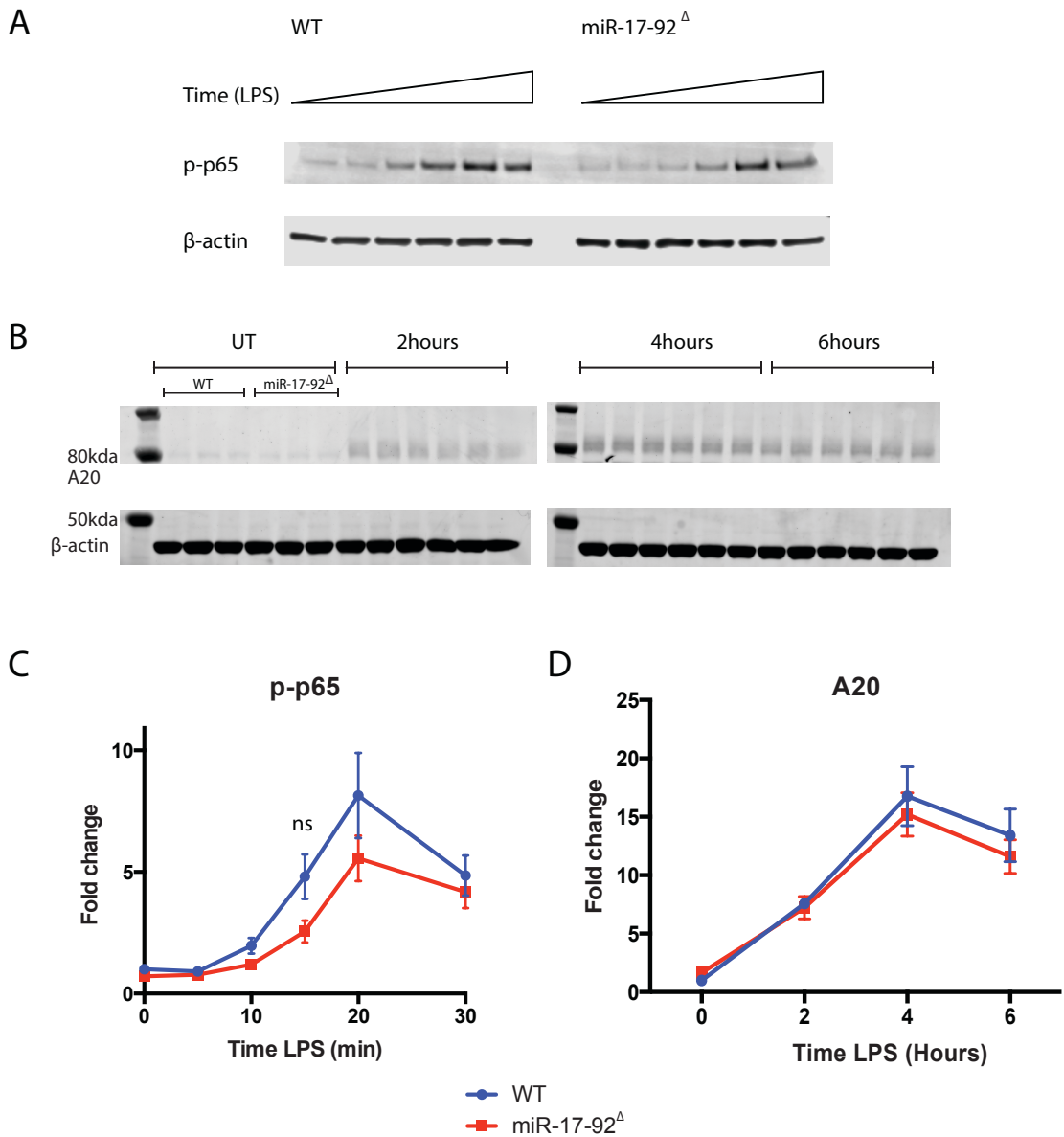
Figure 16:

Protein response of BMDMs to LPS stimulation. **A.** BMDMs were treated with LPS for 0, 5, 10, 15, 20 or 30 minutes before lysing and immunoblotted for p-p65. **B.** BMDMs were treated with LPS for 0, 2, 4 or 6 hours with LPS lysed and immunoblotted for A20. **C, D.** Relative intensity of p-p65 and A20 to β-actin respectively, represented as fold-change to miR-17-92fl untreated. Blots are representative of and graphs are of 3 experiments, plotting mean± SEM, analyzed with Mann-Whitney test, unpaired, nonparametric test
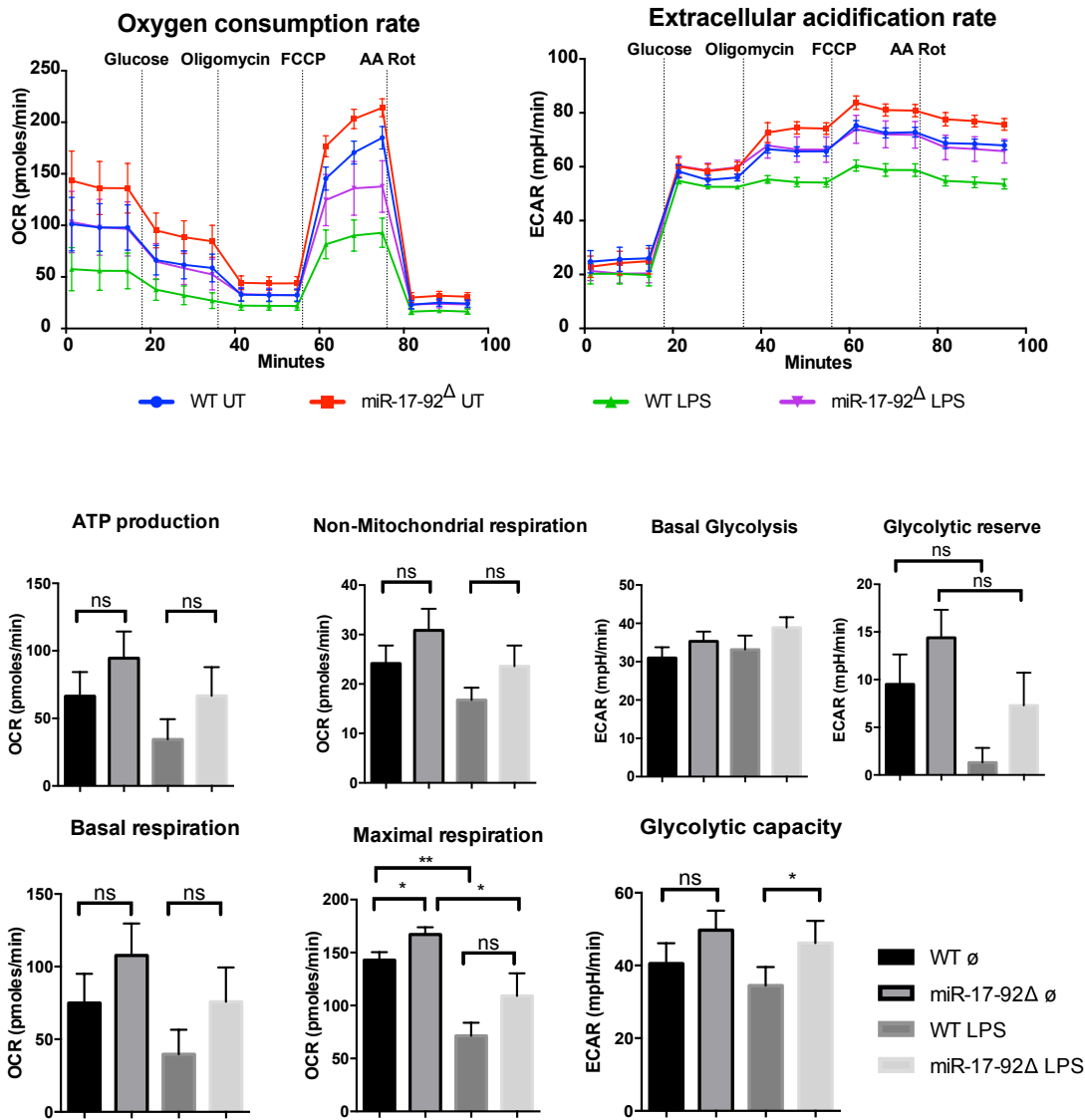
Figure 17:

Metabolic changes in response to LPS stimuli. miR-17-92fl/fl and littermate miR-17-92$^\Delta$ BMDMs were stimulated for 8hour with LPS (30ng/ml) and then were subjected to a sea-horse assay. Analyzed with Mann-Whitney test, unpaired, nonparametric test. (*P<0.05 and **P<0.01)

4.4 iCLIP

In an attempt to discover what genes are directly regulated by the miR-17-92 cluster, BMDMs from miR-17-92fl/fl and miR-17-92$^{\Delta}$ mice were used to perform an iCLIP experiment. This procedure begins with the cross-linking of RNA with any protein within 1Å using UV-C (254 nm) radiation. Following this, cells are lysed, the RNA is digested to manageable lengths, then a protein of interest, in this case, AGO, is immunoprecipitated, the cross-linked RNA is extracted and a library of cDNA is made. This resulting library can be sequenced to determine what and relative quantities of genes are regulated at a specific moment by miRNA. Techniques like this have been employed to determine the non-canonical binding of miR-155 and further our understanding of miRNA-mRNA interactions [124]. As it has been noted that iCLIP and other similar techniques are technically demanding and challenging, with low yields, many recent advances have made several steps more accessible, but much must still be done to improve the final library yield and accuracy [125, 126].

RNA-protein interactions were fixed using UV-radiation to cross-link, then an AGO-IP was performed to enrich the RNA-miRNA interacting population. Figure 18A and B show the successful enrichment of AGO protein from lysates, with minimal contaminations. However the recovery of useable cDNA for sequencing was poor. Even after 28 PCR cycles to amplify the libraries, there was an uneven amount of cDNA in conditions from mice, as indicated in 18C.

4.5 miRNA expression in BMDMs

To investigate the global expression of miRNA and to observe wether the reduction of miR-17-92 cluster had an effect on other miRNA, miRNA was measured using the Nanostring mouse miRNA V1.5. Total RNA was purified from BMDMs of 3 littermate pairs and left untreated and LPS stimulated. Figure 19 shows all miRNAs detected show largely the same expression, with exception to the miRNA from the miR-17-92 cluster, which were significantly reduced. Importantly, the Nanostring data shows that the difference in miRNA expression is not as significant as the previous qPCRs had indicated in figure 7. This opens the possibility that the LysM-Cre driven deletion of the miR-17-92 cluster may not be as effective as previously thought.

4.6 Design of modular Nanostring Panel for macrophage inflammation

Nanostring technology is a technique of detecting individual mRNA molecules of a specific species and counting them in an diagnostically accurate manner to interpret fine modulation
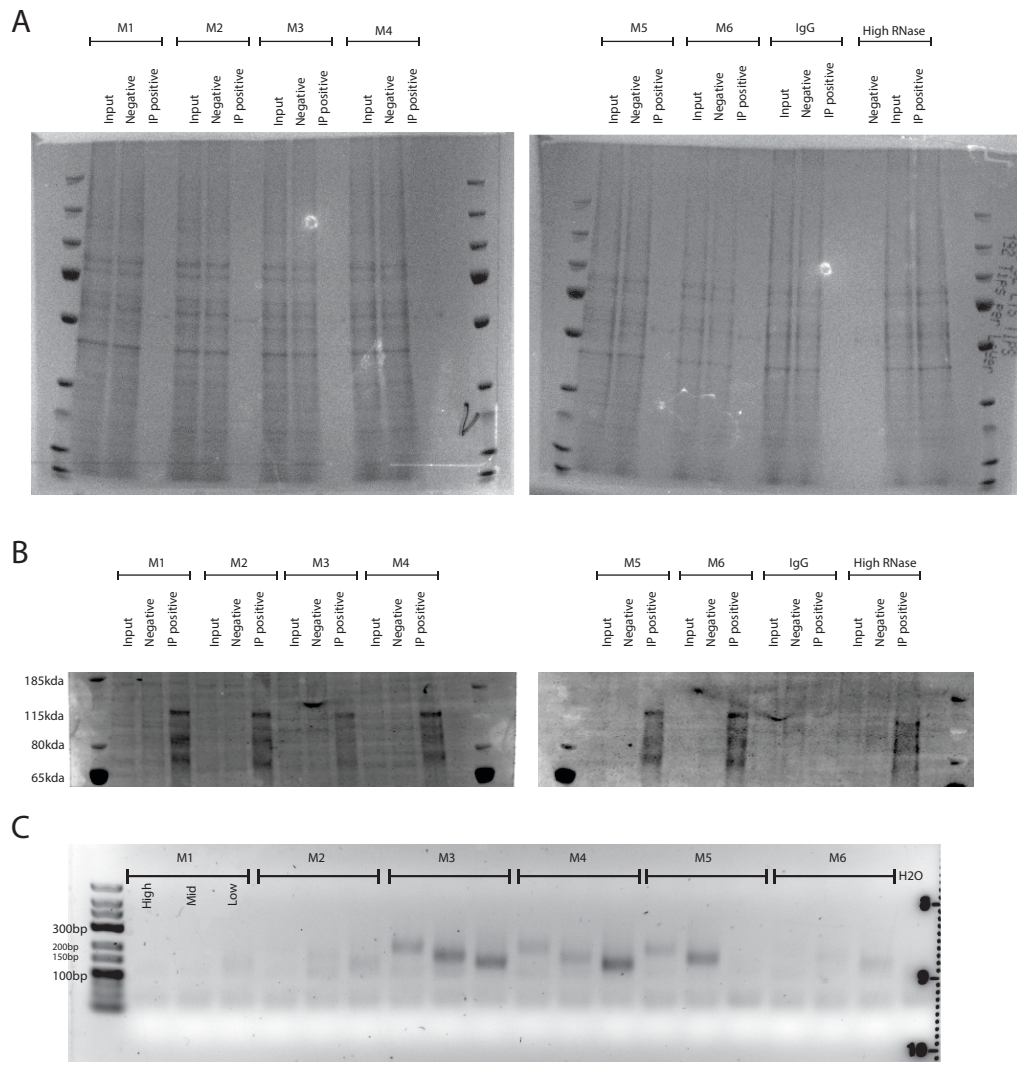
Figure 18:

iCLIP results. Samples of iCLIP experiments, where the samples are separated by the animal they came from M1-6. **A.** Coomassie stain of BIS-TRIS gels, indicating there was a reduction in total protein following the IP. **B.** Western blot for AGO, indicating enrichment of protein following IP. **C.** PCR amplification following 32 cycles of the different fractions of cDNA libraries. This indicates low yield of cDNA species.
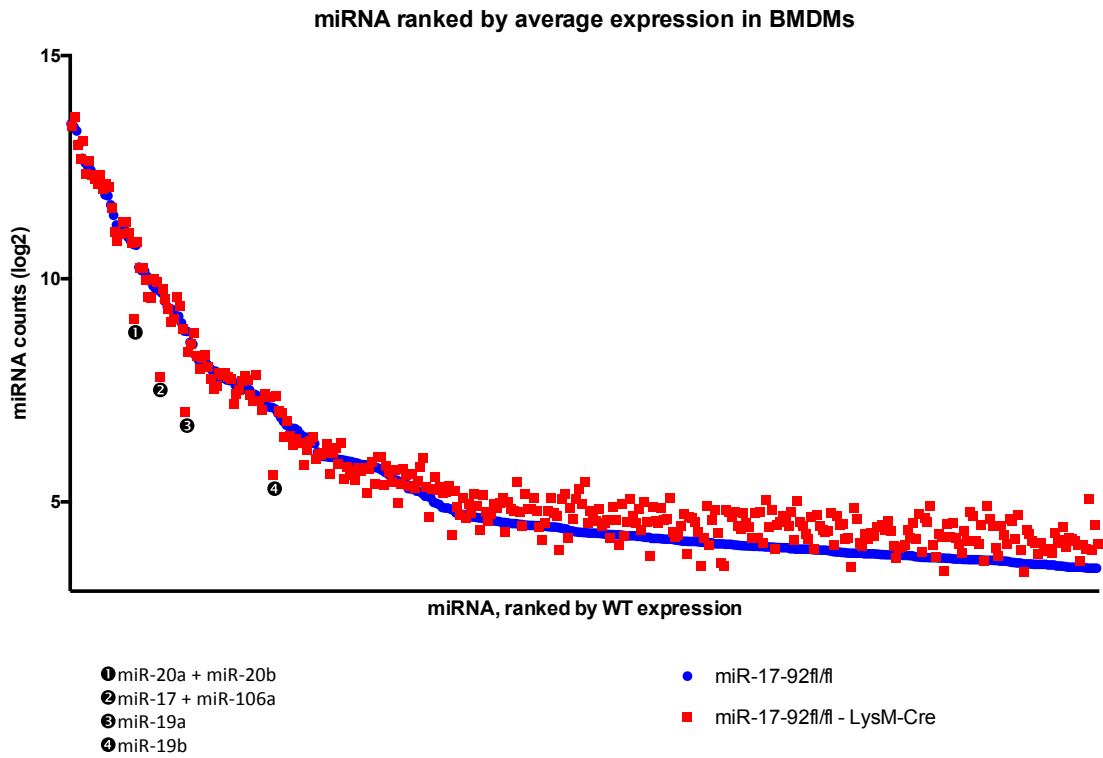
miRNA ranked by average expression in BMDMs

❶ miR-20a + miR-20b
❷ miR-17 + miR-106a
❸ miR-19a
❹ miR-19b

● miR-17-92fl/fl
■ miR-17-92fl/fl - LysM-Cre

Figure 19:

Expression of global miRNA determined by Nanostring. Most miRNA are expressed equally between the WT and LysM-Cre BMDMs. miR-17-92 cluster member miRNAs show a clear reduction, as indicated. Data is of 3x miR-17-92$^\Delta$ mice and Littermate controls.

	miR-17-92Δ:UT vs WT:UT		miR-17-92Δ:LPS vs WT:LPS		WT:LPS vs WT:UT		miR-17-92Δ:LPS vs miR-17-92Δ:UT	
	Fold Change	Adjusted P Value	Fold Change	Adjusted P Value	Fold Change	Adjusted P Value	Fold Change	Adjusted P Value
mmu-miR-106a+mmu-miR-17	-1.2106 ****	< 0.0001	-1.0741 ****	< 0.0001	-0.2820	> 0.9999	-0.1455	> 0.9999
mmu-miR-19a	-1.0193 ****	< 0.0001	-0.9050 ****	< 0.0001	-0.1699	> 0.9999	-0.0556	> 0.9999
mmu-miR-19b	-0.9916 ****	< 0.0001	-0.8796 ****	< 0.0001	-0.3916	> 0.9999	-0.2796	> 0.9999
mmu-miR-20a+mmu-miR-20b	-1.4061 ****	< 0.0001	-1.2123 ****	< 0.0001	-0.2115	> 0.9999	-0.0178	> 0.9999
mmu-miR-362-3p	0.1846	> 0.9999	0.2271 **	0.0048	-0.1061	0.8885	-0.0636	> 0.9999
mmu-miR-674	-0.9966	> 0.9999	-0.3154	> 0.9999	-0.9017 *	0.0244	-0.2205	0.5425
mmu-miR-2135	0.1199	> 0.9999	0.5712	> 0.9999	0.3279 ***	0.0002	0.7792 ****	< 0.0001
mmu-miR-1224	-0.1679	> 0.9999	0.2134	> 0.9999	0.3080	> 0.9999	0.6892 *	0.0157
mmu-miR-199a-3p	0.1558	0.0535	-0.0426	> 0.9999	-0.2235	> 0.9999	-0.4219	> 0.9999
mmu-miR-155	0.0443	> 0.9999	0.2202	> 0.9999	0.4187	> 0.9999	0.5946	0.0641
mmu-miR-146a	0.7318	> 0.9999	0.2190	> 0.9999	0.9494	> 0.9999	0.4366	> 0.9999

Table 7:

miRNA expression assessed by Nanostring of miR-17-92$^\Delta$ BMDMS. miRNA that are significantly changed following LPS stimulation between WT and LysM-Cre BMDMs. Same pairs of mice as in Figure 19. 2-way ANOVA with Tukey Multiple comparisons test was performed, *p<0.032 **p<0.0021 ***p<0.002 ****p<0.001.

of gene expression, unmodulated by amplification biases. The challenge put to me was to design a panel of genes that can be used by many projects in the institute, and easily changed depending on the needs of the investigators. As the vast majority of projects use macrophages, dendritic cells and neutrophils, these were the core cell types considered when designing this panel. Secondly, as most individuals were analyzing the modulation of secreted cytokines and other immune activation markers, these genes were given priority for inclusion.

To achieve this, the Elements chemistry was chosen, allowing the analysis of up to 192 genes per sample, across 12 samples to be completed in 2 days. By dividing the genes into "bins" of 24 genes, 8 panels can be multiplexed to assess different clusters of genes depending on their function.

Using this project design, researchers can quickly adapt the nanostring panel to their requirements, and investigate required bins only. Furthermore, when a new set of genes is required, only the bins of tags must be ordered, instead of a whole new kit. Several variants of this panel has been used to investigate the patient samples, the effect of small molecules on human monocytes, the effect of infarction on mouse heart derived macrophages, DCs and myocardyocytes.

To investigate the effect of LPS on transcription in miR-17-92$^\Delta$ BMDMs, the panel chosen was with TypeI IFN and metabolism and stress, based upon previous results that metabolic processes may be influenced (Figure 17). BMDMs from either miR-17-92$^\Delta$ mice, or littermate WT controls showed almost identical responses, as outlined in figure 21. Previous studies have found that while miRNA do ultimately regulate protein expression, measurements of RNA is still an effective method of detecting miRNA activity [127, 128, 129, 38]. While the Nanostring is measuring a limited selection of genes, the panel was designed to specifically measure the innate response, and as such has shown that there is nearly no difference between the miR-17-92$^\Delta$BMDMs transcriptional response compared to the WT littermate controls. This speaks volumes not only of the accuracy of the nanostring, but how similar the two genotypes are to each other, and how little the miR-17-92 cluster has an effect on in macrophages. From this, it is concluded that *in vitro* prepared BMDMs from miR-17-92$^\Delta$ mice are almost indistinguishable from their WT littermate controls when examining gene expression, indicating that reduction of the miR-17-92 cluster does not have an effect on LPS-induced transcription of genes, in
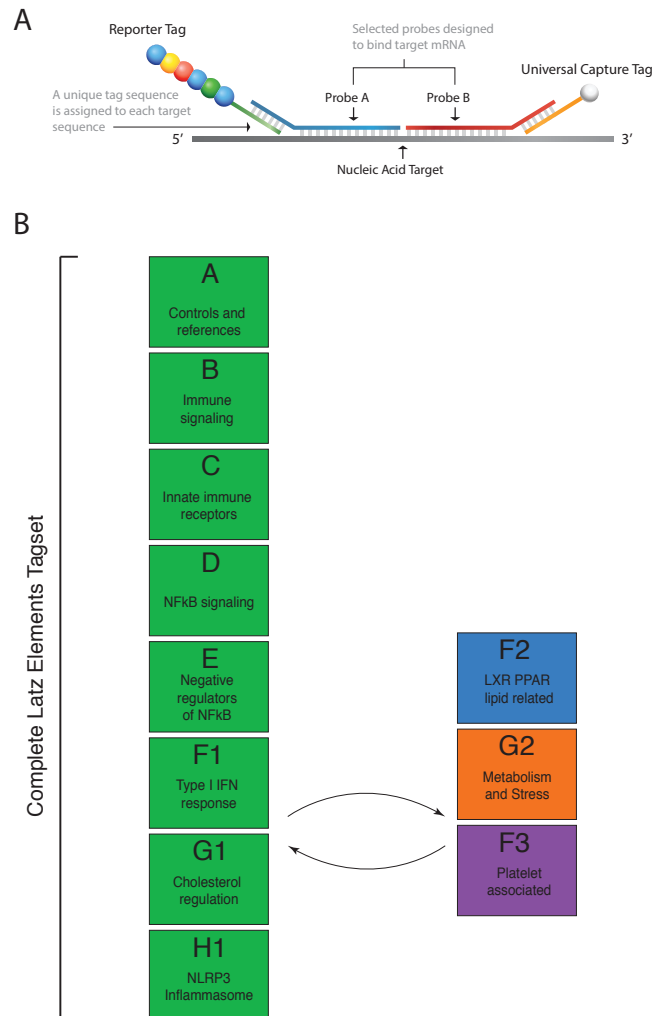
Figure 20:

Nanostring Elements Modular design theory. **A.** Diagram showing how the Nanostring nCounter® Elements™ Reagents works. Diagram adapted from the nCounter® Elements™ XT Reagents User Manual, available online. **B.** Bins of 24 genes with a central theme (annotated with letters) can be mixed together is a specific order to create a 192 gene custom Nanostring assay, specifically designed to analyze macrophages, neutrophils and dendritic cells. If another panel of genes is preferred, it can be replaced with a replacement panel (annotated with number), designed to measure a separate theme of genes.
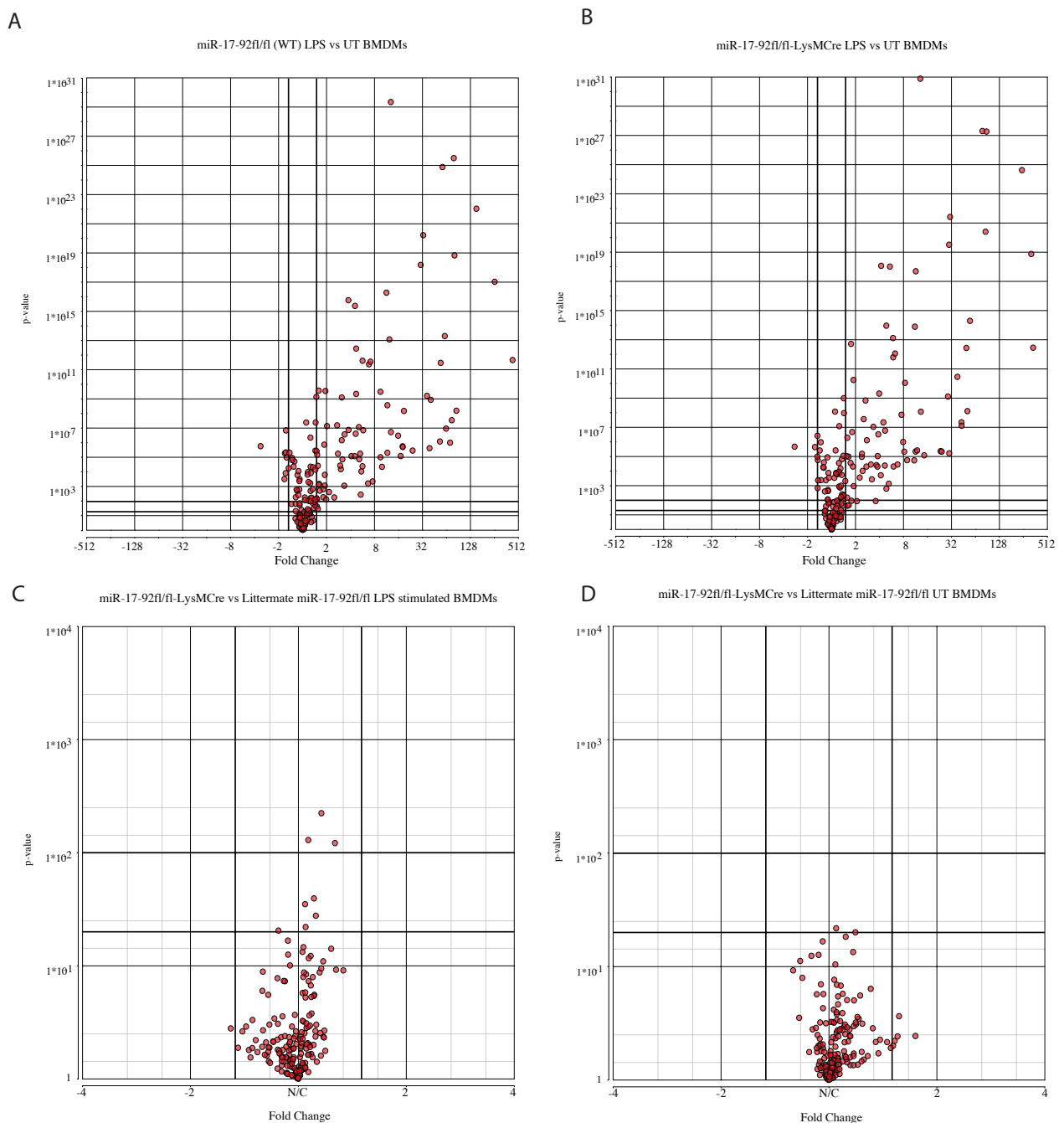
Figure 21:

Nanostring analysis of gene expression of miR-17-92fl/fl - LysMCre BMDMs. Volcano plots of fold gene expression and significance between miR-17-92fl/fl BMDMs and miR-17-92fl/fl LysmCre BMDMs analysed with the modular Nanostring Elements containing Type I IFN, and Metabolism and Stress panels. **A.** Effect of LPS stimulation on miR-17-92fl/fl (WT) BMDMs. **B.** Effect of LPS stimulation on miR-17-92$^\Delta$ BMDMs. **C.** Comparison of miR-17-92$^\Delta$ and littermate miR-17-92fl/fl BMDMs stimulated with LPS. **D.** Comparison of miR-17-92$^\Delta$ and littermate miR-17-92fl/fl BMDMs at basal gene expression (unstimulated). WT=8 miR-17-92$^\Delta$=10 p-Values are Bonferroni multiple comparisons corrected.

agreement with findings from the 24 hour LPS stimulation (Fig. 14).

4.7   *In Vivo* response to LPS of miR-17-92$^\Delta$macrophages.

4.7.1   Selection of cells from *in vivo* experiments.

When performing the *in vivo* experiments, it was important to use magnetic beads to select a specific population of cells that expressed the modulated miR-17-92 cluster, and not take a mixed population. To test this, WT mice were sacrificed for their spleen, blood, and peritoneal lavage, and then each subjected to either F4/80 or CD11b magnetic MACS selection. Following selection, the cells were stained for either F4/80 or CD11b and analysed by FACS. As shown in figure 22, enrichment with Cd11b was comparable to F4/80 enrichment of the peritoneal lavage cells. However Cd11b magnetic selection was superior when collecting CD11b, F4/80 double positive cells, and even F4/80+ CD11b- cells. For this reason, CD11b magnetic selection was chosen to collect cells ex vivo from mouse tissues.

4.7.2   *In vivo* miRNA response to LPS challenge.

To investigate the effect of the miR-17-92 cluster in an *in vivo* setting, miR-17-92$^\Delta$mice and littermate controls were injected with either PBS or LPS intraperitoneally, and monitored for 6 hours, to mimic an acute inflammatory response to infection. Mice were sacrificed and their spleen, blood and peritoneal lavage were taken, and cells were magnetically selected for CD11b selection. As the peritoneal cells had the major difference in miR-17-92 expression, these were of most interest (see figure 10). Using the Nanostring, global miRNA expression was measured from either PBS or LPS injection of 24 mice, (2 were removed due to poor performance of the assay). Figure 23 indicates that there was a lot of variation in the Nanostring miRNA datasets. Much of the variation however can be explained by several non-experimental variables, including the age and gender of the animals. The largest variable however is the effect came from the cage that the animals were housed in prior to the experiment taking place. Figure 23C shows that when correcting for the cage the animal is from, error within the dataset is reduced. It must also be noted that the cage the mice were housed in also determines the animal's age and gender, as mice of the same gender and litter are housed together, regardless of genotype. However, the contribution of age and gender alone are quite small compared to the effect of the cage (Figure 23B). The PCAs shown in Figure 24 show that with cage correction, the datasets have not been overcorrected. Furthermore, each of the conditions clusters separately, indicat-

Figure 22:

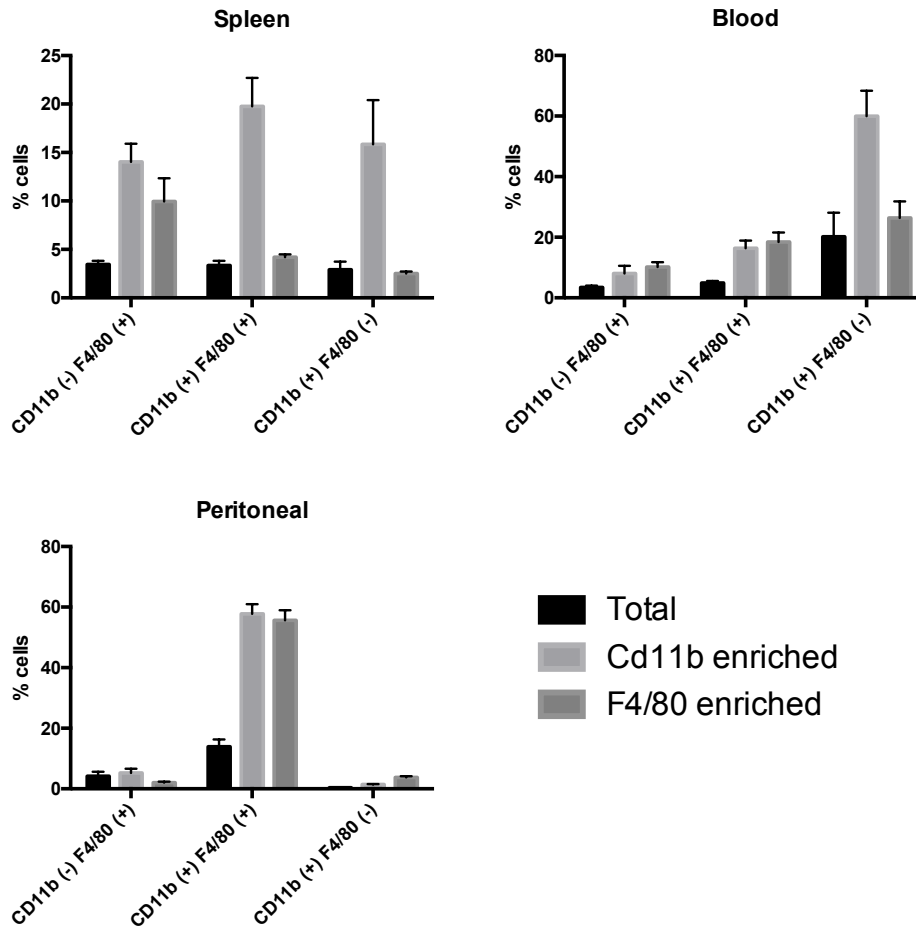***Comparison of CD11b and F4/80 selection of cells from Spleen, Peritoneum and whole blood.*** FACS enrichment of CD11b and F4/80 cells. The spleen, blood and peritoneal lavage were prepared and then magnetically sorted for F4/80 or CD11b expressing cells. After selection, cells were stained for F4/80 and Cd11b and FACS analysis was performed. Values here are % number of cells in a sample. n=6 Mean with SEM.

ing that there are subtle differences between them. Interestingly, cage effects on mice have been previously reported,

miRNA expression and fold changes from peritoneal CD11b+ from 4.7.2 are represented here as volcano plots in Fig. 27. The vast majority of miRNA are unchanged either between the two genotypes, or following challenge, as indicated here. After correcting for changes due to the cages, the miRNA expression was graphed as mean with SEM and found 2-way ANOVA was performed, with Tukey's multiple comparisons test. Unsurprisingly, most of the miRNA showed no to little difference between the conditions, or showed a small change between stimulated and non-stimulated conditions. Fig. 25 shows miRNA that have a significant difference between stimulated and unstimulated conditions, but no significant differences between the WT and miR-17-92$^\Delta$ littermates. 23 miRNA showed a significant change in the miR-17-92$^\Delta$ mice alone, and only two showed significance on in the WT, and 6 showed a significant change within each genotype. This is a further indication that there is global dysregulation of miRNA in the miR-17-92$^\Delta$.

To investigate which pathways may be regulated by the significantly changed miRNA from the peritoneal cells, the predicted targets were collated from Targetscan [105] and then Pathway enrichment was performed using Partek. Table 8 outlines the results of this analysis. While un-surprisingly, most of the top predicted pathways that are likely to be regulated by the modulated miRNA are cancer and pluripotency related, the first immune-related pathway prediction is in position 14, the TGF-β pathway. Furthermore, NF-κB and TLR pathways do not appear until near the end of the list, with extremely poor enrichment scores, indicating that the vast majority of predicted targets that are likely to be modified in the cells are not involved in immune functions at all. This is further backed up by the lack of difference when immunologically challenging the cells.

An interesting explanation for the many changes in miRNA expression is the loss of miR-20a, may free up the component required for it, and many other miRNA maturation, Khsrp. This is further investigated in Supplementary section 7.3, on page 84.

4.7.3 *In vivo* Cytokine response to LPS challenge.

Further investigation of the peritoneal lavage and sera of mice challenged with LPS revealed that there was no significant differences in any cytokines produced by the miR-17-92$^\Delta$. In the sera of the mice, where no observable difference in miR-17-92 expression was observed (figure 10),
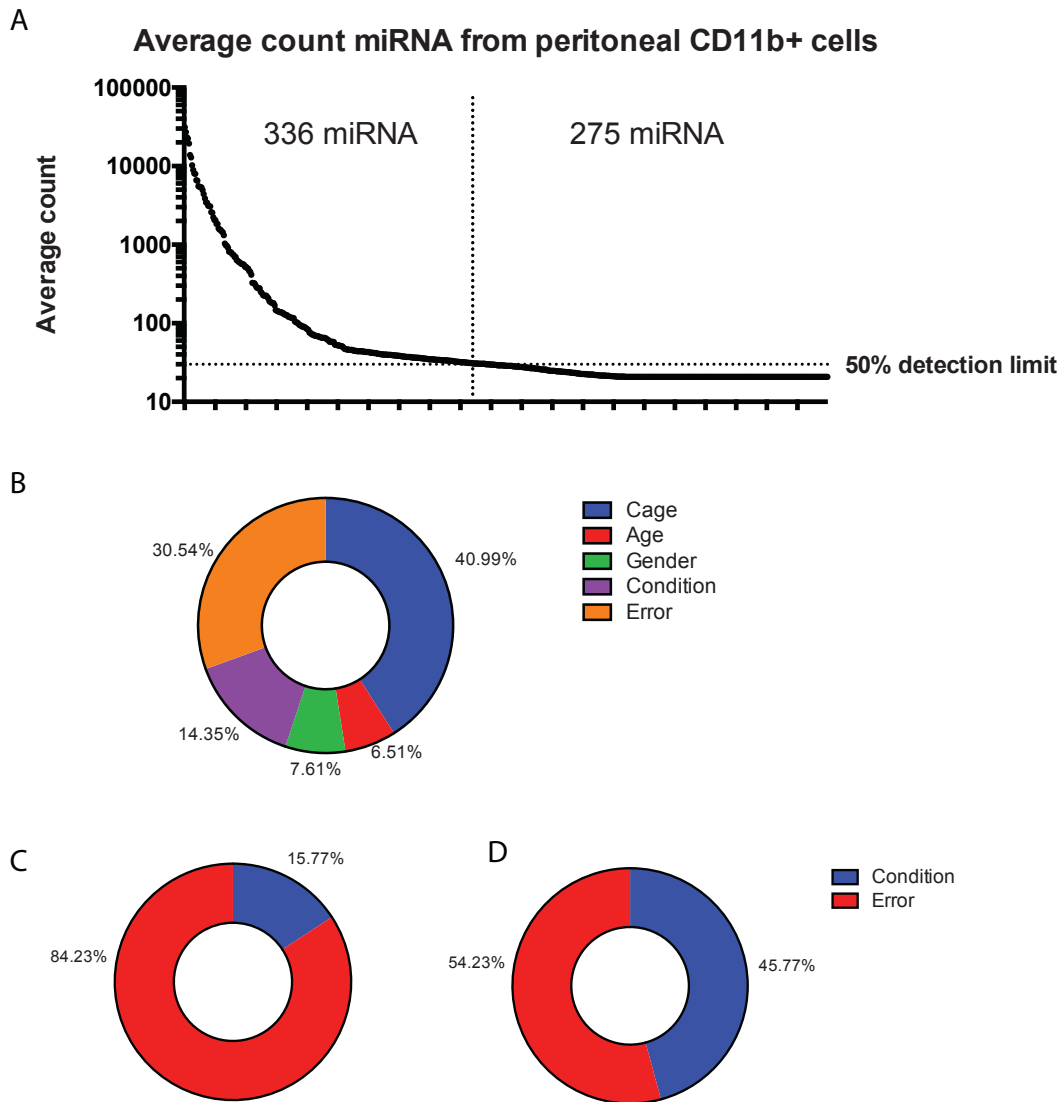
Figure 23:

Quality and variance analysis of miRNA detected by Nanostring from peritoneal cells.
Detection of miRNA levels using nanostring of CD11b+ peritoneal cells from PBS or LPS in-
jected animals. **A.** Average counts of all miRNAs are plotted, and threshold where miRNAs
are detected in at least 50% of samples is plotted on Y-axis. X-axis shows the cutoff, with 336
miRNAs detected, and 275 miRNAs considered undetected. Sources of variation from *in vivo*
peritoneal miRNA Nanostring. **B.** The total sources of variation considering all factors. Cage
and gender are co-dependant. **C.** Error in dataset before Cage correction. **D.** Error in dataset
following Cage correction.

Rank (of 303)	Pathway Name	Enrichment Score	Enrichment p-value
1	Signaling pathways regulating pluripotency of stem cells	17.1312	3.63E-08
2	Pathways in cancer	16.1717	9.48E-08
3	Breast cancer	14.74	3.97E-07
4	Axon guidance	14.0179	8.17E-07
5	Focal adhesion	13.72	1.10E-06
6	Insulin signaling pathway	12.874	2.56E-06
7	Regulation of actin cytoskeleton	12.7857	2.80E-06
8	Hippo signaling pathway	11.5886	9.27E-06
9	Rap1 signaling pathway	11.3819	1.14E-05
10	cAMP signaling pathway	11.1281	1.47E-05
14	TGF-beta signaling pathway	10.394	3.06E-05
20	Wnt signaling pathway	8.97955	0.00012596
25	PI3K-Akt signaling pathway	7.7107	0.000448008
29	Autophagy - animal	7.25848	0.000704176
37	mTOR signaling pathway	6.64151	0.00130506
44	AMPK signaling pathway	6.06366	0.00232587
45	cGMP-PKG signaling pathway	6.01207	0.00244902
46	AGE-RAGE signaling pathway in diabetic complications	5.86058	0.00284958
63	Notch signaling pathway	4.7038	0.00906079
116	Mitophagy - animal	2.32971	0.0973242
118	Inflammatory mediator regulation of TRP channels	2.10901	0.121358
122	p53 signaling pathway	1.90447	0.148901
130	HIF-1 signaling pathway	1.7237	0.178405
155	TNF signaling pathway	1.04162	0.352883
170	Inflammatory bowel disease (IBD)	0.65004	0.522025
173	RIG-I-like receptor signaling pathway	0.635646	0.529593
181	Apoptosis	0.499891	0.606597
206	IL-17 signaling pathway	0.225157	0.798391
213	Toll-like receptor signaling pathway	0.16209	0.850365
257	Cytokine-cytokine receptor interaction	0.0230742	0.97719
284	NF-kappa B signaling pathway	0.00186474	0.998137
286	Rheumatoid arthritis	0.000875383	0.999125

Table 8:

Partek Pathway Enrichment of predicted targets. Predicted targets calculated by Targetscan of miRNA that were found to be significantly changed in peritoneal mø between miR-17-92fl/fl and miR-17-92$^\Delta$ mice, injected with LPS. Not all predictions are tabulated, sets of missing predictions are depicted as gaps in the table. Of 303 ranked pathways, NF-κB and related pathways appear at the bottom of the list, with almost no significance.
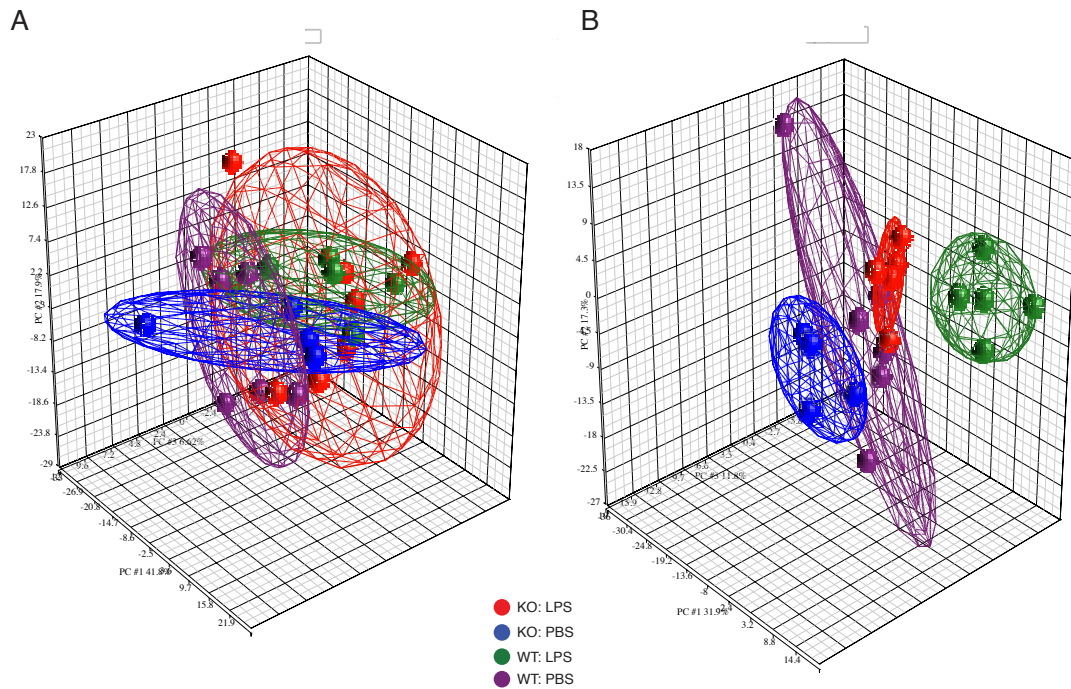
Figure 24:

Effect of cage correction on miRNA expression PCA. Each dot represents a single animal. A. PCA of dataset before Cage correction. B. PCA of dataset following Cage correction.

it was reasoned that there would be little difference in cytokine response to IP LPS challenge. Indeed, there was no observable differences between miR-17-92$^\Delta$and WT littermates, except a slightly elevated Cxcl1. In the peritoneal lavage, where there was a large difference in miR-17-92 expression however, there is also no observable differences, mirroring the *in vitro* results (figure 13). IL-10 and IL-13 appear slightly reduced, while IL-23 is mildly enhanced, however none of these observations are significant. IL-13 however is secreted by Th2, NKT and Mast cells among others [130], but not macrophages. It is interesting to note that macrophages are required to maintain IL-13 signalling from Th2 cells *in vitro* [131], and that the miR-17-92 cluster has already been shown to enhance Th2-driven responses [42]. These raise the possibility that the miR-17-92 cluster does affect macrophage interaction with T-cells and play a role in type 2 cytokine responses.

Of note, Il-23 is mildly enhanced in the miR-17-92$^\Delta$ mice compared to the WT littermates when looking in the peritoneal lavage, while IL-10 is slightly reduced. This has been previously observed that IL-10 is critical in regulating IL-23 release from macrophages [132].

These results mimic those of the *in vitro*, namely that modulating the miR-17-92 cluster in macrophages has no effect on cytokine release when stimulated with LPS *in vivo*. Further
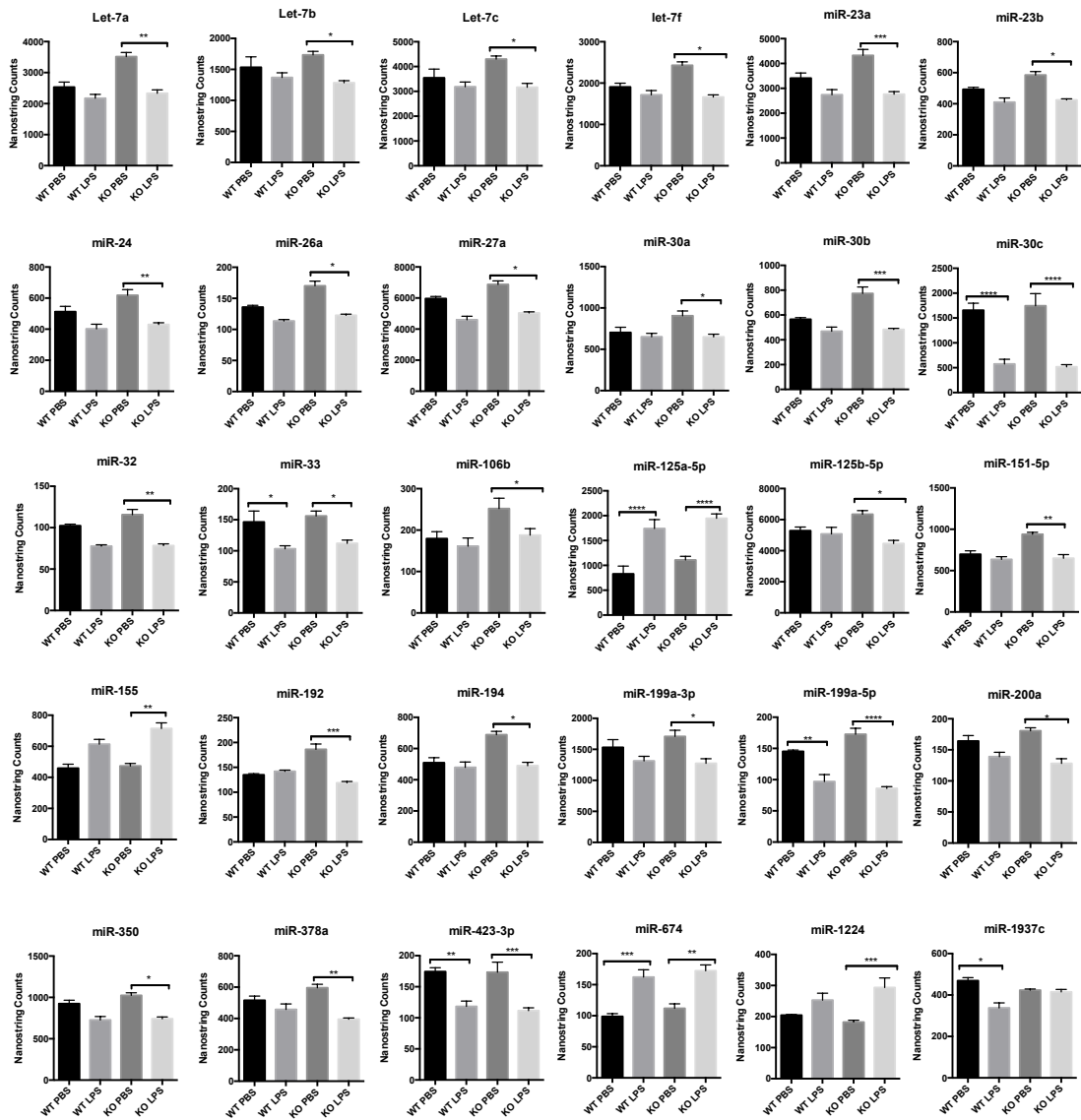
Figure 25:

Significantly differently expressed miRNA within miR-17-92$^\Delta$ or WT peritoneal cells stimulation. miRNA expression following 2-way ANOVA with Tukey multiple comparisons of differences between miR-17-92fl/fl and miR-17-92fl/fl - LysM-Cre -/+ peritoneal CD11b+ lavage cells following PBS or LPS injection. miRNA shown here have no significant difference between the miR-17-92$^\Delta$ and WT groups, but do show a change within their respective conditions. *p<0.032 **p<0.0021 ***p<0.002 ****p<0.001
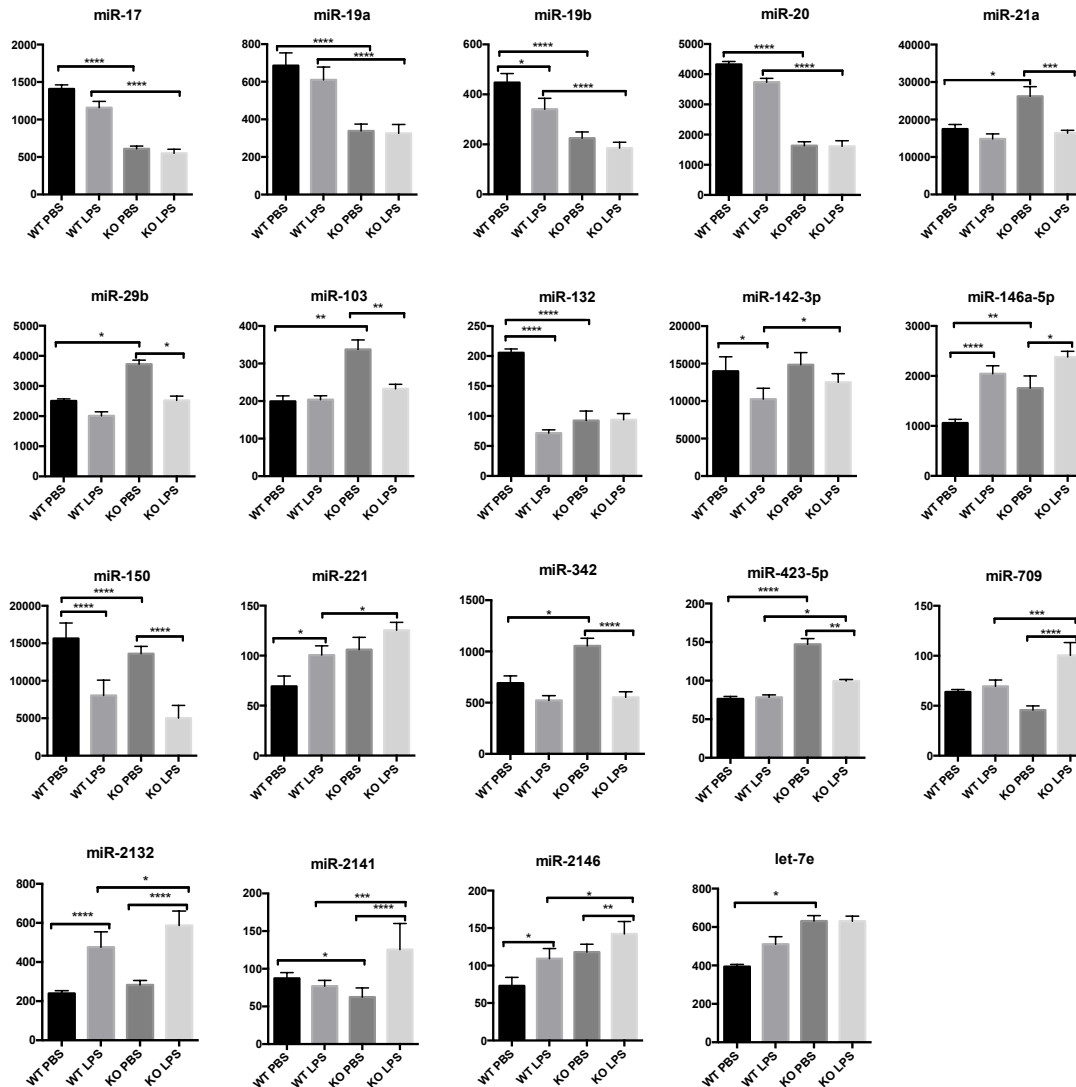
Figure 26:

Significantly differently expressed miRNA between miR-17-92$^\Delta$ and WT littermate peritoneal cells. miRNA expression following 2-way ANOVA with Tukey multiple comparisons test of differences between WT and miR-17-92$^\Delta$ peritoneal CD11b+ lavage cells following PBS or LPS injection. Data is shown as Nanostring Digital counts on the y-axis. miRNA shown here have a significant difference between the miR-17-92$^\Delta$ and WT mice. *p<0.032 **p<0.0021 ***p<0.002 ****p<0.001
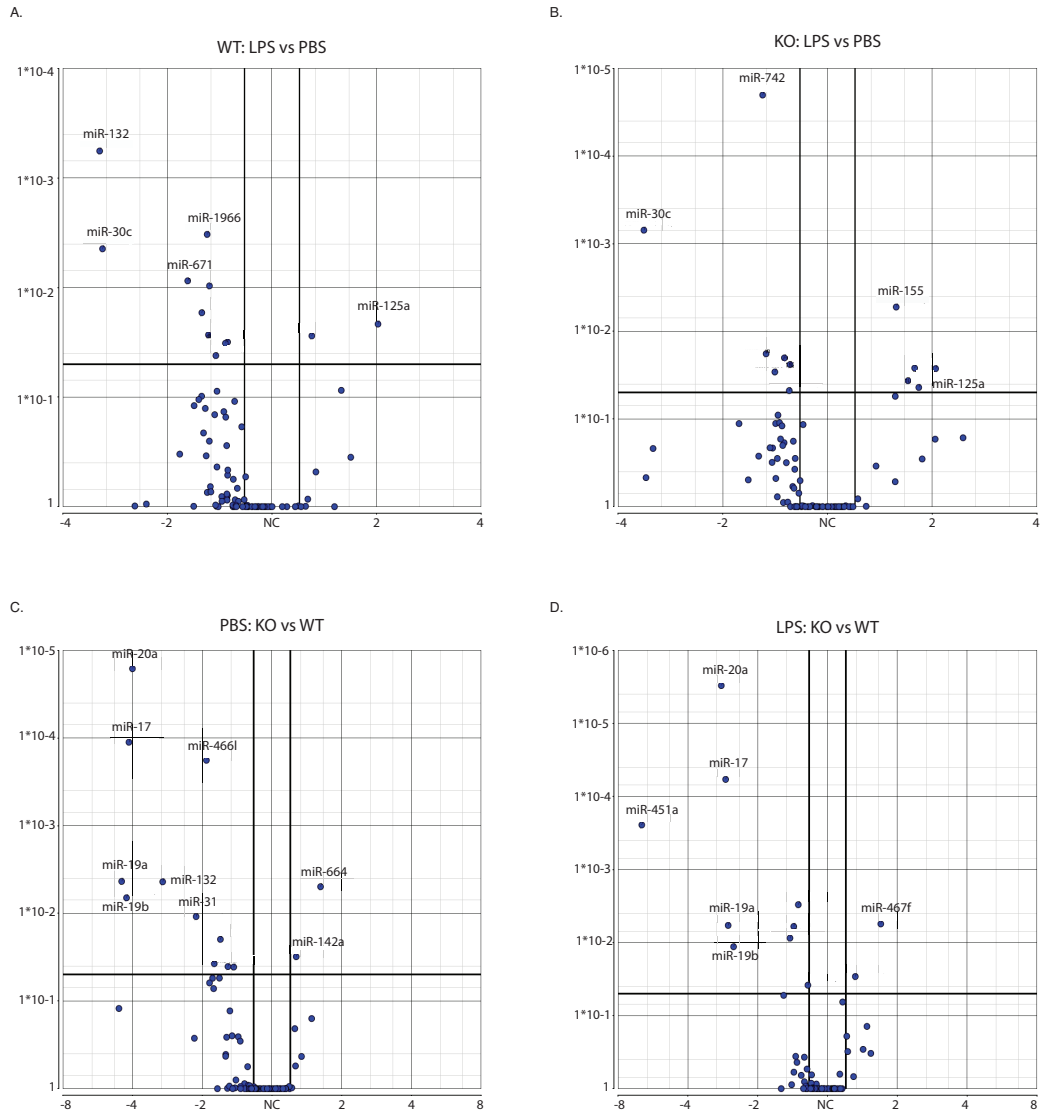
Figure 27:

Volcano plots of miRNA peritoneal expression. miRNA detected from peritoneal CD11b+ cells using the Nanostring. **A:** The effect of LPS on WT peritoneal cells. **B.** The effect of LPS on miR-17-92$^\Delta$ peritoneal cells. **C.** Comparison of PBS treated miR-17-92$^\Delta$ and WT littermate mice. **D.** Comparison of LPS treated miR-17-92$^\Delta$ and WT littermate mice. All data is FDR step-up corrected. X-axis show fold change and Y-axis show p-value.

work should be done to verify if the regulation of the cluster does effect macrophage communication and interaction with other cells, such as Th2 cells, and modulate their own responses.

As a test to see if there were any other measurable differences between the WT and miR-17-92$^\Delta$mice, the peritoneal CD11b+ cells from the LPS and PBS injected mice were analysed using 3' sequencing. 28768 genes in total were identified, with 1280 and 1097 genes up- and down-regulated in the miR-17-92$^\Delta$mice, and 1073 and 869 genes in the WT mice respectively, using FDR step-up correction for multiple comparisons. When comparing the WT and miR-17-92$^\Delta$samples directly, there was no difference observed when comparing the PBS injected mice. However, two genes were significantly different between the LPS treated samples, *Lyz1*, and *Gm20390* (Fig. 30 D). Neither of these genes harbor MREs for any of the miR-17-92 miRNA, indicating that the differences observed are not due to direct miRNA interaction with the transcripts, but are caused by some other means. *GM20390* is a transcript caused by the fusion of the *Nme2* and *Nme1* genes. As this has been identified by 3' sequencing only, it is possible, yet not necessarily the case, that the gene actually being identified is *Nme2*, as a BLAST confirmed that there is a striking similarity in the 3' end of *Nme2* and *GM20390*.

Interestingly, there are also differences, yet insignificant, in *Lyz2* and *Mir17HG* expression. It is likely that the miR-17-92$^\Delta$are trying to express more *Mir17HG*, in response to lowered levels of mature miR-17-92 miRNA. This mirrors what was seen when examining the expression of the Mir17HG by qPCR (Fig. 14).

Sera Cytokines
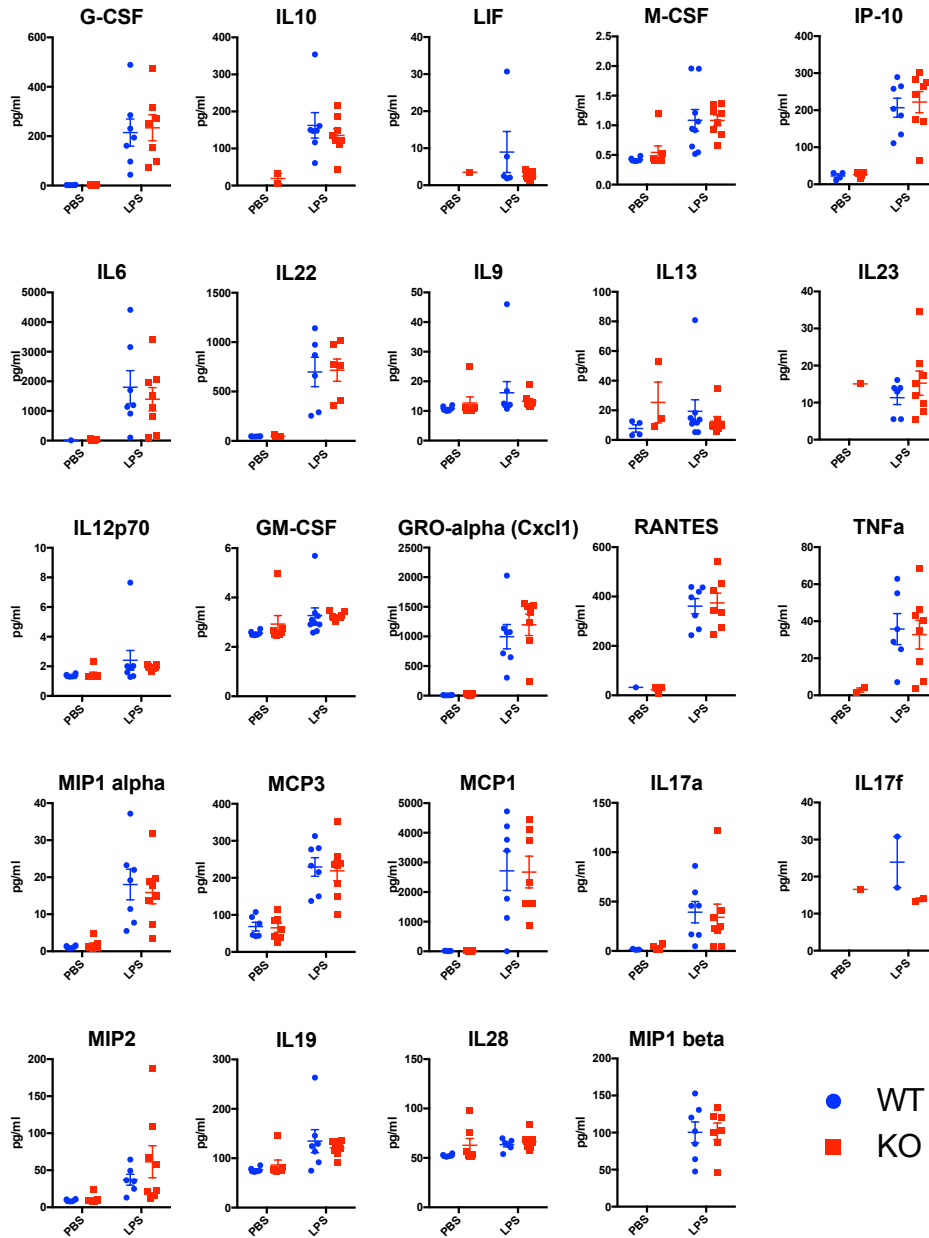
Figure 28:

In vivo cytokine detection from sera. Mice injected IP with either LPS or PBS were sacrificed and a small amount of blood was collected with EDTA. The sera from this was diluted 1:3 and measured using the Magpix multiplex custom assay. No statistical significance is observed when performing a 2 way ANOVA, with Tukey's multiple comparison test.

Peritoneal cytokines
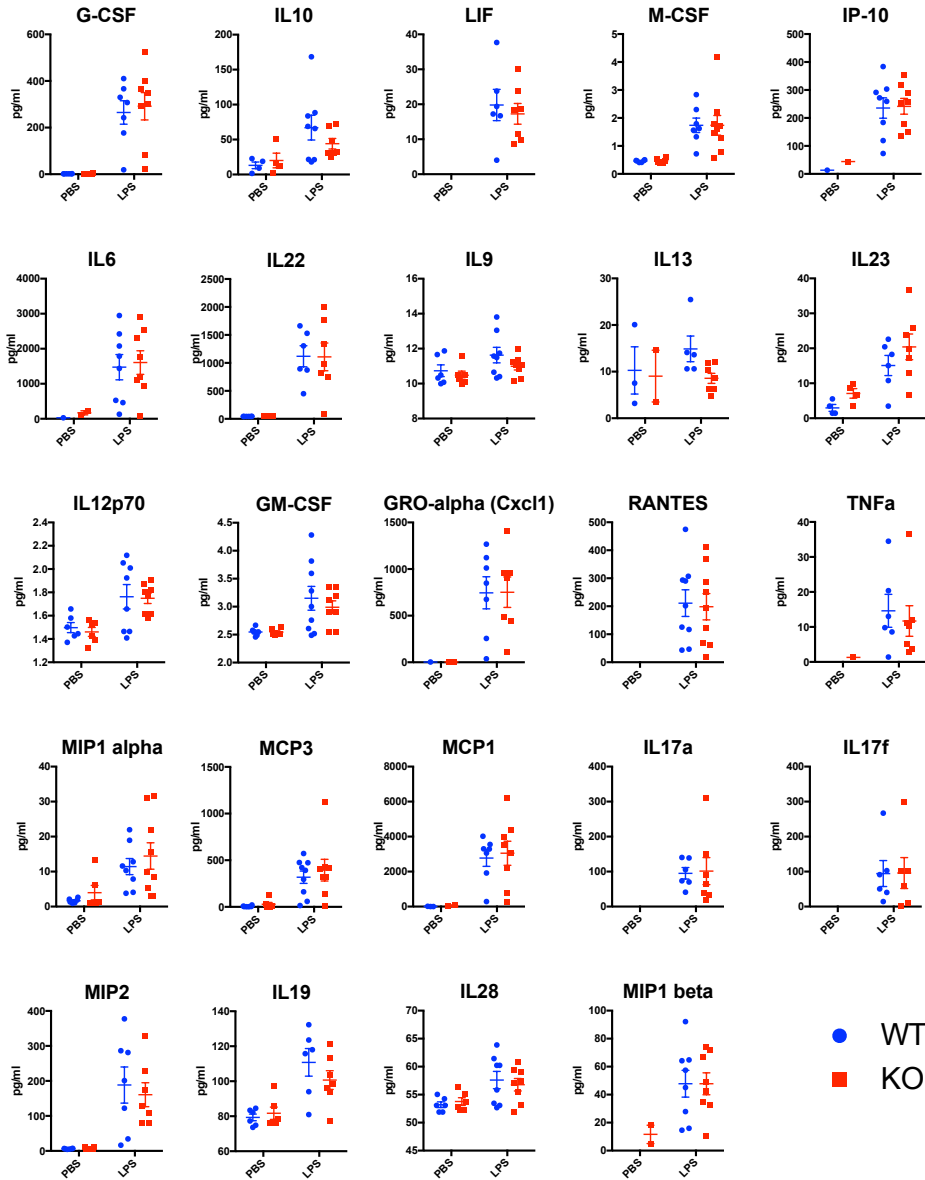
Figure 29:

In vivo cytokine detection from peritoneal lavages. Mice injected IP with either LPS or PBS were sacrificed and a peritoneal lavage was collected. This was diluted 1:3 and measured using the Magpix multiplex custom assay. No statistical significance is observed when performing a 2 way ANOVA, with Tukey's multiple comparison test.
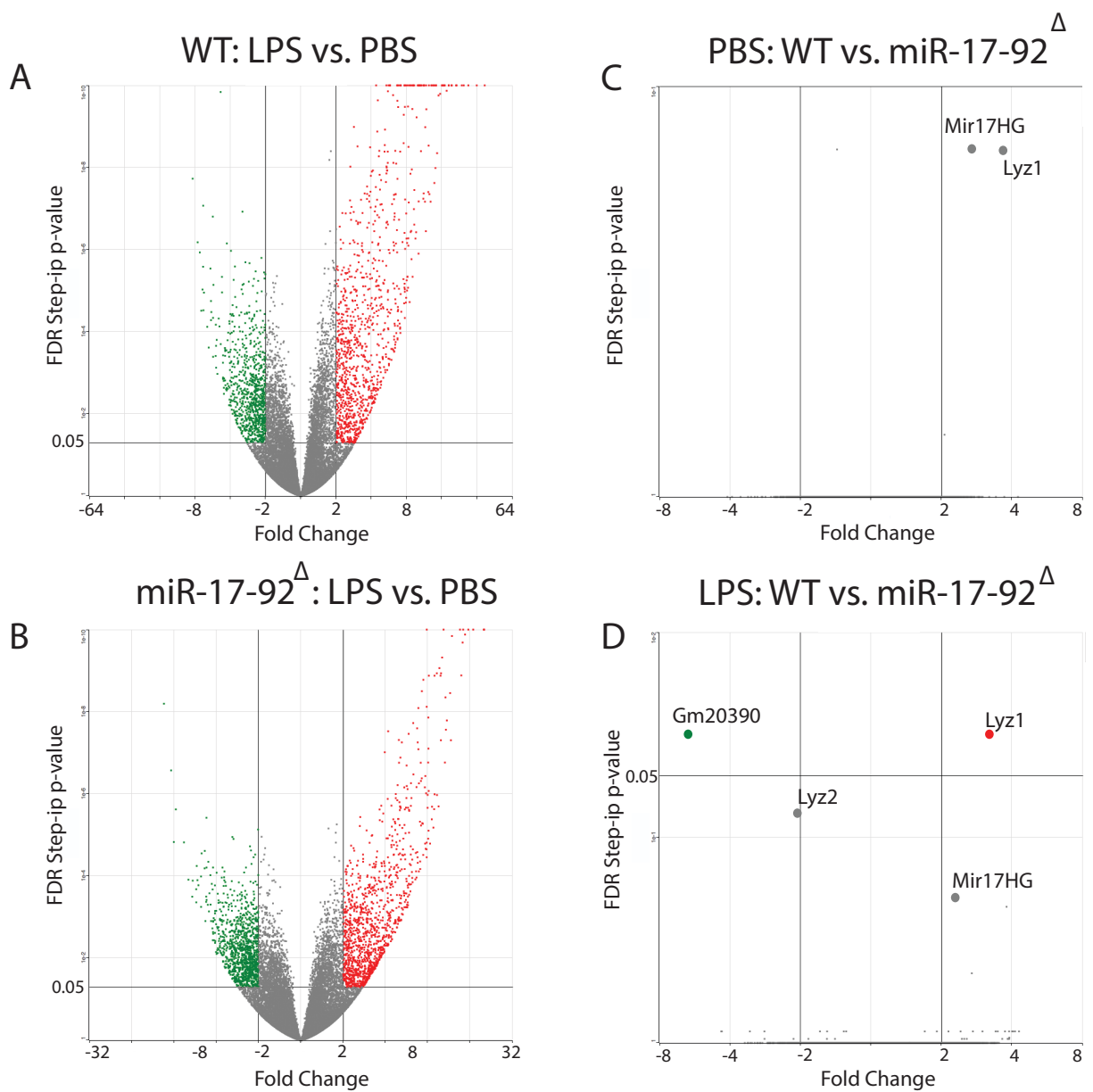
Figure 30:

3'-seq from CD11b+ peritoneal cells. Volcano plots of RNA-sequencing data from peritoneal cells *in vivo* experiment, using FDR corrected p-values. Comparison of **A.** LPS and PBS injected WT mice, **B.** LPS and PBS injected miR-17-92$^\Delta$ mice, **C.** PBS injected WT and miR-17-92$^\Delta$ **D.** LPS injected WT and miR-17-92$^\Delta$. Down-regulated genes are in green, and up-regulated genes are in red.

5 Discussion

This study focused on the role of the complete miR-17-92 cluster and its potential role regulating the innate immune response in macrophages. This is based on the work indicating that miR-19b targets *Tnfaip3*, *Rnf11*, *Kdm2a* and *Zbt16* [40]. This coordinated suppression of genes with similar roles meant that miR-19b could deftly promote NF-κB activity. These results relied on the use of AMOs, which are more than capable of sufficiently and specifically inhibiting miRNA activity, they are not physiologically representative of a diseased state where the miRNA are modified in an organism. To further this research, the miR-17-92$^\Delta$ mouse was generated to identify if perturbations of the miR-17-92 cluster as a whole would have effects on the innate immune system, specifically through NF-κB, in macrophages. The results from the experiments using this animal model however suggest that even though minor perturbations of miRNA are known to often cause disease, reduction of the miR-17-92 cluster does not have a huge effect in macrophages specifically.

miR-19a was recently discovered to be significantly upregulated following Tnfα stimulation of macrophage and dendritic cells from the colon in mice [133]. Its expression however is mostly associated with tumour tissues, not with normal tissues [133]. Furthermore, the same paper describes increased p-p65 and COX-2 following miR-19a mimic injection, and increased levels of both mRNA and protein of Tnfα, Il-1β, Il-6 and Il-17. However, in this study the epxression of this cluster decreased following stimulation, as observed in both mature miRNA (Nanostring, Fig. 26) and prim-miRNA forms(qPCR, Fig. 14). This highlights the contrasting nature of macrophages from different tissues, and the likelihood that regulation of powerful modulators, such as miRNAs is likely significantly different depending on the location and context of cells.

To further this point, it has been published that the miR-17-92 cluster must be down-regulated in macrophages for normal function, whereas enforced expressing inhibited macrophage maturation [115]. In a separate study, miR-17 and -20a down-regulation was found to be critical in monocytic cells because of a negative feedback loop, as the miR-17 family of miRNA repress the expression of RUNX1 [134]. This critical transcription factor is important for the maturation of haemopoetic progenitor cells to myeloid cells, and enhances the expression of the M-CSFR. These discoveries indicate that a relaxed expression of miR-17 is likely critical for normal macrophage function. Interestingly though, in the data here, expression of the *Mir17HG* is decreased following LPS stimulation. It is possible that this is a reaction to the regulation

of NF-κB signalling by the cluster. It is also possible that this lull in transcription is due to the overwhelming transcription of other genes in response to the LPS challenge.

However, it must be noted that the expression of the cluster in macrophages is still well-represented in the landscape of all miRNAs when following normal lab protocols to produce either L929, or M-CSF derived BMDMs. Indeed, while the expression is slightly reduced from total Bone Marrow (Fig. 8) in WT BMDMs, given there was no appreciable difference between miR-17-92$^\Delta$ and WT cells when it came to macrophage cytokine production. It is conceivable that loss of the miR-17-92 cluster has counteracting positive and negative effects, both inhibiting NF-κB activation and promoting macrophage maturation, effectively having opposing effects that results in a net lack of change.

Furthermore, other groups have claimed that the mir-17-92 cluster still has roles in macrophages, such as regulating autophagy proteins in cystic fibrosis [135]. Using antagomiRs, it was shown that miR-17 and miR-20a target both *Atg7* and *Atg16l1*, while mice that were injected intratracheally with antagomiRs had enhanced expression of these genes in their macrophages. These mice were also able to clear *Burkholderia cenocepacia* infection in the lungs better, presumably though autophagy-related mechanisms. An issue with this study is the reliance on huge doses of antagomiRs, resulting in non-physiological responses, especially as the little had been shown if there were any off-target effects of using such therapies [136].

A confounding observation is this study is that there is a reduction of Tnfα released from BMDMs infected with Cre-expressing virus, but no observed difference using the miR-17-92$^\Delta$ BMDMs (Fig. 5 and Fig. 13). It is possible that because the BMDMs for the viral experiments were infected 3 days after beginning of culture, by day 7, when the cells were used, we could observe a difference in cytokine release. The miR-17-92$^\Delta$ BMDMs should have Cre recombinase expressed from day 1 (Fig. 8), meaning the cells have had a reduced miR-17-92 expression for a longer time. There could conceivably be a compensatory mechanism that is unobserved in the cells infected with the Cre- virus that is confounding the results. Furthermore, Cre toxicity may also have a role to play, although was not further investigated in this study.

There are many complications when it comes to miRNA research, but it seems that there are also many redundancies in miRNA expression too that are, as of yet, not well understood. In the CD11b+ cells from the peritoneum of miR-17-92$^\Delta$ mice , levels of miR-125 and miR-221 are elevated, and both are also published to target A20 (Fig. 26) [95, 137]. While it is unclear wether the loss of the miR-17-92 cluster directly deregulated the expression of these

miRNAs, or if the expression of other transcription factors has been affected, it does indicate that the modulating the miR-17-92 cluster does affect the expression of others. This shift in the expression of so many miRNA, such as miR-125, which have competing effects of the miR-17-92 cluster, would allow stabilising the expression of genes. This might alleviate the effects initially hypothesized to be observed. Significant care must be taken when claiming that a miRNA regulates a certain gene, as physiological contexts may allow for these redundancies to be tolerated. This represents another facet where the miR-17-92 cluster may have opposing effects, especially when examining macrophage function [115, 134]. As an example, while miR-19 has been shown to be a positive regulator of NF-κB signaling [40], miR-20 is a negative regulator [12]. Strong modulation of a single miRNA or group of miRNA may not translate to a physiological state.

One critical problem with the model generated in this study is the deletion of the miR-17-92 cluster was incomplete in all tissues tested. While the deletion is most prominent in both BMDMs and peritoneal cells, there is no observable reduction in miRNA in either the blood or splenic CD11b+ fraction (Fig. 10). However, the original paper that describes the invention of the LysM-Cre mouse indicates that there are between 83-90% deletion of the target gene observed in the splenic fraction and peritoneal fractions, and attributes this to the residual macrophages within that are highly differentiated [100]. It is intriguing that there is poor deletion observed in the splenic and peripheral blood compartments, as both these populations of cells are usually old enough to observe cre-driven deletion. This raises several possibilities; the miR-17-92 cluster, or miRNAs within, are critical for the survival of circulating macrophages, the cell turnover in these compartments is too quick to observe effects, or that there is not enough LysM-Cre induction, resulting in a lack of deletion [116]. However, as previously noted, deletion of the cluster is not compatible with life, and generating miR-17-92KO lines using cre-recombinase does have difficulties regarding cell proliferation [37, 42]. It is also perhaps not the fault of the LysM-Cre model, as it has been used successfully for other miRNA research, where the cells survived [66]. In future studies, an inclusion of a LysM-Cre mouse without a gene-flox would be advisable, given that there are reports that intracellular DNA fragments from Cre-recombinase activity can activate STING [138]. While there are no aberrant STING or interferon responses observed in this study, it may also explain the significance of the difference in *Lyz1* expression in the sequencing data (Fig. 30).

Gut microbiota explains many susceptibilities to diseases [139]. Much variation due to gut micro-

biota can be explained due to cage differences where the mice are housed [140]. Furthermore, as mice that are littermates are stored in the same cage together, depending on their sex, it makes it ideal in this study to examine littermate control mice while investigating miR-17-92fl/fl mice. Of interest, no papers were found outlining the effect of cage differences and drift on the expression of miRNA, and in peritoneal cells. While it is quite likely that the differences in miRNA expression or just artifacts of the parental genetic background, if this is the case it would really speak volumes to how small the changes are in miRNA expression in direct response to the loss of the miR-17-92 cluster.

One possibility that must be entertained is that by perturbing this cluster alone, other miRNA may fill in the void left. miRNA regulate the expression of protein noise by decreasing the noise of lowly expressed proteins, however they increase the noise of highly expressed genes [141]. As indicated by the Nanostring of total miRNA from the peritoneal cells of mice, the global miRNA noise is enhanced following the deletion of the miR-17-92 cluster. It is possible that then genes such as A20 have more noise at lower expression levels now that the regulating miRNA are removed, however when stimulated, their noise levels are left unchecked, allowing for more variability. This variability is unpredictable, and thus, in a mixed population of cells, any effect is lost due to noise.

However, other evidence is more direct, as miR-125a and b are both inhibitors of A20 [95]. Interestingly, both of these miRNA are expressed higher in the KO cells than the WT cells when looking at the nanostring data of the peritoneal cells from the *in vivo*. This may then explain how there is no observable effect on A20 in the KO cells, Furthermore, there may be other more complicated means of the cell regulating dysregulation of the miR-17-92 cluster that have not be appreciated yet.

Other groups have also attributed miR-19 as a major component of inflammation. Injection of miR-19a mimics into the peritoneum of mice enhanced the formation of colon cancers in a DSS + azoxymethoane driven colitis-associated colon cancer model. The study also shows enhanced sera presence of several cytokines including Tnfα, IL-6 and Il-1β, to name a few. The paper further attributes this progression in cancer to miR-19a targeting *Tnfaip3* in tumours. Of critical note though, this model is flawed, as injection of mimics enhances the expression many thousand-fold, and brings some questions of physiological relevance. There is also no mention of how the mimics are taken up by cells, only the enhanced expression in tumours of ~1.7 fold [133]. The model that is used here in this study represents a more physiological representation

of miRNA dysregulation.

The delicate interplay between miRNAs and targets following stimulation was eloquently examined by Mann et al recently, where miR-155 was induced rapidly following stimulation and NF-κB activation. miR-155 inhibited *SOCS1* and *SHIP1,* allowing for a robust and full response. This ensured a later induction and accumulation of miR-146a, which could inhibit *IRAK1* and *TRAF6,* leading to a smooth but quick decrease in inflammatory responses and miR-155 expression, which release *SOCS1* and *SHIP1* expression once more, further accelerating the shutdown of inflammatory response. This study also uses the LysM-Cre model for myeloid specific deletion of miRNA, indicating that this model is a viable model for miRNA research [66].

Many previous studies have found that miRNA interaction with mRNA leads to reductions in mRNA that are also correlated with changes in protein levels [127, 128, 129]. However, a more recent paper has indicated that the miR-17-92 cluster does not necessarily regulate gene expression at the transcriptional level, but has a greater observable effect at the protein level [142]. There may be more merit in trying to observe effects on direct targets by means other than qPCR then. While this may be the case, there however is still no change of protein as determined by western blot, nor cytokine release, when investigating the miR-17-92$^\Delta$ cells. This however does not exclude the possibility of transcriptional differences that are a result of protein dysregulation in genes such as A20.

Further complicating the matter, A20 expression is regulated by NF-κB, which in turn downregulates its own expression. By disrupting the miR-17-92, and hopefully stabilising A20 expression, there would be reduced NF-κB activity, but conversely, lower A20 expression too. It would therefore be difficult t fully characterise the anti-inflammatory role of the miR-17-92 cluster through measurements of A20, and may explain why there is no observable change in A20 expression by protein analysis.

Moreover, there are reports that indicate changes to miRNA expression does not correlate to an appreciation in their function [143], and that only highly expressed miRNAs tend to show significant target repression [144]. This is a potential reason why there is no observable effect of reducing the miR-17-92 cluster in macrophages in this study; that the expression is too low in the first place. Furthermore, by altering the expression, there is potentially not a distinct change in their loading, and so the cell continues to behave as normal. This may be entirely why there is little literature on the role of the miR-17-92 cluster in macrophages, but why there is a relative glut in research using B-cells.

This lends credence to the use of CLIP experiments to investigate the effect of the miR-17-92 cluster and targeting direct mRNA targets. While the experiments performed for this thesis were not a complete success, previous efforts in PAR-CLIP of EBV-infected Human B-cells had promising results [145]. While the data was not acquired from true miR-17-92 overexpressing/knockout cells, they are still useful to identify *bone fide* miR-17-92 targets. Among the targets identified included *RNF11, TNFAIP3, SOCS1* and *CYLD*, and other metabolic genes including *HIF1α*. This still lends hope to the fact that the miR-17-92 cluster does regulate negative regulators of NF-κB, however, as this data was collected in B-cells, this is not representative of the biology in macrophages, indicating that they must still be investigated further.

An area that has not been explored in this current study is the possibility of long non-coding RNA (lncRNA) regulation of the miR-17-92 cluster. It has been hypothesized that lncRNA may regulate miRNA expression via binding and sequestering them away from functional targets [146]. There is huge diversity of lncRNA in its many forms available and expressed from the genome [147, 148, 149], and lncRNA are known to have roles in the progression of innate immune diseases and cell types [150]. Furthermore, miR-19 has been posited to be regulated by HOTAIR, a more well-known lncRNA, where its expression was inversely proportional to HOTAIR expression, which alleviated the regulation of PTEN [151]. HOTAIR is considered pro-inflammatory, and while most of its effects are as a scaffold molecule (reviewed in [152]), it is overexposed in PBMCs from Arthritis patients [150], it enhances CCL2 expression [153] and also TNFα due to enhanced expression in sepsis conditions [154]. Furthermore, more recently, another lncRNA, circ-ITCH has been described, and credited in regulating miR-17 [155]. It would be interesting to investigate if changes of the miR-17-92 cluster also change the expression of other lncRNAs.

6 Conclusion

Previous work has established members of this cluster as pro-inflammatory, regulating T cell, B cell and epithelial cell driven inflammation. This study tried to investigate wether the miR-17-92 cluster has an appreciable effect on the function of macrophages in the context of inflammatory diseases. While the miR-17-92 cluster was successfully reduced in macrophages *in vivo* and ex vivo by greater than 50%, which is reasonable to assume in a physiological context, surprisingly there was no appreciable change to the function and response of macrophages to immune stimuli. It is likely that the miR-17-92 cluster affects other pathways and genes more than the hypothesized targets, such as *Tnfaip3*. This is because miRNAs role in cells is context dependent, and the abundance of other, yet unappreciated targets, is greater.

Furthermore, stimulation of the macrophage reveals there is a small difference in metabolic processes, however there is no appreciable difference when examining cytokine release and gene expression, when analysed using a custom modular Nanostring kit. When examining the function of macrophages *in vivo*, it appears that there are changes to the expression of other miRNA, yet this does not translate to changes in either cytokine release nor gene expression.

Together, these results indicate that while the miR-17-92 cluster does play a role in inflammatory diseases in other cells types, it likely does not contribute to the primary cytokine response from macrophages. This highlights firstly, the different roles that miRNA play in different tissues and cell types, and seondly, that *in vitro* studies do not always translate to *in vivo* physiological results. It is possible that using other methods to dampen the effect of the miR-17-92 cluster may yield different results, however physiological relevance is brought into question then.

This study is not exhaustive, and there is some evidence that indicates there are potentially competing effects of the miR-17-92 cluster in macrophages. Further investigation into the binding of miR-17-92 cluster members could potentially reveal as-yet undiscovered redundancy mechanisms in macrophages. Furthermore, inhibition and analysis of individual miRNA from the miR-17-92 cluster may yield interesting results that may not be compounded by reducing expression of the entire cluster of miRNA. These experiments could investigate other roles for these miRNAs in macrophages, including inflammation, activating and facilitating responses of other cells, and initiating Type 2 response from T cells.

7 Supplementary Information

7.1 Publications of miR-17-92 cluster members regulating genes.

While miRNA analysis using algorithms to predict binding works reasonably well, it does not always translate to biological action. Following from the information in Fig. 6, supplementary table 6 provides an up-to-date list of research articles that show interaction of members of the miR-17-92 cluster and genes involved in the regulation of innate immune signalling and responses.

Gene	miRNA family	Publications
Tnfaip3	miR-19, miR-18	[40, 42, 45]
Rnf11	miR-19	[40, 97]
Fbxl11	miR-19	[40]
Cyld	miR-19	[98]
Atg16l1	miR-17	[156]
Itch	miR-17	[157]
Ikzf1	miR-92	[158, 159]
Ikzf4	miR-17	[160]
Socs1	miR-19	[161, 42]
Socs3	miR-19	[96, 162]
Socs6	miR-17	[163]
Hif1a	miR-17, miR-18	[164, 122, 121]
Pten	miR-19, miR-17, miR-92	[39, 158]
Fxr1	miR-92	[165]
S1pr1	miR-17, miR-19, miR-92	[159]
Bcl2l11	miR-19, miR-17, miR-92	[166, 37, 158]

Table 9:
List of publications that confirmed miR-17-92 regulation of negative regulators of NFkB.

7.2 2'OMe AMO sequence specific binding of TLR7

Figure 31 was generated from experiments performed and published in the paper "Sequence-dependent off-target inhibition of TLR7/8 sensing by synthetic microRNA inhibitors" [136]. By transfecting AMOs into BMDMs using DOTAP, a common method to deliver small RNA molecules, and subsequently stimulate TLR7, there was a reduction in TNFa release by inhibiting miR-19a and interestingly with miR-92a as well. However, the use of a 2'OMe control non-targeting AMO reduced the release of mTNFa further, when compared with a non-2'OMe control RNA. Importantly, when using miR-17-92$^\Delta$ BMDMs, with reduced miR-17-92 expression, this inhibitory effect is still observed, indicating that the observed phenomenon is not dependent on the AMOs
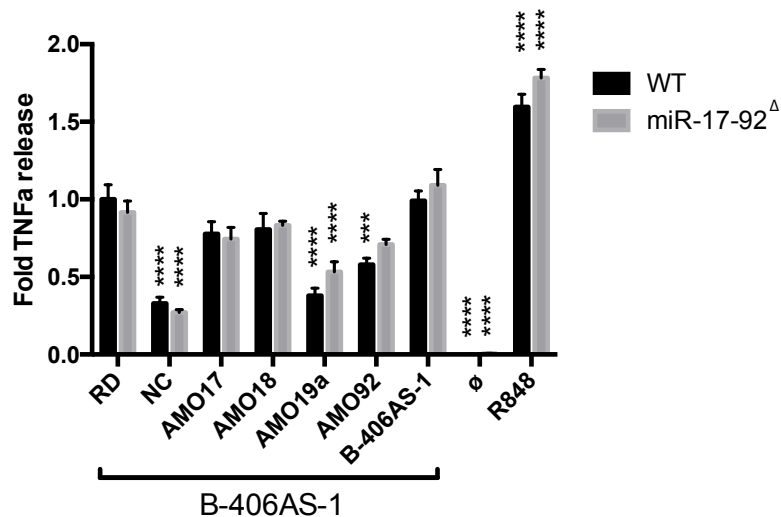
Figure 31:

Zen AMO off target effects. BMDMs of miR-17-92$^\Delta$ mice or littermate controls were isolated and transfected with 40 nM of the indicated 2′OMe AMO or non-2′OMe control RNA (RD) endo-somally using DOTAP, then stimulated with 180 nM of the ssRNA B-406AS-1. After overnight stimulation, the supernatants were tested for mTNFa release. Data is of 3 independent experiments, and normalised to RD. Two-way ANOVA was performed comparing the RD control, with Dunnett's multiple comparisons test, and an alpha set to 0.05.

ability to target and sequester miRNA, but rather inhibit TLR7 signalling itself.

From this, the authors then began to investigate how 2′OMe AMOs can bind, but not activate TLR7 in a sequence-dependent manner. This provides a another complication to AMO-dependent miRNA research that users must be considerate of.

7.3 Khsrp regulation of miRNA modulated by the aberrant expression of miR-20a

KH-type splicing regulatory protein (Khsrp) interacts with and regulated many mRNA expression in cells, and in 2009 was discovered to also regulate and promote the expression of many miRNAs too [34]. By knocking down Khsrp, the expression of several miRNA was significantly reduced (between 1.2 and 1.5 fold). Among these miRNA is miR-20, the most highly expressed of the miR-17-92 cluster in macrophages. Interestingly, even though its expression is very high, the accessibility of Khsrp to its binding site is very difficult in the folding of the pri-miR-17-92 molecule. By taking the miRNAs that were reduced in Khsrp knock-down conditions of THP-1 cells, and examining their expression from peritoneal CD11b+ cells extracted from PBS injected mice, many of these miRNA are expressed at a slightly higher level with reduced miR-

17-92 expression. This could indicate that by reducing Khsrp-processable miR-20a, it allows for Khsrp to bind and mature many other miRNA.
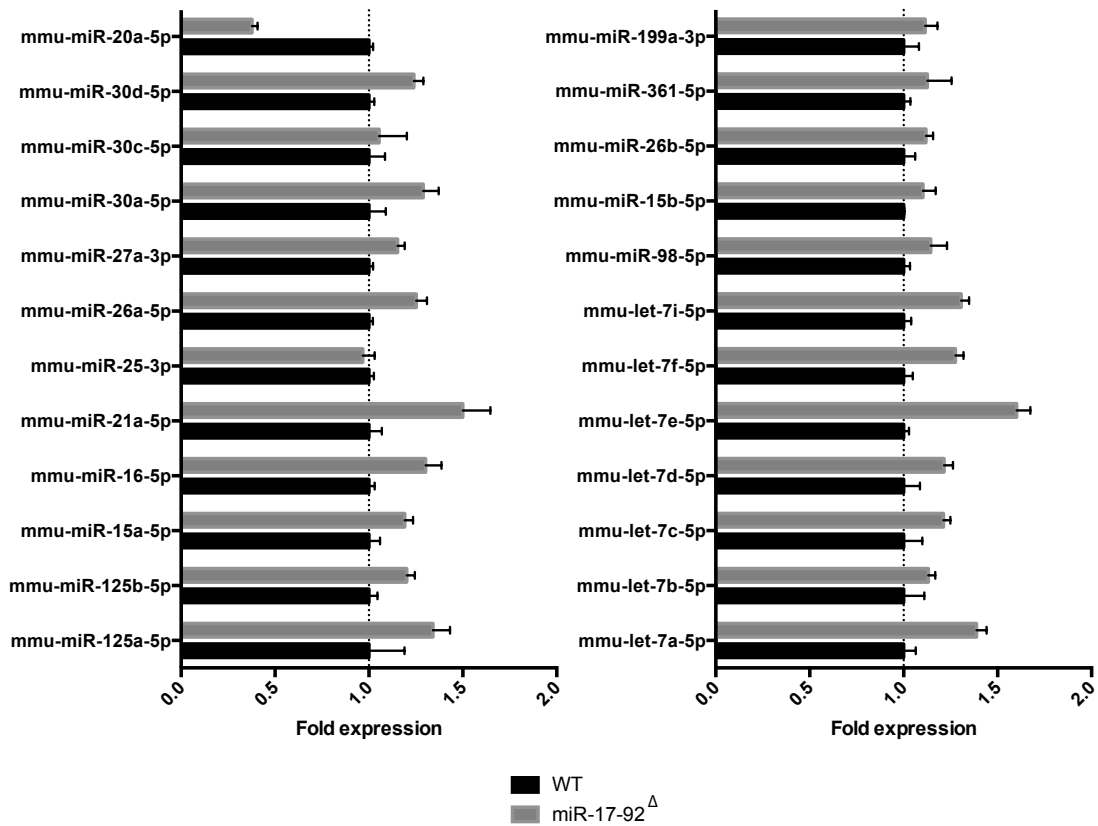
Figure 32:

Fold change of Khsrp regulated miRNA. Expression of miRNA from PBS injected mice that are known to be regulated by Khsrp. Expression is represented as fold change over the WT expression.

7.4 QAQC of 3'-sequencing of RNA from CD11b+ peritoneal cells.

To compliment the sequencing performed using the *in vivo* samples, Supplemental figure 33 shows that the samples performed the same an were all high quality, however when examining the differences, there was little to discern. Importantly, the difference in LPS compared to untreated was far more significant than the difference in the genotype, regardless of wether the sample was stimulated or not. Furthermore, when comparing the samples they would not cluster with the genotype, instead only by stimulation, with some outliers. This indicates that even though the mice had a reliable knock down of miRNA, this did not translate to an appreciable difference in gene expression anywhere in the transcriptome.
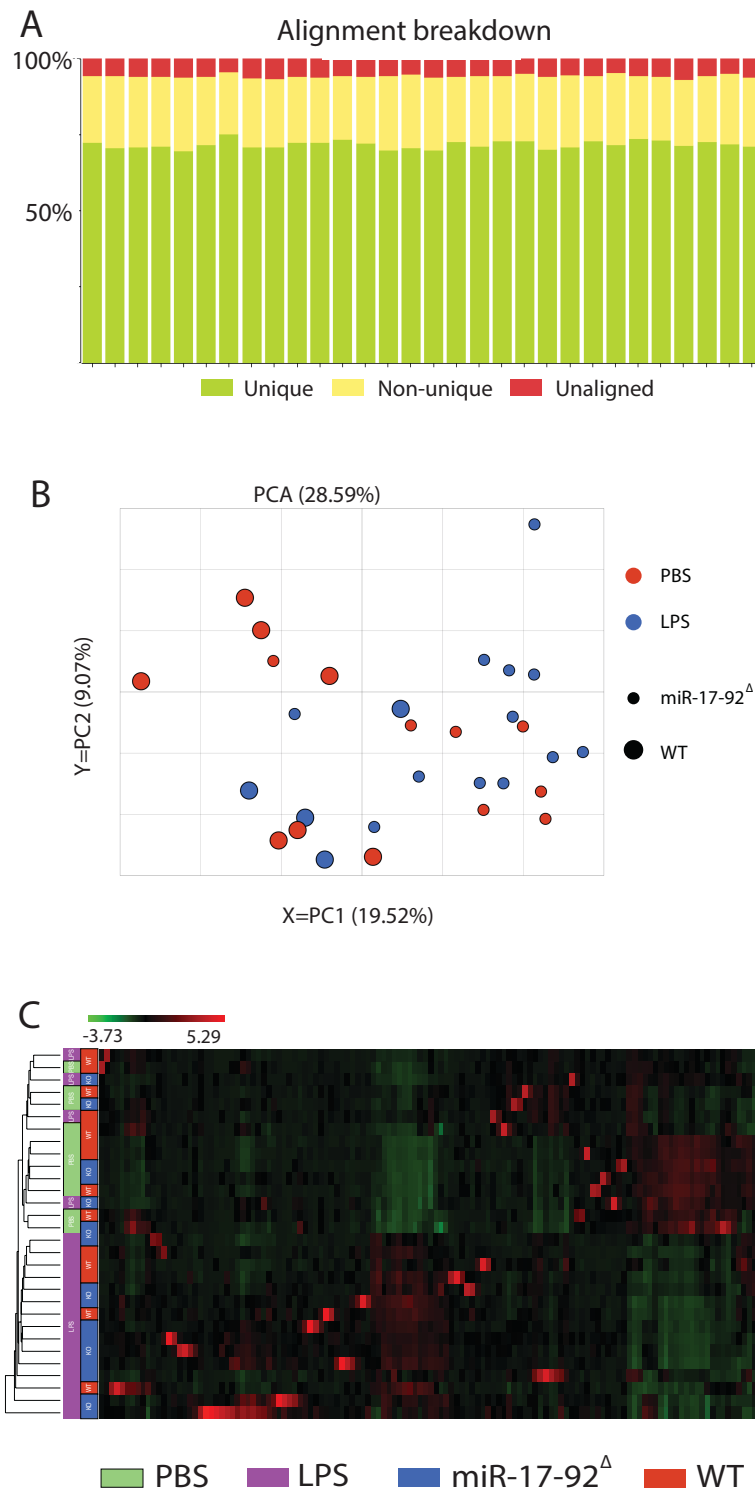
Figure 33:

Post-Alignment QAQC from Sequencing data. A. The overall quality of the reads was excellent, indicating that the results were reliable. **B.** The PCA of all samples indicates that the difference in LPS stimulation is greater than the differences caused by the genotypes. C. Heatmap with clustering using Euclidean distance, showing that the treatment of the samples clusters much more reliably than the genotypes.

7.5   Log2 Gene expression as determined by Nanostring

Table 10 (until page 91) has a list of the expression values of all genes analysed with the Nanostring, and used in Figure 62. P-values, corrected for multiple comparisons with the Bonferroni test (Extremely stringent) are included. Importantly, the BMDMs responded extremely well to LPS. However, the differences between the two genotypes are negligible. Some genes, such as *Cyld*, does show a significant change following stimulation in the miR-17-92$^\Delta$, but not in the littermate controls. There is however, no significant differences between the miR-17-92$^\Delta$ and littermate controls, indicating that there are subtle, yet potentially insignificant changes to gene expression.

| Gene Name	Mean expression log2				Bonferroni corrected p-values			
	WT LPS	miR-17-92$^\Delta$ UT	WT LPS	miR-17-92$^\Delta$ LPS	KO vs WT LPS	KO vs WT UT	LPS vs UT KO	LPS vs UT WT
Acadm	10.48	10.56	10.26	10.40	1	1	1	0.39
Actb	17.79	17.76	17.79	17.77	1	1	1	1
Ager	3.69	3.66	3.55	3.49	1	1	1	1
Aim2	7.73	7.96	7.84	8.03	1	1	1	1
Ass1	10.66	10.78	10.99	11.14	1	1	0.27	1
Atat1	7.14	7.15	7.47	7.46	1	1	0.23	0.39
Atf3	11.27	11.32	11.32	11.23	1	1	1	1
Atp5J	11.04	11.05	11.05	11.11	1	1	1	1
Bst2	12.64	12.54	12.66	12.57	1	1	1	1
Casp1	10.22	10.28	10.75	10.71	1	1	3.12E-03	6.78E-04
Casp4	9.10	9.03	11.33	11.31	1	1	2.23E-12	6.81E-11
Casp8	9.15	9.08	9.06	8.96	1	1	1	1
Ccl17	3.36	3.67	7.05	6.65	1	1	2.08E-04	3.59E-05
Ccl2	11.91	12.27	14.83	14.55	1	1	0.33	0.09
Ccl20	3.36	3.59	5.76	5.46	1	1	7.98E-03	1.08E-03
Ccl22	5.31	5.50	8.84	8.42	1	1	2.82E-06	5.19E-07
Ccl3	11.23	11.77	15.32	15.22	1	1	3.79E-03	1.58E-03
Ccl4	9.54	10.13	14.83	14.68	1	1	8.80E-04	4.54E-04
Ccl5	8.33	8.60	12.92	12.46	1	1	1.71E-03	6.64E-04
Ccl7	10.37	10.69	12.80	12.54	1	1	1	0.69
Cd40	6.67	6.87	12.01	11.72	1	1	1.59E-07	2.21E-07
Ch25h	8.15	8.80	11.40	11.39	1	1	9.94E-03	1.90E-03
Chuk	9.62	9.64	9.84	9.83	1	1	0.03	0.02
Clec4e	10.18	10.57	13.81	14.05	1	1	2.60E-12	1.60E-11
Cltc	13.12	13.12	13.07	13.11	1	1	1	1
Csf3	2.96	3.39	6.94	6.42	1	1	9.63E-04	6.34E-05
Cxcl1	7.17	6.89	14.42	14.83	1	1	4.86E-23	1.77E-20
Cxcl10	8.10	8.08	13.86	13.70	1	1	7.48E-11	6.50E-10
Cxcl2	10.46	10.31	16.30	16.61	1	1	1.02E-25	2.46E-23
Cxcl3	6.02	6.17	12.36	12.59	1	1	8.09E-19	2.80E-17
Cxcl5	3.85	4.07	5.58	5.75	1	1	0.07	0.17

Table 10: ***Gene expression between miR-17-92$^\Delta$ and WT BMDMs.***

Gene Name	WT LPS	miR-17-92$^\Delta$ UT	WT LPS	miR-17-92$^\Delta$ LPS	KO vs WT LPS	KO vs WT UT	LPS vs UT KO	LPS vs UT WT
Cyld	8.92	8.99	9.24	9.31	1	1	0.03	0.12
Ddit3	9.66	9.65	9.20	9.37	1	1	1	1
Ddx41	3.10	3.16	3.57	3.49	1	1	1	1
Dectin1	11.13	11.17	11.01	11.14	1	1	1	1
Edn1	3.11	3.91	9.26	8.81	1	1	1.24E-03	1.92E-04
Eef1g	13.66	13.60	13.68	13.65	1	1	1	1
G6pdx	12.21	12.20	12.00	12.05	1	1	0.40	0.03
Gapdh	15.68	15.69	15.70	15.68	1	1	1	1
Gbp1	3.19	3.25	3.79	3.46	1	1	1	1
Gbp2	8.02	8.10	10.24	10.05	1	1	6.21E-05	4.66E-05
Gbp3	7.61	7.64	9.96	9.80	1	1	9.44E-06	1.64E-05
Gls	11.31	11.40	11.65	11.71	1	1	5.72E-03	8.41E-03
Got1	10.80	10.68	10.65	10.62	1	1	1	1
Gpt	6.33	6.27	6.17	6.30	1	1	1	1
Gsto1	10.84	10.84	10.94	10.95	1	1	0.06	1
Hk1	10.94	11.00	11.11	11.13	1	1	1	1
Hprt	10.01	10.07	10.09	10.11	1	1	1	1
Hsa90aa1	12.76	12.84	13.19	13.21	1	1	0.01	9.28E-03
Idh2	9.25	9.19	9.13	9.05	1	1	0.48	1
Ifi204	11.45	11.34	12.04	11.85	1	1	1	1
Ifit2	9.25	9.24	10.57	10.30	1	1	1	1
Ifit3	10.54	10.35	10.97	10.74	1	1	1	1
Ifitm3	13.82	13.93	14.24	14.22	1	1	1	0.29
Ifna1	3.61	3.59	3.48	3.62	1	1	1	1
Ifnb1	3.25	3.29	7.42	6.80	1	1	9.36E-04	3.39E-04
Ifng	3.82	4.00	4.69	4.35	1	1	1	0.29
Ikbkb	9.75	9.89	10.65	10.59	1	1	2.09E-03	2.60E-04
Ikbkg	9.50	9.58	9.39	9.49	1	1	1	1
Il10	5.89	5.91	10.12	9.63	1	1	1.75E-06	1.28E-06
Il11	3.61	3.65	4.21	4.07	1	1	1	1
Il12a	3.20	3.51	4.86	4.68	1	1	0.06	2.65E-03
Il12b	3.14	3.78	9.56	9.45	1	1	1.59E-06	1.23E-06
Il13	3.96	3.63	4.68	4.52	1	1	9.99E-03	0.37
Il15	8.28	8.34	10.31	9.98	1	1	7.29E-03	1.60E-03
IL16	6.41	6.66	5.74	6.08	1	1	3.60E-03	1.97E-03
Il18	7.68	7.68	8.05	7.97	1	1	1	1
IL18bp	7.20	7.23	7.38	7.39	1	1	1	1
Il18r1	3.87	3.77	4.73	4.70	1	1	0.22	1
Il1a	4.61	4.91	13.36	13.31	1	1	7.17E-11	4.13E-10
Il1b	7.21	7.11	15.23	15.43	1	1	2.72E-17	1.80E-15
Il1r1	5.63	5.39	5.95	5.96	1	1	0.10	1
Il1r2	5.93	6.12	6.32	6.44	1	1	1	1
Il1rap	7.83	7.84	8.08	8.08	1	1	0.03	0.10
Il1rl1	5.43	5.36	5.79	6.02	1	1	1	1
Il1rl2	5.43	5.51	5.85	5.95	1	1	0.80	1
Il1rn	10.69	10.86	13.06	12.78	1	1	0.01	2.58E-03
Il23a	3.64	4.21	9.37	8.81	1	1	9.45E-04	1.58E-04

Table 10: *Gene expression between miR-17-92$^\Delta$ and WT BMDMs.*

Gene Name	miR-17-92$^\Delta$ WT LPS	UT	WT LPS	miR-17-92$^\Delta$ LPS	KO vs WT LPS	KO vs WT UT	LPS vs UT KO	LPS vs UT WT
Il27	4.29	4.52	8.47	8.09	1	1	7.89E-04	3.79E-04
Il33	4.08	4.27	5.00	4.72	1	1	1	0.03
Il6	3.70	4.31	9.92	9.73	1	1	9.29E-06	5.53E-06
Irak1	9.96	10.00	9.80	9.83	1	1	2.34E-03	0.02
Irak3	8.01	8.29	9.49	9.55	1	1	2.16E-03	1.09E-03
Irak4	9.65	9.66	9.31	9.42	1	1	0.09	3.67E-03
Irf3	9.15	9.19	9.23	9.30	1	1	1	1
Irf7	9.64	9.56	10.18	9.96	1	1	1	1
Irg1	8.42	8.82	14.35	14.60	1	1	1.04E-12	9.44E-12
Isg15	10.46	10.53	12.92	12.58	1	1	0.04	0.02
Itch	9.92	9.96	9.94	9.96	1	1	1	1
Ldha	14.19	14.14	14.18	14.15	1	1	1	1
Map3k7	9.46	9.45	9.55	9.62	1	1	7.87E-04	1
Mapk14	10.03	10.07	10.29	10.29	1	1	1	1
Mapk3	11.54	11.53	11.50	11.53	1	1	1	1
Mb21d1	7.52	7.72	8.45	8.37	1	1	1	0.17
Mdh2	11.92	11.90	11.89	11.90	1	1	1	1
Mefv	5.20	5.48	7.70	8.05	1	1	1.57E-11	4.63E-10
Mnda	11.94	11.91	13.54	13.36	1	1	0.01	0.01
Mx2	6.73	6.64	9.46	9.03	1	1	0.15	0.12
Myd88	9.58	9.71	10.60	10.57	1	1	4.31E-05	1.40E-05
Naip2	9.75	9.90	9.68	9.79	1	1	1	1
Naip5	7.37	7.46	7.08	7.23	1	1	1	1
Naip6	7.91	7.93	7.63	7.65	1	1	0.51	1
Nfe2L2	12.62	12.69	13.29	13.50	0.92	1	3.93E-11	5.18E-08
Nfkb1	10.73	10.82	12.65	12.57	1	1	1.90E-05	2.56E-05
Nfkbia	12.39	12.38	16.07	16.08	1	1	2.65E-29	8.68E-28
Nfkbib	8.95	9.09	11.19	11.08	1	1	9.97E-08	8.72E-08
Nlrc3	8.44	8.42	7.74	7.84	1	1	7.81E-05	2.75E-05
Nlrc4	7.24	7.29	7.88	7.92	1	1	1.95E-03	7.36E-03
Nlrc5	7.74	7.78	7.97	7.95	1	1	1	1
Nlrp10	4.70	4.64	4.40	4.50	1	1	1	1
Nlrp12	3.13	3.07	3.63	3.57	1	1	1	1
Nlrp1a	6.52	6.45	5.94	6.01	1	1	0.08	0.01
Nlrp1B	5.55	5.54	5.26	5.29	1	1	1	1
Nlrp3	10.67	10.94	13.44	13.51	1	1	3.28E-10	8.11E-10
Nlrp6	3.05	3.07	3.31	3.24	1	1	1	1
Nlrx1	6.72	6.88	5.98	6.19	1	1	4.61E-04	1.02E-03
Nod1	6.65	6.74	8.09	8.08	1	1	5.66E-06	1.24E-05
Nod2	6.60	6.74	10.09	10.25	1	1	4.15E-16	1.01E-14
Oas1b	5.69	5.67	6.33	6.06	1	1	1	1
Oas1g	9.47	9.55	10.16	10.05	1	1	0.91	0.13
Oas3	8.77	8.69	8.91	8.83	1	1	1	1
Oaz1	13.56	13.58	13.56	13.61	1	1	1	1
Otud7b	8.48	8.37	8.63	8.51	1	1	1	1
Peli1	9.87	10.03	12.40	12.26	1	1	3.45E-05	2.70E-05
Pgd	13.14	13.14	13.01	13.05	1	1	1	0.31

Table 10: *Gene expression between miR-17-92$^\Delta$ and WT BMDMs.*

Gene Name	miR-17-92$^\Delta$ WT LPS	UT	WT LPS	miR-17-92$^\Delta$ LPS	KO vs WT LPS	KO vs WT UT	LPS vs UT KO	LPS vs UT WT
Phgdh	8.78	8.83	8.90	8.99	1	1	1	1
Pik3ap1	12.91	12.88	12.93	12.88	1	1	1	1
Pkm1	13.61	13.62	13.49	13.51	1	1	0.06	0.06
Pkm2	13.63	13.68	13.50	13.55	1	1	0.03	0.08
Ppia	15.49	15.56	15.51	15.60	1	1	1	1
Ppm1a	10.00	10.07	10.32	10.39	1	1	1.71E-05	8.59E-05
Prkaa1	10.52	10.53	10.48	10.53	1	1	1	1
Prps1	7.51	7.50	7.41	7.51	1	1	1	1
Ptgs2	7.27	7.30	12.46	12.55	1	1	7.11E-09	1.17E-07
Pycard	6.48	6.63	6.44	6.35	1	1	1	1
Rela	10.65	10.71	11.61	11.62	1	1	1.16E-08	5.48E-08
Relb	9.14	9.06	11.05	11.13	1	1	1.76E-16	3.31E-14
Ripk1	8.62	8.63	8.19	8.18	1	1	2.15E-04	2.16E-03
Rnf11	8.84	8.95	9.18	9.25	1	1	0.02	0.02
Rpl19	14.58	14.60	14.73	14.75	1	1	1.72E-06	7.94E-06
Rps6ka5	7.12	7.37	8.75	8.64	1	1	1.33E-03	1.30E-04
Rsad2	8.83	8.82	11.33	11.05	1	1	8.59E-03	7.94E-03
Saa3	6.12	6.57	12.10	12.00	1	1	1.61E-05	2.08E-05
Sdha	10.84	10.85	10.86	10.90	1	1	1	1
Sdhb	12.03	12.03	11.86	11.90	1	1	1	0.74
Serpinb2	5.64	5.74	8.96	8.89	1	1	3.67E-03	8.66E-03
Shpk	5.67	5.70	5.86	5.71	1	1	1	1
Sigirr	5.27	5.44	5.05	5.21	1	1	1	1
Slc27A1	12.53	12.48	12.15	12.16	1	1	0.01	8.35E-03
Slc6A3	3.67	3.64	4.34	4.43	1	1	5.62E-03	0.15
Smpdl3b	7.53	7.56	7.57	7.69	1	1	1	1
Socs1	6.81	7.29	10.35	10.04	1	1	7.25E-03	9.39E-04
Socs3	8.06	8.01	14.36	14.47	1	1	1.11E-25	6.02E-24
Stat1	11.55	11.39	11.65	11.46	1	1	1	1
Tank	10.20	10.43	11.83	11.85	1	1	2.97E-07	1.52E-07
Tax1bp1	10.81	10.82	11.36	11.34	1	1	2.18E-06	7.92E-06
Tbk1	9.80	9.90	10.38	10.39	1	1	1.83E-03	7.25E-04
Tbp	8.24	8.25	8.22	8.18	1	1	1	1
Tgfb1	9.55	9.56	9.48	9.64	1	1	1	1
Ticam1	8.32	8.47	8.84	8.88	1	1	1	1
Ticam2	8.37	8.27	8.66	8.67	1	1	1	1
Tirap	7.66	7.69	7.71	7.66	1	1	1	1
Tlr1	7.70	7.83	9.27	9.13	1	1	0.02	7.11E-03
Tlr2	10.97	10.95	13.16	13.39	1	1	1.98E-16	8.05E-14
Tlr3	7.66	7.63	7.78	7.64	1	1	1	1
Tlr4	10.98	10.90	10.28	10.30	1	1	2.08E-03	8.81E-04
Tlr5	5.87	5.76	5.12	5.18	1	1	0.30	0.06
Tlr6	7.18	7.16	7.52	7.56	1	1	0.20	1
Tlr7	9.63	9.65	9.84	9.88	1	1	1	1
Tlr8	10.70	10.66	10.16	10.17	1	1	7.90E-04	9.22E-04
Tlr9	9.10	8.84	8.40	8.28	1	1	0.09	0.02
Tmem173	9.27	9.22	9.14	9.13	1	1	1	1

Table 10: ***Gene expression between miR-17-92$^\Delta$ and WT BMDMs.***

Gene Name	WT LPS	miR-17-92$^\Delta$ UT	WT LPS	miR-17-92$^\Delta$ LPS	KO vs WT LPS	KO vs WT UT	LPS vs UT KO	LPS vs UT WT
Tnf	10.31	10.54	15.24	15.44	1	1	6.30E-18	1.26E-16
Tnfaip3	9.60	9.68	14.63	14.62	1	1	7.87E-20	1.16E-18
Tnfaip8l2	10.53	10.45	8.78	8.91	1	1	4.35E-04	3.32E-04
Tnfrsf1a	11.16	11.19	10.91	10.87	1	1	5.21E-03	0.32
Tnip1	9.16	9.41	11.99	12.06	1	1	1.80E-10	5.39E-10
Tnip2	8.42	8.51	9.03	8.94	1	1	0.04	1.29E-03
Tnip3	11.40	11.48	13.15	12.95	1	1	1.57E-04	5.16E-05
Traf1	8.04	8.13	11.29	11.19	1	1	1.85E-08	6.20E-08
Traf3	8.50	8.48	9.03	9.14	1	1	1.06E-04	0.01
Traf6	9.21	9.22	9.78	9.72	1	1	2.08E-07	1.39E-07
Trex1	9.93	10.03	12.11	11.95	1	1	1.92E-03	1.61E-03
Trim21	8.83	8.99	9.94	9.71	1	1	1	0.46
Trim30a	10.53	10.43	10.81	10.62	1	1	1	1
Tubb5	12.03	11.94	11.60	11.59	1	1	0.01	2.98E-03
Ube2n	6.93	7.05	7.14	7.24	1	1	1	1
Usp18	8.81	8.81	9.80	9.65	1	1	1	1
Usp21	8.16	8.23	8.06	8.07	1	1	1	1
Xbp1	11.74	11.74	11.61	11.68	1	1	1	1
Zfand6	10.65	10.70	10.86	10.88	1	1	0.03	0.03

Table 10: **Gene expression between miR-17-92$^\Delta$ and WT BMDMs.**

8 Abbreviations

Abbreviation	Full phrase or term
AMO	AntagomiR
ANOVA	Analysis of Varience
BM	Bone Marrow
BMDM	Bone Marrow Derived Macrophage
BSA	Bovine Serum Albumin
βME	Beta-Mercaptoethanol (2-Mercaptoethanol)
cDNA	Copy DNA
DC	Dendritic cell
DESeq2	Differential gene expression analysis based on the negative binomial distribution
ELISA	Enzyme-Linked immunosorbent assay
FCS	Fetal Calf Serum
fl	flox
iCLIP	Individual nucleotide Cross-linking and Immunoprecipitation
IFN	Interferon
Il	Interleukin
ILC	Innate Lymphoid cell
IP	Intraperitoneal
L929	L929 cell conditioned medium
LPS	Lipopolysaccharide
Mø	Macrophage
M-CSF	Macrophage Colony Stimulating Factor
miR-17-92$^{\Delta}$	miR-17-92fl/fl - LysMCre cell/mouse
miRNA	microRNA
mRNA	Messenger RNA
NF-κB	Nuclear Factor kappa B family
PAMP	Pathogen Associated Molecular Pattern
PBMC	Peripheral blood mononuclear cell

Abbreviation	Full phrase or term
PCR	Polymerase Chain Reaction
pre-miRNA	precursor-miRNA
pri-miRNA	Primary miRNA Transcript
PRR	Pattern Recognition Receptor
qPCR	Quantitative Real-Time PCR
RNA	Ribonucleic Acid
RISC	RNA-induced silencing complex
RT	Reverse Transcription
TNFa	Tumour necrosis factor alpha
TLR	Toll-Like Receptor
UT	Untreated
LysM-Cre	Lysozyme 2 (Lyz2) driven Cre recombinase
WT	Wild type: miR-17-92fl/fl mouse

9 Publications

1. Michael P. Gantier, **H. James Stunden**, Claire E. McCoy, Mark A. Behlke, Die Wang, Maria Kaparakis-Liaskos, Soroush T. Sarvestani, Yuan H. Yang, Dakang Xu, Sinéad C. Corr, Eric F. Morand and Bryan R. G. Williams. A miR-19 regulon that controls NF-κB signaling. Nucleic Acids Research 40, 8048–8058 (2012).

2. **H. James Stunden**, Eicke Latz. PKR stirs up inflammasomes. Cell Res 23, 168–170 (2013).

3. Soroush T. Sarvestani, **H. James Stunden**, Mark A. Behlke, Samuel C. Forster, Claire E. McCoy, Michelle D. Tate, Jonathan Ferrand, Kim A. Lennox, Eicke Latz, Bryan R.G. Williams and Michael P. Gantier. Sequence-dependent off-target inhibition of TLR7/8 sensing by synthetic microRNA inhibitors. Nucleic Acids Research 43, 1177–1188 (2015).

4. Geneviève Pépin, Charlotte Nejad, Jonathan Ferrand, Belinda J. Thomas, **H. James Stunden**, Elaine Sanij, Chwan-Hong Foo, Cameron R. Stewart, Jason E. Cain, Philip G. Bardin, Bryan R. G. Williams, and Michael P. Gantier. Topoisomerase 1 Inhibition Promotes Cyclic GMP-AMP Synthase-Dependent Antiviral Responses. MBio. 2017 Oct 3;8(5).

5. Lorenz Fülle, Nancy Steiner, Markus Funke, Fabian Gondorf, Franziska Pfeiffer, Julia Siegl, Friederike V. Opitz, Silvana Haßel, Anna Belen Erazo, Oliver Schanz, **H. James Stunden**, Michael Blank, Carsten Gröber, Kristian Händler, Marc Beyer, Heike Weighardt, Eicke Latz, Joachim L.Schultze, Günter Mayer, Irmgard Förster. RNA aptamers recognizing murine CCL17 inhibit T cell chemotaxis and reduce contact hypersensitivity in vivo. Molecular Therapy; 2017 Oct 12;:1–38.

6. Laia Civit, Seyed Mohammad Taghdisi, Anna Jonczyk, Silvana K. Haßel, Carsten Gröber, Michael Blank, **H. James Stunden**, Marc Beyer, Joachim Schultze, Eicke Latz, Günter Mayer. Systematic evaluation of cell-SELEX enriched aptamers binding to breast cancer cells. Biochimie. 2017 Oct 17.

7. Charlotte Nejad, **H. James Stunden**, Michael. P. Gantier. A guide to miRNAs in inflammation and innate immune responses. The FEBS Journal, 285(20), 3695–3716 (2018).

10 Acknowledgements

11 Erklärung

Hiermit versichere ich, dass ich die vorliegende Arbeit persönlich, selbstständig und ohne Benutzung anderer als der angegebenen Quellen und Hilfsmittel angefertigt habe, sowie direkt oder indirekt übernommene Daten und Konzepte unter Angabe der Quelle kenntlich gemacht habe.

Ich habe keine früheren Promotionsversuche unternommen und die Arbeit wurde bisher weder im In- noch im Ausland in gleicher oder ähnlicher Form einer anderen Prüfungsbehörde vorgelegt.

Für die Erstellung der vorgelegten Arbeit und/oder die Gelegenheit zur Promotion habe ich keine fremde Hilfe, insbesondere keine entgeltliche Hilfe von Vermittlungs- bzw. Beratungsdiensten in Anspruch genommen.

Datum   Unterschrift

References

[1] Bartel, D. P. MicroRNAs: genomics, biogenesis, mechanism, and function. *Cell* **116**, 281–297 (2004).

[2] Lee, R. C., Feinbaum, R. L. & Ambros, V. The C. elegans heterochronic gene lin-4 encodes small RNAs with antisense complementarity to lin-14. *Cell* **75**, 843–854 (1993).

[3] Fire, A. *et al.* Potent and specific genetic interference by double-stranded RNA in Caenorhabditis elegans. *Nature* **391**, 806–811 (1998).

[4] Kloosterman, W. P. & Plasterk, R. H. A. The diverse functions of microRNAs in animal development and disease. *Developmental Cell* **11**, 441–450 (2006).

[5] Schirle, N. T., Sheu-Gruttadauria, J. & MacRae, I. J. Structural basis for microRNA targeting. *Sci. Immunol* (2014).

[6] Lewis, B. P., Burge, C. B. & Bartel, D. P. Conserved seed pairing, often flanked by adenosines, indicates that thousands of human genes are microRNA targets. *Cell* **120**, 15–20 (2005).

[7] Lim, L. P. *et al.* Microarray analysis shows that some microRNAs downregulate large numbers of target mRNAs. *Nature* **433**, 769–773 (2005).

[8] Friedman, R. C., Farh, K. K.-H., Burge, C. B. & Bartel, D. P. Most mammalian mRNAs are conserved targets of microRNAs. *Genome Res.* **19**, 92–105 (2009).

[9] Reczko, M., Maragkakis, M., Alexiou, P., Grosse, I. & Hatzigeorgiou, A. G. Functional microRNA targets in protein coding sequences. *Bioinformatics* **28**, 771–776 (2012).

[10] Paraskevopoulou, M. D. *et al.* DIANA-microT web server v5.0: service integration into miRNA functional analysis workflows. *Nucleic Acids Research* **41**, W169–73 (2013).

[11] Philippe, L. *et al.* TLR2 expression is regulated by microRNA miR-19 in rheumatoid fibroblast-like synoviocytes. *The Journal of Immunology* **188**, 454–461 (2012).

[12] Philippe, L. *et al.* MiR-20a regulates ASK1 expression and TLR4-dependent cytokine release in rheumatoid fibroblast-like synoviocytes. *Ann. Rheum. Dis.* **72**, 1071–1079 (2013).

[13] Philippe, L., Alsaleh, G., Bahram, S., Pfeffer, S. & Georgel, P. The miR-17☐92 Cluster: A Key Player in the Control of Inflammation during Rheumatoid Arthritis. *Front Immunol* **4**, 70 (2013).

[14] Li, X. *et al.* miR-146a-5p Antagonized AGEs- and P.g-LPS-Induced ABCA1 and ABCG1 Dysregulation in Macrophages via IRAK-1 Downregulation. *Inflammation* **38**, 1761–1768 (2015).

[15] Li, K., Ching, D., Luk, F. S. & Raffai, R. L. Apolipoprotein E Enhances MicroRNA-146a in Monocytes and Macrophages to Suppress Nuclear Factor-?B-Driven Inflammation and Atherosclerosis. *Circulation Research* **117**, e1–e11 (2015).

[16] Shi, C. *et al.* MicroRNA-21 knockout improve the survival rate in DSS induced fatal colitis through protecting against inflammation and tissue injury. *PLoS ONE* **8**, e66814 (2013).

[17] Ha, M. & Kim, V. N. Regulation of microRNA biogenesis. *Nat Rev Mol Cell Biol* **15**, 509–524 (2014).

[18] Han, J. *et al.* Molecular basis for the recognition of primary microRNAs by the Drosha-DGCR8 complex. *Cell* **125**, 887–901 (2006).

[19] Bohnsack, M. T., Czaplinski, K. & Görlich, D. Exportin 5 is a RanGTP-dependent dsRNA-binding protein that mediates nuclear export of pre-miRNAs. *RNA* **10**, 185–191 (2004).

[20] Kim, V. N., Han, J. & Siomi, M. C. Biogenesis of small RNAs in animals. *Nat Rev Mol Cell Biol* **10**, 126–139 (2009).

[21] Carthew, R. W. & Sontheimer, E. J. Origins and Mechanisms of miRNAs and siRNAs. *Cell* **136**, 642–655 (2009).

[22] Eulalio, A. *et al.* Deadenylation is a widespread effect of miRNA regulation. *RNA* **15**, 21–32 (2009).

[23] Hutvágner, G. & Zamore, P. D. A microRNA in a multiple-turnover RNAi enzyme complex. *Sci. Immunol* **297**, 2056–2060 (2002).

[24] Paddison, P. J., Caudy, A. A., Bernstein, E., Hannon, G. J. & Conklin, D. S. Short hairpin RNAs (shRNAs) induce sequence-specific silencing in mammalian cells. *Genes & Development* **16**, 948–958 (2002).

[25] van Rooij, E. & Kauppinen, S. Development of microRNA therapeutics is coming of age. *EMBO Mol Med* **6**, 851–864 (2014).

[26] Babar, I. A. *et al.* Nanoparticle-based therapy in an in vivo microRNA-155 (miR-155)-dependent mouse model of lymphoma. *Proceedings of the National Academy of Sciences* (2012).

[27] Pofahl, M., Wengel, J. & Mayer, G. Multifunctional nucleic acids for tumor cell treatment. *Nucleic Acid Ther* **24**, 171–177 (2014).

[28] Meng, L. *et al.* Small RNA zippers lock miRNA molecules and block miRNA function in mammalian cells. *Nat Commun* **8**, 13964 (2017).

[29] Olive, V. *et al.* A component of the mir-17-92 polycistronic oncomir promotes oncogene-dependent apoptosis. *Elife* **2**, e00822 (2013).

[30] Esquela-Kerscher, A. & Slack, F. J. Oncomirs - microRNAs with a role in cancer. *Nat Rev Cancer* **6**, 259–269 (2006).

[31] Ota, A. *et al.* Identification and characterization of a novel gene, C13orf25, as a target for 13q31-q32 amplification in malignant lymphoma. *Cancer Research* **64**, 3087–3095 (2004).

[32] O'Donnell, K. A., Wentzel, E. A., Zeller, K. I., Dang, C. V. & Mendell, J. T. c-Myc-regulated microRNAs modulate E2F1 expression. *Nature* **435**, 839–843 (2005).

[33] Chakraborty, S. & Krishnan, Y. A structural map of oncomiR-1 at single-nucleotide resolution. *Nucleic Acids Research* **45**, 9694–9705 (2017).

[34] Trabucchi, M. *et al.* The RNA-binding protein KSRP promotes the biogenesis of a subset of microRNAs. *Nature* **459**, 1010–1014 (2009).

[35] Guil, S. & Cáceres, J. F. The multifunctional RNA-binding protein hnRNP A1 is required for processing of miR-18a. *Nat Struct Mol Biol* **14**, 591–596 (2007).

[36] He, L. *et al.* A microRNA polycistron as a potential human oncogene. *Nature* **435**, 828–833 (2005).

[37] Ventura, A. *et al.* Targeted deletion reveals essential and overlapping functions of the miR-17 through 92 family of miRNA clusters. *Cell* **132**, 875–886 (2008).

[38] Han, Y.-C. *et al.* An allelic series of miR-17 □ 92-mutant mice uncovers functional specialization and cooperation among members of a microRNA polycistron. *Nat Genet* **47**, 766–775 (2015).

[39] Olive, V. *et al.* miR-19 is a key oncogenic component of mir-17-92. *Genes & Development* **23**, 2839–2849 (2009).

[40] Gantier, M. P. *et al.* A miR-19 regulon that controls NF-κB signaling. *Nucleic Acids Research* **40**, 8048–8058 (2012).

[41] Baumjohann, D. *et al.* The microRNA cluster miR-17□92 promotes TFH cell differentiation and represses subset-inappropriate gene expression. *Nat Immunol* (2013).

[42] Simpson, L. J. *et al.* A microRNA upregulated in asthma airway T cells promotes TH2 cytokine production. *Nat Immunol* **15**, 1162–1170 (2014).

[43] Serr, I. *et al.* miRNA92a targets KLF2 and the phosphatase PTEN signaling to promote human T follicular helper precursors in T1D islet autoimmunity. *Proc Natl Acad Sci USA* **113**, E6659–E6668 (2016).

[44] Brock, M. *et al.* MicroRNA-18a enhances the interleukin-6-mediated production of the acute-phase proteins fibrinogen and haptoglobin in human hepatocytes. *Journal of Biological Chemistry* **286**, 40142–40150 (2011).

[45] Trenkmann, M. *et al.* Tumor necrosis factor α-induced microRNA-18a activates rheumatoid arthritis synovial fibroblasts through a feedback loop in NF-κB signaling. *Arthritis Rheum* **65**, 916–927 (2013).

[46] Singh, P. B. *et al.* MicroRNA regulation of type 2 innate lymphoid cell homeostasis and function in allergic inflammation. *J. Exp. Med.* (2017).

[47] Aken, B. L. *et al.* Ensembl 2017. *Nucleic Acids Research* **45**, D635–D642 (2017).

[48] Janeway, C. A. & Medzhitov, R. Innate immune recognition. *Annu. Rev. Immunol.* **20**, 197–216 (2002).

[49] Hayden, M. S. & Ghosh, S. NF-κB in immunobiology. *Cell Res* **21**, 223–244 (2011).

[50] Cohen, P. The TLR and IL-1 signalling network at a glance. *J. Cell. Sci.* **127**, 2383–2390 (2014).

[51] Silva, M. T. & Correia-Neves, M. Neutrophils and macrophages: the main partners of phagocyte cell systems. *Front Immunol* **3**, 174 (2012).

[52] Gordon, S. *Elie Metchnikoff: father of natural immunity.*, vol. 38 (Sir William Dunn School of Pathology, University of Oxford, Oxford, UK. siamon.gordon@path.ox.ac.uk, 2008).

[53] Kim, K.-W., Zhang, N., Choi, K. & Randolph, G. J. Homegrown Macrophages. *Immunity* **45**, 468–470 (2016).

[54] Mass, E. *et al.* Specification of tissue-resident macrophages during organogenesis. *Sci. Immunol* **353**, aaf4238–aaf4238 (2016).

[55] Murray, P. J. & Wynn, T. A. Protective and pathogenic functions of macrophage subsets. *Nat. Rev. Immunol.* **11**, 723–737 (2011).

[56] Taganov, K. D., Boldin, M. P., Chang, K.-J. & Baltimore, D. NF-kappaB-dependent induction of microRNA miR-146, an inhibitor targeted to signaling proteins of innate immune responses. *Proc Natl Acad Sci USA* **103**, 12481–12486 (2006).

[57] Hou, J. *et al.* MicroRNA-146a feedback inhibits RIG-I-dependent Type I IFN production in macrophages by targeting TRAF6, IRAK1, and IRAK2. *J Immunol* **183**, 2150–2158 (2009).

[58] Nahid, M. A., Pauley, K. M., Satoh, M. & Chan, E. K. L. miR-146a Is Critical for Endotoxin-induced Tolerance: IMPLICATION IN INNATE IMMUNITY. *J Biol Chem* **284**, 34590–34599 (2009).

[59] Shaked, I. *et al.* MicroRNA-132 potentiates cholinergic anti-inflammatory signaling by targeting acetylcholinesterase. *Immunity* **31**, 965–973 (2009).

[60] Wang, H. *et al.* Nicotinic acetylcholine receptor alpha7 subunit is an essential regulator of inflammation. *Nature* **421**, 384–388 (2003).

[61] Pavlov, V. A. *et al.* Selective alpha7-nicotinic acetylcholine receptor agonist GTS-21 improves survival in murine endotoxemia and severe sepsis. *Crit. Care Med.* **35**, 1139–1144 (2007).

[62] McCoy, C. E. *et al.* IL-10 inhibits miR-155 induction by toll-like receptors. *Journal of Biological Chemistry* **285**, 20492–20498 (2010).

[63] Jablonski, K. A., Gaudet, A. D., Amici, S. A., Popovich, P. G. & Guerau-de Arellano, M. Control of the Inflammatory Macrophage Transcriptional Signature by miR-155. *PLoS ONE* **11**, e0159724 (2016).

[64] Boldin, M. P. *et al.* miR-146a is a significant brake on autoimmunity, myeloproliferation, and cancer in mice. *J. Exp. Med.* **208**, 1189–1201 (2011).

[65] Lu, Z.-J. *et al.* MicroRNA-155 promotes the pathogenesis of experimental colitis by repressing SHIP-1 expression. *World J. Gastroenterol.* **23**, 976–985 (2017).

[66] Mann, M. *et al.* An NF-κB-microRNA regulatory network tunes macrophage inflammatory responses. *Nat Commun* **8**, 851 (2017).

[67] Sen, R. & Baltimore, D. Multiple nuclear factors interact with the immunoglobulin enhancer sequences. *Cell* **46**, 705–716 (1986).

[68] Oeckinghaus, A. & Ghosh, S. The NF-kappaB family of transcription factors and its regulation. *Cold Spring Harb Perspect Biol* **1**, a000034 (2009).

[69] Oeckinghaus, A., Hayden, M. S. & Ghosh, S. Crosstalk in NF-κB signaling pathways. *Nat Immunol* **12**, 695–708 (2011).

[70] Sen, R. & Smale, S. T. Selectivity of the NF-κB response. *Cold Spring Harbor perspectives in …* (2010).

[71] Zhang, Q., Lenardo, M. J. & Baltimore, D. 30 Years of NF-κB: A Blossoming of Relevance to Human Pathobiology. *Cell* **168**, 37–57 (2017).

[72] Wertz, I. E. *et al.* De-ubiquitination and ubiquitin ligase domains of A20 downregulate NF-kappaB signalling. *Nature* **430**, 694–699 (2004).

[73] Newton, K. *et al.* Ubiquitin chain editing revealed by polyubiquitin linkage-specific antibodies. *Cell* **134**, 668–678 (2008).

[74] Newton, K. & Dixit, V. M. Signaling in innate immunity and inflammation. *Cold Spring Harb Perspect Biol* **4** (2012).

[75] Karin, M. How NF-kappaB is activated: the role of the IkappaB kinase (IKK) complex. *Oncogene* **18**, 6867–6874 (1999).

[76] Akira, S. & Takeda, K. Toll-like receptor signalling. *Nat. Rev. Immunol.* **4**, 499–511 (2004).

[77] Shih, V. F.-S., Tsui, R., Caldwell, A. & Hoffmann, A. A single NFκB system for both canonical and non-canonical signaling. *Cell Res* **21**, 86–102 (2011).

[78] O'Neill, L. A. J., Golenbock, D. & Bowie, A. G. The history of Toll-like receptors - redefining innate immunity. *Nature Publishing Group* **13**, 453–460 (2013).

[79] Smale, S. T. Selective Transcription in Response to an Inflammatory Stimulus. *Cell* **140**, 833–844 (2010).

[80] Tong, A.-J. *et al.* A Stringent Systems Approach Uncovers Gene-Specific Mechanisms Regulating Inflammation. *Cell* **165**, 165–179 (2016).

[81] Kondo, T., Kawai, T. & Akira, S. Dissecting negative regulation of Toll-like receptor signaling. *Trends in Immunology* **33**, 449–458 (2012).

[82] Hou, Y. *et al.* Activation of the nuclear factor-κB pathway during postnatal lung inflammation preserves alveolarization by suppressing macrophage inflammatory protein-2. *Am. J. Physiol. Lung Cell Mol. Physiol.* **309**, L593–604 (2015).

[83] Lang, T. & Mansell, A. The negative regulation of Toll-like receptor and associated pathways. *Immunol. Cell Biol.* (2007).

[84] Boldin, M. P. & Baltimore, D. MicroRNAs, new effectors and regulators of NF-κB. *Immunol. Rev.* **246**, 205–220 (2012).

[85] Liew, F. Y., Xu, D., Brint, E. K. & O'Neill, L. A. J. Negative regulation of toll-like receptor-mediated immune responses. *Nat. Rev. Immunol.* **5**, 446–458 (2005).

[86] Opipari, A. W., Boguski, M. S. & Dixit, V. M. The A20 cDNA induced by tumor necrosis factor alpha encodes a novel type of zinc finger protein. *J Biol Chem* **265**, 14705–14708 (1990).

[87] Dixit, V. M. *et al.* Tumor necrosis factor-alpha induction of novel gene products in human endothelial cells including a macrophage-specific chemotaxin. *J Biol Chem* **265**, 2973–2978 (1990).

[88] Pahl, H. L. Activators and target genes of Rel/NF-κB transcription factors. *Oncogene* (1999).

[89] Tsitsiou, E. & Lindsay, M. A. microRNAs and the immune response. *Curr Opin Pharmacol* **9**, 514–520 (2009).

[90] O'Neill, L. A., Sheedy, F. J. & McCoy, C. E. MicroRNAs: the fine-tuners of Toll-like receptor signalling. *Nat. Rev. Immunol.* **11**, 163–175 (2011).

[91] Yang, L. *et al.* miR-146a controls the resolution of T cell responses in mice. *J. Exp. Med.* **209**, 1655–1670 (2012).

[92] Curtale, G. *et al.* Negative regulation of Toll-like receptor 4 signaling by IL-10-dependent microRNA-146b. *Proceedings of the National Academy of Sciences* **110**, 11499–11504 (2013).

[93] Tili, E. *et al.* Modulation of miR-155 and miR-125b levels following lipopolysaccharide/TNF-alpha stimulation and their possible roles in regulating the response to endotoxin shock. *The Journal of Immunology* **179**, 5082–5089 (2007).

[94] O'Connell, R. M., Taganov, K. D., Boldin, M. P., Cheng, G. & Baltimore, D. MicroRNA-155 is induced during the macrophage inflammatory response. *Proc Natl Acad Sci USA* **104**, 1604–1609 (2007).

[95] Hsu, A. C.-Y. *et al.* MicroRNA-125a and -b inhibit A20 and MAVS to promote inflammation and impair antiviral response in COPD. *JCI Insight* **2**, e90443 (2017).

[96] Collins, A. S., McCoy, C. E., Lloyd, A. T., O'Farrelly, C. & Stevenson, N. J. miR-19a: An Effective Regulator of SOCS3 and Enhancer of JAK-STAT Signalling. *PLoS ONE* **8**, e69090 (2013).

[97] Ashraf, U. *et al.* MicroRNA-19b-3p Modulates Japanese Encephalitis Virus-Mediated Inflammation via Targeting RNF11. *Journal of Virology* **90**, 4780–4795 (2016).

[98] Ye, H. *et al.* MicroRNA and transcription factor co-regulatory network analysis reveals miR-19 inhibits CYLD in T-cell acute lymphoblastic leukemia. *Nucleic Acids Research* (2012).

[99] Sauer, B. Functional expression of the cre-lox site-specific recombination system in the yeast Saccharomyces cerevisiae. *Mol. Cell. Biol.* **7**, 2087–2096 (1987).

[100] Clausen, B. E., Burkhardt, C., Reith, W., Renkawitz, R. & Förster, I. Conditional gene targeting in macrophages and granulocytes using LysMcre mice. *Transgenic Res.* **8**, 265–277 (1999).

[101] Hornung, V. *et al.* Silica crystals and aluminum salts activate the NALP3 inflammasome through phagosomal destabilization. *Nature Publishing Group* **9**, 847–856 (2008).

[102] Love, M. I., Huber, W. & Anders, S. Moderated estimation of fold change and dispersion for RNA-seq data with DESeq2. *Genome Biol* **15**, 550 (2014).

[103] Bresler, S. C. *et al.* Gene expression profiling of anti-CTLA4-treated metastatic melanoma in patients with treatment-induced autoimmunity. *Lab. Invest.* (2016).

[104] Huppertz, I. *et al.* iCLIP: protein-RNA interactions at nucleotide resolution. **65**, 274–287 (2014).

[105] Agarwal, V., Bell, G. W., Nam, J.-W. & Bartel, D. P. Predicting effective microRNA target sites in mammalian mRNAs. *Elife* **4**, 101 (2015).

[106] Gantier, M. P. *et al.* Analysis of microRNA turnover in mammalian cells following Dicer1 ablation. *Nucleic Acids Research* **39**, 5692–5703 (2011).

[107] Burkitt, M. D., Williams, J. M., Townsend, T., Hough, R. & Pritchard, D. Mice lacking NF-κB1 exhibit marked DNA damage responses and more severe gastric pathology in response to intraperitoneal tamoxifen administration. *Cell Death Dis* **8**, e2939 (2017).

[108] Behjati, S. & Frank, M. H. The effects of tamoxifen on immunity. *Curr. Med. Chem.* **16**, 3076–3080 (2009).

[109] Boillée, S. *et al.* Onset and progression in inherited ALS determined by motor neurons and microglia. *Sci. Immunol* **312**, 1389–1392 (2006).

[110] Schmidt-Supprian, M. & Rajewsky, K. Vagaries of conditional gene targeting. *Nat Immunol* **8**, 665–668 (2007).

[111] Loonstra, A. *et al.* Growth inhibition and DNA damage induced by Cre recombinase in mammalian cells. *Proc Natl Acad Sci USA* **98**, 9209–9214 (2001).

[112] Abram, C. L., Roberge, G. L., Hu, Y. & Lowell, C. A. Comparative analysis of the effi-
ciency and specificity of myeloid-Cre deleting strains using ROSA-EYFP reporter mice.
J. Immunol. Methods **408**, 89–100 (2014).

[113] Rüegger, S. & Großhans, H. MicroRNA turnover: when, how, and why. *Trends in Bio-
chemical Sciences* **37**, 436–446 (2012).

[114] Marzi, M. J. *et al.* Degradation dynamics of microRNAs revealed by a novel pulse-chase
approach. *Genome Res.* **26**, 554–565 (2016).

[115] Pospisil, V. *et al.* Epigenetic silencing of the oncogenic miR-17-92 cluster during PU.1-
directed macrophage differentiation. *EMBO J* **30**, 4450–4464 (2011).

[116] Keshav, S., Chung, P., Milon, G. & Gordon, S. Lysozyme is an inducible marker of
macrophage activation in murine tissues as demonstrated by in situ hybridization. *J.
Exp. Med.* **174**, 1049–1058 (1991).

[117] Blasi, E., Mathieson, B. J., Varesio, L. & Cleveland, J. L. Selective immortalization of
murine macrophages from fresh bone marrow by a raf/myc recombinant murine retrovirus.
Nature **318**, 667–670 (1985).

[118] Liu, M. *et al.* TNF-α is a novel target of miR-19a. *Int. J. Oncol.* **38**, 1013–1022 (2011).

[119] O'Neill, L. A. J., Kishton, R. J. & Rathmell, J. A guide to immunometabolism for immunol-
ogists. *Nature Publishing Group* **16**, 553–565 (2016).

[120] Poitz, D. M. *et al.* Regulation of the Hif-system by micro-RNA 17 and 20a - Role during
monocyte-to-macrophage differentiation. *Mol. Immunol.* **56**, 442–451 (2013).

[121] Lei, Z. *et al.* Regulation of HIF-1alpha and VEGF by miR-20b tunes tumor cells to adapt
to the alteration of oxygen concentration. *PLoS ONE* **4**, e7629 (2009).

[122] Krutilina, R. *et al.* MicroRNA-18a inhibits hypoxia-inducible factor 1α activity and lung
metastasis in basal breast cancers. *Breast Cancer Res.* **16**, R78 (2014).

[123] Akhtar, S. *et al.* Endothelial Hypoxia-Inducible Factor-1α Promotes Atherosclerosis and
Monocyte Recruitment by Upregulating MicroRNA-19a. *Hypertension* **66**, 1220–1226
(2015).

[124] Loeb, G. B. *et al.* Transcriptome-wide miR-155 binding map reveals widespread non-canonical microRNA targeting. *Molecular Cell* **48**, 760–770 (2012).

[125] Van Nostrand, E. L. *et al.* Robust transcriptome-wide discovery of RNA-binding protein binding sites with enhanced CLIP (eCLIP). *Nat Meth* **13**, 508–514 (2016).

[126] Broughton, J. P., Lovci, M. T., Huang, J. L., Yeo, G. W. & Pasquinelli, A. E. Pairing beyond the Seed Supports MicroRNA Targeting Specificity. *Molecular Cell* **64**, 320–333 (2016).

[127] Baek, D. *et al.* The impact of microRNAs on protein output. *Nature* **455**, 64–71 (2008).

[128] Selbach, M. *et al.* Widespread changes in protein synthesis induced by microRNAs. *Nature* **455**, 58–63 (2008).

[129] Eichhorn, S. W. *et al.* mRNA destabilization is the dominant effect of mammalian microRNAs by the time substantial repression ensues. *Molecular Cell* **56**, 104–115 (2014).

[130] Rael, E. L. & Lockey, R. F. Interleukin-13 signaling and its role in asthma. *World Allergy Organ J* **4**, 54–64 (2011).

[131] Borthwick, L. A. *et al.* Macrophages are critical to the maintenance of IL-13-dependent lung inflammation and fibrosis. *Mucosal Immunol* **9**, 38–55 (2016).

[132] Krause, P. *et al.* IL-10-producing intestinal macrophages prevent excessive antibacterial innate immunity by limiting IL-23 synthesis. *Nat Commun* **6**, 7055 (2015).

[133] Wang, T. *et al.* miR-19a promotes colitis-associated colorectal cancer by regulating tumor necrosis factor alpha-induced protein 3-NF-κB feedback loops. *Oncogene* (2016).

[134] Fontana, L. *et al.* MicroRNAs 17-5p-20a-106a control monocytopoiesis through AML1 targeting and M-CSF receptor upregulation. *Nat Cell Biol* **9**, 775–787 (2007).

[135] Tazi, M. F. *et al.* Elevated Mirc1/Mir17-92 cluster expression negatively regulates autophagy and CFTR (cystic fibrosis transmembrane conductance regulator) function in CF macrophages. *Autophagy* **12**, 2026–2037 (2016).

[136] Sarvestani, S. T. *et al.* Sequence-dependent off-target inhibition of TLR7/8 sensing by synthetic microRNA inhibitors. *Nucleic Acids Research* **43**, 1177–1188 (2015).

[137] Zhao, D., zhuang, N., Ding, Y., Kang, Y. & Shi, L. MiR-221 activates the NF-κB pathway by targeting A20. *Biochemical and Biophysical Research Communications* **472**, 11–18 (2016).

[138] Pépin, G., Ferrand, J. & Höning, K. Cre-dependent DNA recombination activates a STING-dependent innate immune response. *Nucleic acids …* (2016).

[139] Gilbert, J. A. *et al.* Microbiome-wide association studies link dynamic microbial consortia to disease. *Nature* **535**, 94–103 (2016).

[140] Mamantopoulos, M. *et al.* Nlrp6- and ASC-Dependent Inflammasomes Do Not Shape the Commensal Gut Microbiota Composition. *Immunity* **47**, 339–348.e4 (2017).

[141] Schmiedel, J. M. *et al.* Gene expression. MicroRNA control of protein expression noise. *Sci. Immunol* **348**, 128–132 (2015).

[142] Jin, H. Y. *et al.* Differential Sensitivity of Target Genes to Translational Repression by miR-17~92. *PLoS Genet* **13**, e1006623 (2017).

[143] Schug, J. *et al.* Dynamic recruitment of microRNAs to their mRNA targets in the regenerating liver. *BMC Genomics* **14**, 264 (2013).

[144] Mullokandov, G. *et al.* High-throughput assessment of microRNA activity and function using microRNA sensor and decoy libraries. *Nat Meth* (2012).

[145] Jin, H. Y. *et al.* MicroRNA-17~92 plays a causative role in lymphomagenesis by coordinating multiple oncogenic pathways. *EMBO J* **32**, 2377–2391 (2013).

[146] Salmena, L., Poliseno, L., Tay, Y., Kats, L. & Pandolfi, P. P. A ceRNA hypothesis: the Rosetta Stone of a hidden RNA language? *Cell* **146**, 353–358 (2011).

[147] Memczak, S. *et al.* Circular RNAs are a large class of animal RNAs with regulatory potency. *Nature* **495**, 333–338 (2013).

[148] Mercer, T. R. *et al.* Targeted RNA sequencing reveals the deep complexity of the human transcriptome. *Nature Publishing Group* **30**, 99–104 (2012).

[149] Huang, Z. *et al.* Identification of Differentially Expressed Long Non-coding RNAs in Polarized Macrophages. *Sci Rep* **6**, 19705 (2016).

[150] Song, J. *et al.* PBMC and exosome-derived Hotair is a critical regulator and potent marker for rheumatoid arthritis. *Clin. Exp. Med.* **15**, 121–126 (2015).

[151] Lai, Y. *et al.* HOTAIR functions as a competing endogenous RNA to regulate PTEN expression by inhibiting miR-19 in cardiac hypertrophy. *Mol. Cell. Biochem.* **62**, 365–9 (2017).

[152] Mercer, T. R. & Mattick, J. S. Structure and function of long noncoding RNAs in epigenetic regulation. *Nat Struct Mol Biol* **20**, 300–307 (2013).

[153] Fujisaka, Y. *et al.* Long non-coding RNA HOTAIR up-regulates chemokine (C-C motif) ligand 2 and promotes proliferation of macrophages and myeloid-derived suppressor cells in hepatocellular carcinoma cell lines. *Oncol Lett* 1–6 (2017).

[154] Wu, H., Liu, J., Li, W., Liu, G. & Li, Z. LncRNA-HOTAIR promotes TNF-α production in cardiomyocytes of LPS-induced sepsis mice by activating NF-κB pathway. *Biochemical and Biophysical Research Communications* **471**, 240–246 (2016).

[155] Yang, C. *et al.* Circular RNA circ-ITCH inhibits bladder cancer progression by sponging miR-17/miR-224 and regulating p21, PTEN expression. *Mol. Cancer* **17**, 19 (2018).

[156] Zhai, Z., Wu, F., Chuang, A. Y. & Kwon, J. H. miR-106b fine tunes ATG16L1 expression and autophagic activity in intestinal epithelial HCT116 cells. *Inflamm. Bowel Dis.* **19**, 2295–2301 (2013).

[157] Sampath, D. *et al.* Specific activation of microRNA106b enables the p73 apoptotic response in chronic lymphocytic leukemia by targeting the ubiquitin ligase Itch for degradation. *Blood* **113**, 3744–3753 (2009).

[158] Mavrakis, K. J. *et al.* A cooperative microRNA-tumor suppressor gene network in acute T-cell lymphoblastic leukemia (T-ALL). *Nat Genet* **43**, 673–678 (2011).

[159] Xu, S. *et al.* Mir-17-92 regulates bone marrow homing of plasma cells and production of immunoglobulin G2c. *Nat Commun* **6**, 6764 (2015).

[160] Liu, S.-Q., Jiang, S., Li, C., Zhang, B. & Li, Q.-J. miR-17-92 cluster targets phosphatase and tensin homology and Ikaros Family Zinc Finger 4 to promote TH17-mediated inflammation. *Journal of Biological Chemistry* **289**, 12446–12456 (2014).

[161] Pichiorri, F. *et al.* MicroRNAs regulate critical genes associated with multiple myeloma pathogenesis. *Proceedings of the National Academy of Sciences* **105**, 12885–12890 (2008).

[162] Cheng, X. *et al.* miR-19b downregulates intestinal SOCS3 to reduce intestinal inflammation in Crohn's disease. *Sci Rep* **5**, 1–15 (2015).

[163] Wu, Q. *et al.* miR-17-5p promotes proliferation by targeting SOCS6 in gastric cancer cells. *FEBS Letters* **588**, 2055–2062 (2014).

[164] Montoya, M. M. *et al.* A Distinct Inhibitory Function for miR-18a in Th17 Cell Differentiation. *J Immunol* **199**, 559–569 (2017).

[165] Cheever, A., Blackwell, E. & Ceman, S. Fragile X protein family member FXR1P is regulated by microRNAs. *RNA* **16**, 1530–1539 (2010).

[166] Mavrakis, K. J. *et al.* Genome-wide RNA-mediated interference screen identifies miR-19 targets in Notch-induced T-cell acute lymphoblastic leukaemia. *Nat Cell Biol* **12**, 372–379 (2010).